LOCATION AND TIMING: A GENETIC ANALYSIS OF THIRD PHARYNGEAL POUCH DEVELOPMENT

by

VIRGINIA E. BAIN

(Under the direction of Nancy R. Manley)

ABSTRACT

The third pharyngeal pouch is formed between E8.5 and E9 in mice. The thymus and the parathyroid both form from third pouch endoderm at later stages of development. Although domain specific markers have been identified, the exact pathway responsible for patterning the thymus and parathyroid from third pouch endoderm is still unknown. Furthermore, several questions remain about morphogenesis of the thymus and parathyroid once these domains are established. In this study, we take advantage of the Cre loxp system in mice to regulate genes in a tissue specific manner. By deleting or ectopically expressing genes previously identified as being required for some part of third pouch patterning or morphogenesis, we aim to learn more about the pathway in which these genes function.

In our study of third pouch patterning we find that Shh signaling from neural crest mesenchyme and pouch endoderm both participate in patterning of the third pharyngeal pouch

and that signaling from either source is sufficient to support parathyroid fate. We find that Shh signaling and *Tbx1* expression does not guarantee *Gcm2* expression although this may be caused by an additional inhibitory factor. Finally we find the first evidence that *Foxn1* expression is inhibited by *Tbx1* expression in vivo.

In our study of thymus and parathyroid morphogenesis we find that AP-2α is required for separation of thymus from ectodermal cleft. We also find that ectodermal cleft fails to downregulate *Fgf8* expression and has ectopic expression of *Pax1* in the absence of AP-2a. We find that ectodermal cleft expressing endodermal identity genes is able to express *Foxn1* and *Gcm2*; however, cleft fails to organize expression of either gene. Finally we find that thymus function is either decreased or delayed.

Index words: Organogenesis, Development, Thymus, Parathyroid, Third pharyngeal pouch endoderm, Ectodermal cleft, Neural crest mesenchyme, *Sonic hedgehog* (*Shh*), *Foxn1, Gcm2, Tbx1, Fgf8, Bmp4, AP2α*

LOCATION AND TIMING: A GENETIC ANALYSIS OF THIRD PHARYNGEAL POUCH DEVELOPMENT

by

VIRGINIA E. BAIN

B.A. Agnes Scott College, 2004

A Dissertation Submitted to the Graduate Faculty of The University of Georgia in Partial Fulfillment of the Requirements for the Degree

DOCTOR OF PHILOSOPHY

ATHENS, GEORGIA

2011

LOCATION AND TIMING: A GENETIC ANALYSIS OF THIRD PHARYNGEAL POUCH DEVELOPMENT

by

VIRGINIA E. BAIN

Major Professor: Nancy R. Manley

Committee: Brian G. Condie
Kimberly D. Klonowski
James D. Lauderdale
Michael R. Strand

Electronic Version Approved:

Maureen Grasso
Dean of the Graduate School
The University of Georgia
December 2011

DEDICATION

I am eternally grateful for the faith and support of so many wonderful people: especially my parents who have done everything in their power to help me. I take this moment to remember my grandmothers, both of whom were enthusiastic about my pursuit of science and neither of whom were able to receive the education they desired or deserved. I dedicate this work to the many people who have believed in me, you have my gratitude.

ACKNOWLEDGEMENTS

First and foremost I wish to thank my advisor, Nancy Manley. Thank you for giving me an environment where the only limit to what I could learn was my imagination and the amount of sleep necessary to maintain cognizance. With your help I feel I have learned so much about developmental biology and life and I will always be glad I was able to join the Manley lab. I especially appreciate the amount of time you have spent helping me to refine my ability to communicate science.

I also wish to thank the wonderful members of my committee. Thanks to Brian for all the technical help with my project and the interesting conversations about a myriad of topics. Thanks to Jim for all the encouragement and support. Thanks to Kim for her enthusiasm and advice. Thanks to Mike for his non-mouse perspective and the many thoughtful questions he has asked about my research.

I wish to thank past and present members of the Condie/Manley lab who have made it a fun and wonderful place to work. Special thanks go to Julie Gordon, who I asked no less than 305 questions during my time in this lab. I also wish to thank Qiaozhi Wei, Jerrod Bryson, Lizhen Chen, Jason Liu, Billie Moore-Scott, Kyoko Masuda, Jie Li, and Shiyun Xiao for their expert technical advice (and encouragement) on the many techniques I learned during my time in the lab. I also wish to thank the same group as well as Julie, Cindy, Chris, Jena, Jamie, Megan[1] and Megan[2], Heidi, Wen, Yuzhi, Luying, Mike, and Mike for their friendship and camaraderie throughout the years.

Thanks to Michelle and Krista who have been wonderful mentees. Both of you are very talented and I had a wonderful time working with you.

I especially wish to thank Pansy Bond, Joelle Szendel, Nina Hauke, and Janice Lunsford, all of whom have helped me with quagmire of graduate school paperwork, complicated reagent requests, and who have been charming people to know.

Thanks to Kim Cardenas for all the encouragement over the years. Thanks to everyone from the Richie and Blackburn labs for their reagents and support. Thanks to all members of the Lauderdale lab, especially Jiha, Kenji, Vijay, and Vani.

I thank the mouse room staff for their help over the years in keeping my mice safe and generating embryos.

I also wish to thank the faculty and graduate students of the Genetics Department and Cell Biology. I especially wish to thank Lori King for all of her encouragement and straight talk over the years. My thanks also go to the DDR crowd.

Finally I wish to thank my family, especially my parents and my husband. I appreciate your support and understanding and am very grateful for your encouragement.

TABLE OF CONTENTS

Page

LIST OF TABLES

Page

LIST OF FIGURES

Page

CHAPTER 1

INTRODUCTION AND LITERATURE REVIEW

The third pharyngeal pouch: a system for endodermal development.

In early embryogenesis, cells of the blastula are totipotent until gastrulation at which point they are divided into three groups: endoderm, mesoderm, and ectoderm. Before these layers form, the developing egg contains an inner cell mass of two layers, the hypoblast and the epiblast. At the time of gastrulation, the outer layer of the inner cell mass, the epiblast, migrates inwards via the primitive streak to form endoderm and mesenchyme. The developing endoderm of a vertebrate has two main functions, that of forming the digestive tract of the organism and that of forming the respiratory tract as well as several glandular organs essential for mineral regulation and immunity. The developing endoderm can be divided in to four sections. The most posterior segment is the first to have migrated through the primitive streak and forms the hindgut which includes the large intestine. The third region forms the midgut and includes the small intestine. The second region forms the dorsal foregut and includes the esophagus and stomach as well as the pharyngeal pouches. The first region forms the ventral foregut which includes the liver and pancreas. The endoderm depends on crosstalk with surrounding mesoderm and ectoderm to properly develop (Wells and Melton, 1999).

The question of how a population of cells can differentiate from multipotent precursors to functional and fully fated tissue is central to developmental biology. Endoderm at its' earliest stage is a single cell-layer thick and accounts for just 500 cells in a mouse embryo; however, these cells will eventually contribute to many different structures such as esophagus, lung,

stomach, intestine, thymus, parathyroid, thyroid, pancreas, and liver and will entail significantly more than 500 cells (Grapin-Botton and Melton, 2000). Development of the thymus and the parathyroid from third pharyngeal pouch endoderm is one example of fate change from multipotent endoderm to fated organs with very different function and morphology. In this thesis, I will address how 'uniform' endoderm differentiates into regionalized and fated organs utilizing the system of third pharyngeal pouch development (Fig. 1.1).

The pharyngeal region encompasses several essential structures.

Pharyngeal pouches are endodermal outpockets that develop between brachial arches. These pouches contribute to structure via musculature and form several organs within mammals. Early chordates and fish have six pharyngeal pouches; however, in mammals and birds the lowest pouches are vestigial or absent. In mice and humans the first four pouches have been well characterized. The first pharyngeal pouch contributes to the tubotympanic recess of the ear (Mallo et al., 1996). The second pharyngeal pouch forms the palatine tonsils in humans and has no known function in mice (Grevellac and Tucker, 2010). The third pharyngeal pouch forms the thymus and parathyroid in mice and humans (Manley and Capecchi, 1995; Gordon et al., 2001). Additional parathyroid forms from the fourth pharyngeal pouch in humans. The ultimobranchial bodies, which contribute to the thyroid, are formed from the fourth pharyngeal pouch in mice and the fifth pharyngeal pouch in humans (Hilfer et al., 1984; Merida-Velasco et al., 1989). The follicular cells of the thyroid come from the thyroid diverticulum found at the base of the pharynx (Missero et al., 1998). Pharyngeal pouches develop both temporally and spatially and contributions from endoderm and surrounding neural crest mesenchyme are both important for normal development.

Many signals and genes are essential to pharyngeal development.

At E7.5 in mice all endoderm is a single sheet of cells (Wells, 1999). At this stage retinoic acid signaling is important for posterior pharyngeal pouch development and is critical for giving anterior – posterior identity (Bayha et al., 2009). Mice deficient in *retinaldehyde dehydrogenase 2* (*RALDH2*) are embryonic lethal between E9.5 and E10.5 and have severe defects in trunk, hindbrain, and heart formation (Niederreither et al., 1999; Niederreither et al., 2000; Niederreither et al., 2001). Further work with *RALDH2* mutants, which lack the ability to make retinoic acid, shows that most of the *RALDH2* mutant phenotype can be rescued by supplementation of retinoic acid between E7.5 and E10.5. The upper arches and the first pharyngeal pouch are rescued (Niederreither et al., 2002). However, even with supplemented retinoic acid the second through fourth pouches fail to form properly. Ectopic thymi are found at low prevalence in rescued *RALDH2* mutants but parathyroids are never found (Niederreither et al., 2003). Furthermore, even in the retinoic acid rescue of *RALDH2* embryos *Hoxa1*, *Hoxb1*, and *Fgf8* levels were down regulated. The authors conclude that the posterior pharyngeal pouches are highly sensitive to retinoic acid signaling and that *RALDH2* in mesoderm adjacent to posterior pouches produces high retinoic acid volumes in very specific locations to pattern the posterior pharyngeal arches and pouches (Niederreither et al., 2003). Treatment of mouse embryos with a panretinoic acid receptor antagonist results in loss of the third and fourth pharyngeal pouches (Wendling et al., 2000). Further evidence for retinoic acid providing anterior – posterior identity comes from work in chicken ectopically expressing retinoic acid in the most anterior brachial arches. When retinoic acid soaked beads were implanted in anterior brachial arch, thyroid marker *Nkx2.1* was repressed and these arches expressed posterior identity genes such as Hox genes instead (Bayha et al., 2009).

At E8.5 *Tbx1* is expressed in pharyngeal endoderm and an endoderm specific deletion of *Tbx1* mimics the full mutant phenotype of *Tbx1*. *Tbx1* is a transcription factor and not a mesenchymal signal; however, *Tbx1* is downstream of *Sonic hedgehog* (*Shh*) and upstream of *Fgf8* and *Fgf3* putting it in the middle of several mesenchymal signals. (Arnold et al., 2005). *Tbx1* expression in endoderm is required for survival of pharyngeal pouches and mice that are *Tbx1* null or have a deletion of endodermal *Tbx1* lack both thymus and parathyroid due to absence of pouch endoderm (Jerome and Papaioannou, 2001; Arnold et al., 2006; Zhang et al., 2006). *Tbx1* heterozygous mice have an ectopic parathyroid and mice with *Tbx1* over expression have either an ectopic or missing parathyroids, depending on dosage (Merscher et al., 2001; Liao et al., 2004). Incorrect *Tbx1* dosage is also associated with migration failure of the thymus and parathyroids (Liao et al., 2004). *Tbx1* may work with *Crkl* in regulation of retinoic acid signaling. Mice heterozygous for both *Tbx1* and *Crkl* had increased levels of retinoic acid in the pharyngeal regions indicating an inability to metabolize retinoic acid and had anterior ectopic expression of retinoic acid target genes. These mice also were aparathyroid with high prevalence and had hypoplastic ectopic thymi (Guris et al., 2006). Work with *Ripply3* deficient mice suggests that *Tbx1* uses *Ripply3* to regulate (and restrict) *Pax9* within the pharyngeal pouch (Okubo et al., 2011).

At E9.5 *Fgf3* and *Fgf8* are found in pharyngeal endoderm and *Fgf10* is found in mesenchyme adjacent to pharyngeal endoderm. *Fgf3* and *Fgf8* are down regulated in the absence of *Tbx1* and heterozygous mutant analysis has shown that they are epistatically linked. While *Fgf10* was activated by *Tbx1* in vitro, double heterozygous mutants did not confirm this interaction in vivo and suggest functional redundancy among FGFs (Aggarwal et al., 2006). Work with overexpression of *Shh* in lung has shown a reduction in *Fgf10* in the

presence of high levels of *Shh* (Bellusci et al., 1997). *Fgf7* and *Fgf10* are expressed in mesenchyme surrounding the thymus and have been shown to interact with *FgfR2-IIIb* to promote thymus growth and TEC differentiation (Revest et al., 2001). *Fgf4* and *Fgf16* are also expressed in pharyngeal endoderm; however, their function there is not yet known (Niswander et al., 1992; Wright et al., 2003). In zebrafish *Fgf3* and *Fgf8* segment the pharyngeal endoderm into pouches. *Fgf8* morpholinos have variable phenotypes and some even had extra pouches that turned into extra cartilage. (Crump et al., 2004). *Fgf8* mouse mutants have defects with pharyngeal arches, the third and fourth pharyngeal pouches are small and difficult to find and the thymus and parathyroids are hypoplastic. *Fgf8* is necessary for neural crest cell migration and survival in these mutants; however, it also is necessary for proper segmentation of the pharyngeal pouches: probably because of the absent pharyngeal arches (Abu-Issa et al., 2002). *Fgf8* is found in both endoderm and ectoderm; however, it serves different roles in each tissue. Ectodermal *Fgf8* is required for formation of fourth pharyngeal arch artery and deleting *Fgf8* only in ectoderm results in the many vascular defects seen in *Fgf8* null mice whereas mutants with deletion of both ectodermal and endodermal *Fgf8* in the third and fourth pharyngeal pouches had defects in thymus and parathyroid as well as aortic valve (Macatee et al., 2003).

Bmp4 is also a prominent player in the pharyngeal region. *Bmp4* is localized to the ventral region of the third pharyngeal pouch by E10.5 and is still present at E11.5 (Patel et al., 2006). In early thymus development, Bmp4 signaling to mesenchyme is required for thymic capsule formation and separation of thymus and parathyroid (Gordon et al., 2010). In later thymus development *Bmp4* from both TEC and neural crest mesenchyme are required for thymus survival, and a smaller primordium with a large lumen is found in the absence of *Bmp4* (Bleul and Boehm, 2005; Gordon et al., 2010).

Wnt signaling is often found to work in concert with Bmps and Fgfs and is found in the pharyngeal region during development. While it is known that T-cells and TEC produce Wnt glycoproteins and that TEC are sensitive to precise regulation of Wnt signaling at later stages, little is known about Wnt in early third pharyngeal embryonic development (Balciunaite et al., 2002; Pongracz et al., 2006; Zuklys et al., 2009). There is some evidence that Wnt-β-catenin signaling is involved in first pharyngeal arch development as well as cardiac outflow tract (Brault et al., 2001). Mesenchymal inactivation of *β-catenin* resulted in hypoplastic ectopic thymus, ectopic parathyroid, and increase in *Tbx1, Gcm2,* and *Fgf8.* Conversely, overexpression of *β-catenin* resulted in lowered *Tbx1* and *Gcm2* expression (Huh and Ornitz, 2010). Additional analysis of $Ctnnb1^{Dermo1\text{-}Cre}$ embryos by members of my lab indicates that the entire embryo is smaller than wild type and that the thymus is not hypoplastic in comparison to body size (Julie Gordon). Furthermore, 3-D reconstruction of thymus and parathyroid suggests that the ratio of thymus to parathyroid within these mutants was normal (personal observation).

Sonic hedgehog (*Shh*) is also essential to pharyngeal pouch development although not required for initial pharyngeal region patterning (Chiang et al., 1996). *Shh* is a secreted glycoprotein that acts as a morphogen and is capable of travelling between 80 and 300 uM from its source (Gritli-Linde et al., 2001). *Shh* and Shh signaling, as indicated by *Patched* expression, are higher in anterior pharyngeal pouches. In the absence of *Shh*, *Fgf8* and *Pax1* expression is increased in the second pouch and first pouch remnant at E10.5 indicating a role for *Shh* in negative regulation of *Fgf8* and *Pax1* to maintain identity of the anterior pouches. Furthermore in the absence of *Shh*, the parathyroid is absent and the thymus covers all present third pouch endoderm (Moore-Scott and Manley, 2005). Further support for Shh signaling having different roles in the anterior and posterior pouch endoderm comes from work in chicken where late

inhibition of Shh signaling via bead implant resulted in an ectopic region of *Gcm2* expression in the first and second pharyngeal pouches (Grevellec et al., 2011).

Third pouch development requires the proper temporal and spatial expression of multiple genes and pathways.

While endodermal in origin, interactions between endoderm, mesenchyme, and ectoderm are necessary for proper thymus and parathyroid formation and mutant phenotypes cover defects from multiple tissue types. These mutants can be divided into groups by failure of initial pouch patterning, failed signaling between endoderm and surrounding tissues, and delayed or failed migration. One group of mutants encompasses defects in patterning of pharyngeal endoderm. *Hoxa3*, *Pax1*, *Pax9*, *Eya1*, and *Six1/4* are all necessary for proper establishment of the third pharyngeal pouch (Manley and Capecchi, 1995; Wallin et al., 1996; Su et al., 2001; Hetzer-Egger et al., 2002; Xu et al., 2002; Zou et al., 2006). Deletion of any of these genes results in hypoplastic or absent parathyroid and thymus and some of these mutants also have delayed or failed separation from pharynx. Another type of patterning failure involves improper interactions with surrounding tissues. *Fgf7/10*, *Splotch*, *Shh*, and *Bmp2/4* are all necessary for proper interactions between pouch endoderm and surrounding mesenchyme which is also required for normal development (Revest et al., 2001; Bleul and Boehm, 2005; Moore-Scott and Manley, 2005; Griffith et al., 2009). *Fgf7/10* is required for proliferation of the thymus in late development and may have currently unknown earlier roles and *Splotch*, *Shh*, and *Bmp2/4* are all involved in patterning and separation of thymus and parathyroid. A third group of mutants involves delayed detachment or failed migration of thymus and parathyroid. *Frs2α*, an Fgf docking protein, as well as *Hoxa3* from neural crest cells are required for normal separation from

the pharynx while *ephrin β2* and Bmp4 signaling from neural crest or endoderm are involved in migration (Kameda et al., 2009; Chen et al., 2010; Foster et al., 2010; Gordon et al., 2010).

Neural crest plays a critical role in thymus and parathyroid development.

Neural crest cells are transient, migratory, pluripotent cells that contribute to neurons, glia, melanocytes, endocrine cells, and mesenchyme essential to development of several organs including thymus, parathyroid, and heart (Le Douarin and Kalcheim, 1999; Conway et al., 2000; Epstein et al., 2000; Jiang et al., 2000; Le Douarin et al., 2004; Griffith et al., 2009). The third pharyngeal pouch. is surrounded by neural crest mesenchyme from E9.5 onward (Le Livre and Le Douarin, 1975; Jiang et al., 2000) and these cells contribute to the capsule surrounding the thymus. There has been much interest in the contributions of neural crest mesenchyme to third pouch development. Neural crest contribution to the pharyngeal region happens after establishment of pharyngeal patterning, as initial patterning is normal when neural crest cells are ablated before migration in chickens (Vetch et al., 1999). Regardless of initial patterning, neural crest cells participate in development of the pharyngeal region as neural crest ablation in chick results in a hypoplastic thymus, parathyroid, and thyroid (Bockman and Kirby, 1984; Bockman and Kirby, 1989). Removal of the neural crest mesenchyme thymic capsule after E12.5 results in arrested thymus development (Auerbach, 1960; Jenkinson et al., 2003). Genetic analysis further confirms neural crest's role in thymus development as mice deficient for *PDGFrα,* which is expressed neural crest mesenchyme, have a hypoplastic thymus and a reduction in the proliferation of TEC (Jenkinson et al., 2007). Signals from neural crest mesenchyme are important for thymus proliferation and maturation. *Fgf7/10* produced in neural crest mesenchyme has been shown to be involved in proliferation of the thymus (Ohuchi et al., 2000; Revest et al., 2001), and *Bmp4,* which is found in both neural crest mesenchyme and pouch

endoderm, has been shown to promote TEC development (Bluel and Boehm, 2005). Most recently work with *Splotch* mice has found an early role for neural crest mesenchyme in third pharyngeal pouch patterning. *Splotch* mice are deficient for *Pax3* which is required for the differentiation, proliferation, and migration of neural crest cells (Conway et al., 2000; Epstein et al., 2000; Pani et al., 2002). In the absence of neural crest mesenchyme, thymus fated tissue increases while parathyroid fated tissue decreases and overall pouch size stays the same indicating a signal (or signals) from neural crest mesenchyme in establishing the boundary between thymus and parathyroid (Griffith et al., 2009).

Understanding the molecular mechanisms that regulate third pouch differentiation and morphogenesis.

Recent work from the Manley lab and our collaborators has attempted to unravel the complex pathway responsible for pharyngeal pouch patterning and organ morphogenesis. The earliest known markers of thymus and parathyroid are *Foxn1* and *Gcm2*. It was found that *Foxn1* and *Gcm2* are organ specific by E10.5 for *Gcm2* within parathyroid and by E11.25 for *Foxn1* within thymus and that at this time thymus and parathyroid were morphologically indistinguishable (Gordon et al., 2001). Further work showed that thymus and parathyroid separate from ectodermal cleft and pharynx by apoptosis around E11.75, that ectoderm does not contribute to third pouch by lineage study, and that transplanted third pouch endoderm was sufficient to form thymus at the kidney capsule without the contribution of pharyngeal mesenchyme or ectoderm (Gordon et al., 2004). Work with *Shh* was particularly interesting to pouch patterning because in the absence of *Shh, Foxn1* extends throughout third pouch endoderm and in to the pharynx while parathyroid marker *Gcm2* is absent. Based on these findings a *Shh* → *Gcm2* regulatory pathway for parathyroid development was proposed (Moore-Scott and

Manley, 2005). Further work with *Gcm2* showed that *Gcm2* was not required for initial parathyroid patterning but instead was required for differentiation and survival of the parathyroid. Because *Tbx1* expression was normal in *Gcm2* null embryos a *Shh* → *Tbx1* → *Gcm2* pathway was proposed (Liu et al., 2007). Work with *Shh* also suggested that *Bmp4* and *Shh* might form opposing gradients within the third pouch (Moore-Scott and Manley, 2005) and this possibility was investigated by looking more closely at *Bmp4* expression at early stages and in *Bmp4* mutants (Patel et al., 2006; Gordon et al., 2010). It was found that Bmp4 signaling to mesenchyme is required for thymic capsule formation and separation of thymus and parathyroid but no direct link between *Foxn1* and *Bmp4* was found (Gordon et al., 2010). Finally, recent work used a text and database screening process to identify possible candidates for early *Foxn1* independent thymus markers. *Isl1* and *Foxg1* were confirmed to be early thymus markers by *in situ* hybridization and their roles in thymus development are still being investigated (Wei and Condie, in press; Wei and Condie, in preparation). My work continues the goals of earlier investigations, using genetic analysis to determine how known genes in and around the third pouch contribute to thymus and parathyroid fate and to investigate the mechanism of separation of third pouch from pharynx and surface ectoderm.

Figures and Figure Legends

Figure 1.1 reprinted with permission from Blackburn and Manley 2004

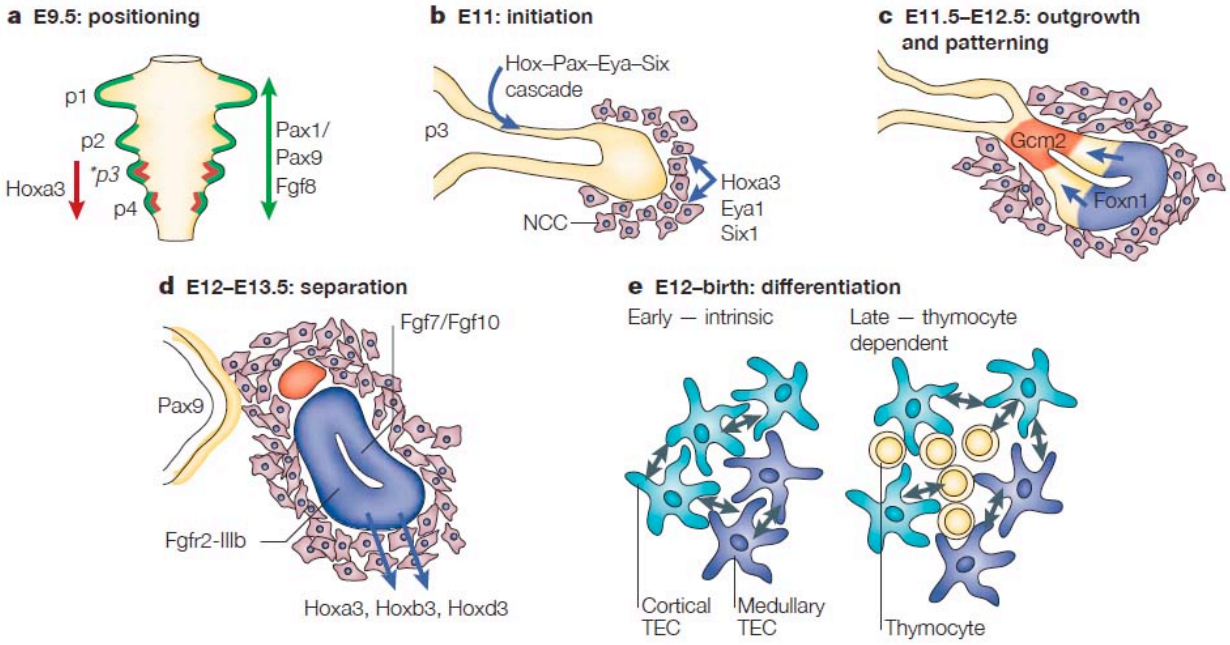

Figure 1.1: Early patterning and morphogenesis of third pharyngeal pouch and its derivatives.

A. Early third pouch endoderm is patterned by Fgf8 and given positional information by Hox genes and Pax genes.
B. The Hox-Eya-Six-Pax transcription factor cascade establishes pouch fate by an as of yet unknown downstream target.
C. After initial fates are established, pouch endoderm and neural crest mesenchyme act to continue patterning the third pharyngeal pouch into thymus and parathyroid.
D. Thymus and parathyroid separate from pharynx, surface ectoderm and each other. Current evidence suggests that signals from neural crest mesenchyme play a role in migration.
E. Foxn1 is required for TEC crosstalk.

References

Abu-Issa, R., G. Smyth, et al. (2002). "Fgf8 is required for pharyngeal arch and cardiovascular development in the mouse." Development 129(19): 4613-4625.

Aggarwal, V. S., J. Liao, et al. (2006). "Dissection of Tbx1 and Fgf interactions in mouse models of 22q11DS suggests functional redundancy." Human molecular genetics 15(21): 3219-3228.

Arnold, J. S., U. Werling, et al. (2006). "Inactivation of Tbx1 in the pharyngeal endoderm results in 22q11DS malformations." Development 133(5): 977-987.

Auerbach, R. (1960). "Morphogenetic interactions in the development of the mouse thymus gland." Developmental biology 2: 271-284.

Balciunaite, G., M. P. Keller, et al. (2002). "Wnt glycoproteins regulate the expression of FoxN1, the gene defective in nude mice." Nature immunology 3(11): 1102-1108.

Bayha, E., M. C. J√ ∏rgensen, et al. (2009). "Retinoic Acid Signaling Organizes Endodermal Organ Specification along the Entire Antero-Posterior Axis." PLoS ONE 4(6): e5845.

Bellusci, S., J. Grindley, et al. (1997). "Fibroblast growth factor 10 (FGF10) and branching morphogenesis in the embryonic mouse lung." Development 124(23): 4867-4878.

Blackburn, C. C. and N. R. Manley (2004). "Developing a new paradigm for thymus organogenesis." Nature reviews. Immunology 4(4): 278-289.

Bleul, C. C. and T. Boehm (2005). "BMP Signaling Is Required for Normal Thymus Development." The Journal of Immunology 175(8): 5213-5221.

Bockman, D. and M. Kirby (1984). "Dependence of thymus development on derivatives of the neural crest." Science 223(4635): 498-500.

Bockman, D. and M. L. Kirby (1989). "Neural crest function in thymus development." Immunol Ser. 45: 451-467.

Brault, V., R. Moore, et al. (2001). "Inactivation of the (Œ≤)-catenin gene by Wnt1-Cre-mediated deletion results in dramatic brain malformation and failure of craniofacial development." Development 128(8): 1253-1264.

Chen, L., P. Zhao, et al. (2010). "Mouse and zebrafish Hoxa3 orthologues have nonequivalent in vivo protein function." Proceedings of the National Academy of Sciences 107(23): 10555-10560.

Chiang, C., Y. Litingtung, et al. (1996). "Cyclopia and defective axial patterning in mice lacking Sonic hedgehog gene function." Nature 383(6599): 407-413.

Conway, S. J., D. J. Henderson, et al. (1997). "Development of a lethal congenital heart defect in the splotch (Pax3) mutant mouse." Cardiovascular Research 36(2): 163-173.

Conway, S. J., J. Bundy, et al. (2000). "Decreased neural crest stem cell expansion is responsible for the conotruncal heart defects within the Splotch (Sp2H)/Pax3 mouse mutant." Cardiovascular Research 47(2): 314-328.

Crump, J. G., L. Maves, et al. (2004). "An essential role for Fgfs in endodermal pouch formation influences later craniofacial skeletal patterning." Development 131(22): 5703-5716.

Danielian, P. S., D. Muccino, et al. (1998). "Modification of gene activity in mouse embryos in utero by a tamoxifen-inducible form of Cre recombinase." Current Biology 8(24): 1323-S1322.

Epstein, J. A., J. Li, et al. (2000). "Migration of cardiac neural crest cells in Splotch embryos." Development 127(9): 1869-1878.

Foster, K., J. Sheridan, et al. (2008). "Contribution of Neural Crest-Derived Cells in the Embryonic and Adult Thymus." The Journal of Immunology 180(5): 3183-3189.

Foster, K. E., J. Gordon, et al. (2010). "EphB‚Äìephrin-B2 interactions are required for thymus migration during organogenesis." Proceedings of the National Academy of Sciences 107(30): 13414-13419.

Franz, T. (1989). "Persistent truncus arteriosus in the Splotch mutant mouse." Anat Embryol (Berl). 180(5): 457-464.

Garg, V., C. Yamagishi, et al. (2001). "Tbx1, a DiGeorge syndrome candidate gene, is regulated by sonic hedgehog during pharyngeal arch development." Developmental biology 235(1): 62-73.

Gordon, J., A. R. Bennett, et al. (2001). "Gcm2 and Foxn1 mark early parathyroid- and thymus-specific domains in the developing third pharyngeal pouch." Mechanisms of Development 103(1-2): 141-143.

Gordon, J., V. A. Wilson, et al. (2004). "Functional evidence for a single endodermal origin for the thymic epithelium." Nature immunology 5(5): 546-553.

Gordon, J., S. R. Patel, et al. (2010). "Evidence for an early role for BMP4 signaling in thymus and parathyroid morphogenesis." Developmental biology 339(1): 141-154.

Gordon, J. and N. R. Manley (2011). "Mechanisms of thymus organogenesis and morphogenesis." Development 138(18): 3865-3878.

Grapin-Botton, A. and D. A. Melton (2000). "Endoderm development: from patterning to organogenesis." Trends in Genetics 16(3): 124-130.

Grevellec, A. and A. S. Tucker (2010). "The pharyngeal pouches and clefts: Development, evolution, structure and derivatives." Seminars in Cell & Developmental Biology 21(3): 325-332.

Grevellec, A., A. Graham, et al. (2011). "Shh signalling restricts the expression of Gcm2 and controls the position of the developing parathyroids." Developmental biology 353(2): 194-205.

Griffith, A. V., K. Cardenas, et al. (2009). "Increased thymus- and decreased parathyroid-fated organ domains in Splotch mutant embryos." Developmental biology 327(1): 216-227.

Gritli-Linde, A., P. Lewis, et al. (2001). "The Whereabouts of a Morphogen: Direct Evidence for Short- and Graded Long-Range Activity of Hedgehog Signaling Peptides." Developmental biology 236(2): 364-386.

Guris, D. L., G. Duester, et al. (2006). "Dose-dependent interaction of Tbx1 and Crkl and locally aberrant RA signaling in a model of del22q11 syndrome." Developmental cell 10(1): 81-92.

Hetzer-Egger, C., M. Schorpp, et al. (2002). "Thymopoiesis requires Pax9 function in thymic epithelial cells." European Journal of Immunology 32(4): 1175-1181.

Hilfer, S. R. and J. W. Brown (1984). "The development of pharyngeal endocrine organs in mouse and chick embryos." Scan Electron Microsc. (Pt 4): 2009-2022.

Huh, S. H. and D. M. Ornitz (2010). "Beta-catenin deficiency causes DiGeorge syndrome-like phenotypes through regulation of Tbx1." Development 137(7): 1137-1147.

Itoi, M., N. Tsukamoto, et al. (2007). "Mesenchymal cells are required for functional development of thymic epithelial cells." International Immunology 19(8): 953-964.

Jenkinson, W. E., E. J. Jenkinson, et al. (2003). "Differential Requirement for Mesenchyme in the Proliferation and Maturation of Thymic Epithelial Progenitors." The Journal of Experimental Medicine 198(2): 325-332.

Jenkinson, W. E., S. W. Rossi, et al. (2007). "PDGFRŒ±-expressing mesenchyme regulates thymus growth and the availability of intrathymic niches." Blood 109(3): 954-960.

Jeong, J., J. Mao, et al. (2004). "Hedgehog signaling in the neural crest cells regulates the patterning and growth of facial primordia." Genes & Development 18(8): 937-951.

Jerome, L. A. and V. E. Papaioannou (2001). "DiGeorge syndrome phenotype in mice mutant for the T-box gene, Tbx1." Nat Genet 27(3): 286-291.

Jiang, X., D. H. Rowitch, et al. (2000). "Fate of the mammalian cardiac neural crest." Development 127(8): 1607-1616.

Kameda, Y., M. Ito, et al. (2009). "FRS2α is required for the separation, migration, and survival of pharyngeal-endoderm derived organs including thyroid, ultimobranchial body, parathyroid, and thymus." Developmental Dynamics 238(3): 503-513.

Le Douarin, N. M., S. Creuzet, et al. (2004). "Neural crest cell plasticity and its limits." Development 131(19): 4637-4650.

Le Douarin, N. M. and F. V. Jotereau (1975). "Tracing of cells of the avian thymus through embryonic life in interspecific chimeras." J Exp Med. 142(1): 17-40.

Le Douarin, N. M. and C. Kalcheim (1999). The Neural Crest (Second Edition) (Developmental and Cell Biology Series).

Liao, J., L. Kochilas, et al. (2004). "Full spectrum of malformations in velo-cardio-facial syndrome/DiGeorge syndrome mouse models by altering Tbx1 dosage." Human molecular genetics 13(15): 1577-1585.

Liu, Z., S. Yu, et al. (2007). "Gcm2 is required for the differentiation and survival of parathyroid precursor cells in the parathyroid/thymus primordia." Developmental biology 305(1): 333-346.

Macatee, T. L., B. P. Hammond, et al. (2003). "Ablation of specific expression domains reveals discrete functions of ectoderm- and endoderm-derived FGF8 during cardiovascular and pharyngeal development." Development 130(25): 6361-6374.

Machado, A. F., L. J. Martin, et al. (2001). "Pax3 and the splotch mutations: structure, function, and relationship to teratogenesis, including gene-chemical interactions." Curr Pharm Des. 7(9): 751-785.

Mallo, M. and T. Gridley (1996). "Development of the mammalian ear: coordinate regulation of formation of the tympanic ring and the external acoustic meatus." Development 122(1): 173-179.

Manley, N. R. and B. G. Condie (2010). "Transcriptional Regulation of Thymus Organogenesis and Thymic Epithelial Cell Differentiation." 92: 103-120.

Merida-Velasco, J. A., J. D. Garcia-Garcia, et al. (1989). "Origin of the ultimobranchial body and its colonizing cells in human embryos." Acta Anat (Basel). 136(4): 325-330.

Merscher, S., B. Funke, et al. (2001). "TBX1 Is Responsible for Cardiovascular Defects in Velo-Cardio-Facial/DiGeorge Syndrome." Cell 104(4): 619-629.

Missero, C., G. Cobellis, et al. (1998). "Molecular events involved in differentiation of thyroid follicular cells." Molecular and Cellular Endocrinology 140(1-2): 37-43.

Moore-Scott, B. A. and N. R. Manley (2005). "Differential expression of Sonic hedgehog along the anterior-posterior axis regulates patterning of pharyngeal pouch endoderm and pharyngeal endoderm-derived organs." Developmental biology 278(2): 323-335.

Niederreither, K., V. Subbarayan, et al. (1999). "Embryonic retinoic acid synthesis is essential for early mouse post-implantation development." Nat Genet 21(4): 444-448.

Niederreither, K., J. Vermot, et al. (2000). "Retinoic acid synthesis and hindbrain patterning in the mouse embryo." Development 127(1): 75-85.

Niederreither, K., J. Vermot, et al. (2001). "Embryonic retinoic acid synthesis is essential for heart morphogenesis in the mouse." Development 128(7): 1019-1031.

Niederreither, K., V. r. Fraulob, et al. (2002). "Differential expression of retinoic acid-synthesizing (RALDH) enzymes during fetal development and organ differentiation in the mouse." Mechanisms of Development 110(1-2): 165-171.

Niederreither, K., J. Vermot, et al. (2002). "Retinaldehyde dehydrogenase 2 (RALDH2)-independent patterns of retinoic acid synthesis in the mouse embryo." Proceedings of the National Academy of Sciences 99(25): 16111-16116.

Niederreither, K., J. Vermot, et al. (2003). "The regional pattern of retinoic acid synthesis by RALDH2 is essential for the development of posterior pharyngeal arches and the enteric nervous system." Development 130(11): 2525-2534.

Niswander, L. and G. R. Martin (1992). "Fgf-4 expression during gastrulation, myogenesis, limb and tooth development in the mouse." Development 114(3): 755-768.

Ohnemus, S., B. Ã. Kanzler, et al. (2002). "Aortic arch and pharyngeal phenotype in the absence of BMP-dependent neural crest in the mouse." Mechanisms of Development 119(2): 127-135.

Ohuchi, H., Y. Hori, et al. (2000). "FGF10 Acts as a Major Ligand for FGF Receptor 2 IIIb in Mouse Multi-Organ Development." Biochemical and Biophysical Research Communications 277(3): 643-649.

Okubo, T., A. Kawamura, et al. (2011). "Ripply3, a Tbx1 repressor, is required for development of the pharyngeal apparatus and its derivatives in mice." Development 138(2): 339-348.

Pani, L., M. Horal, et al. (2002). "Rescue of neural tube defects in Pax-3-deficient embryos by p53 loss of function: implications for Pax-3- dependent development and tumorigenesis." Genes & Development 16(6): 676-680.

Patel, S. R., J. Gordon, et al. (2006). "Bmp4 and Noggin expression during early thymus and parathyroid organogenesis." Gene expression patterns : GEP 6(8): 794-799.

Peters, H., A. Neubuser, et al. (1998). "Pax9-deficient mice lack pharyngeal pouch derivatives and teeth and exhibit craniofacial and limb abnormalities." Genes & Development 12(17): 2735-2747.

Pongracz, J. E., S. M. Parnell, et al. (2006). "Overexpression of ICAT highlights a rolefor catenin-mediated canonical Wnt signalling in early T cell development." European Journal of Immunology 36(9): 2376-2383.

Revest, J.-M., R. K. Suniara, et al. (2001). "Development of the Thymus Requires Signaling Through the Fibroblast Growth Factor Receptor R2-IIIb." The Journal of Immunology 167(4): 1954-1961.

Su, D., S. Ellis, et al. (2001). "Hoxa3 and pax1 regulate epithelial cell death and proliferation during thymus and parathyroid organogenesis." Developmental biology 236(2): 316-329.

Veitch, E., J. Begbie, et al. (1999). "Pharyngeal arch patterning in the absence of neural crest." Current Biology 9(24): 1481-1484.

Wallin, J., H. Eibel, et al. (1996). "Pax1 is expressed during development of the thymus epithelium and is required for normal T-cell maturation." Development 122(1): 23-30.

Wei, Q. and B. G. Condie (in preparation). "Foxg1 regulates Foxn1-independent TEC differentiation."

Wei, Q. and B. G. Condie (in press). "Data mining and in situ hybridization screen identify potential transcription regulators of thymus development." PLoS ONE.

Wells, J. M. and D. A. Melton (1999). "Vertebrate endoderm development." Annual Review of Cell and Developmental Biology 15: 393-410.

Wendling, O., C. Dennefeld, et al. (2000). "Retinoid signaling is essential for patterning the endoderm of the third and fourth pharyngeal arches." Development 127(8): 1553-1562.

Wright, T. J., E. P. Hatch, et al. (2003). "Expression of mouse fibroblast growth factor and fibroblast growth factor receptor genes during early inner ear development." Developmental Dynamics 228(2): 267-272.

Xu, P.-X., W. Zheng, et al. (2002). "Eya1 is required for the morphogenesis of mammalian thymus, parathyroid and thyroid." Development 129(13): 3033-3044.

Zhang, Z., T. Huynh, et al. (2006). "Mesodermal expression of Tbx1 is necessary and sufficient for pharyngeal arch and cardiac outflow tract development." Development 133(18): 3587-3595.

Zou, D., D. Silvius, et al. (2006). "Patterning of the third pharyngeal pouch into thymus/parathyroid by Six and Eya1." Developmental biology 293(2): 499-512.

Zuklys, S., J. Gill, et al. (2009). "Stabilized beta-catenin in thymic epithelial cells blocks thymus development and function." Journal of immunology 182(5): 2997-3007.

CHAPTER 2

PROXIMITY TO SONIC HEDGEHOG SIGNALING INFLUENCES THYMUS AND PARATHYROID DOMAIN PATTERNING.

To be submitted to *Development*. Virginia Bain, Julie Gordon, Michelle Dookwah, Isaias Ramos, and Nancy R. Manley

Abstract:

The thymus and parathyroid both develop from third pharyngeal pouch endoderm. Previous studies show that deleting *Sonic hedgehog* (*Shh*) results in a smaller primordium that is aparathyroid and has the thymus domain shifted toward the pharynx. Similarly, absence of most neural crest mesenchyme after deleting *Pax3* (Splotch mice) causes a domain shift towards a larger thymus and smaller parathyroid within a normal sized pouch. As Shh signaling is active in both the dorsal pouch endoderm and neighboring neural crest mesenchyme, these data raise the question of which target of Shh signaling is the basis for the patterning defects seen in the Shh mutants. We have taken a genetic approach to determine how Shh signaling affects pouch patterning by ectopically activating or deleting the Shh signal transducer *Smoothened* (*Smo*) in either pharyngeal pouch endoderm or neural crest mesenchyme. We find that *Foxn1* and *Gcm2* domain locations and relative sizes within the pouch change in response to deleting or activating Shh signaling. Effects were seen when Shh signaling was manipulated in either neural crest or the endoderm, indicating that Shh signaling affects pouch pattern by both directly acting on the pouch endoderm, and indirectly via neural crest. These results suggest that Shh signaling to both the pouch endoderm and neural crest cells affects thymus and parathyroid organ domain patterning, and that the early third pouch uses precise levels of Sonic hedgehog signaling to restrict the thymus and parathyroid domain borders, While several known Shh downstream targets are present in this region, none of their expression patterns were affected, indicating that these effects of Shh may act via a different mechanism.

Introduction

In mice, thymus and parathyroid organogenesis begin at E9.5 when the third pharyngeal pouch is formed. Current data suggests that formation of the third pharyngeal pouch is required for thymus and parathyroid formation as all known mutants in which the third pouch fails to form lack a thymus and parathyroid (Blackburn and Manley, 2004). The parathyroid marker *Gcm2* is first detectable at E9.5 in the dorsal/anterior endoderm of the third pharyngeal pouch (Gordon et al., 2001). At E10.5 the *Hoxa3-Pax1/9-Eya1-Six1/4* pathway is necessary for early patterning of the third pharyngeal pouch in order to establish a thymus and parathyroid (Manley and Condie, 2010). By E10.5 *Gcm2* is restricted to the dorsal and anterior part of the third pouch which forms the parathyroid (Gordon et al., 2001). The thymus and parathyroid rudiments form at E11 when third pouch endoderm begins to proliferate to form an organ rudiment. By E11.5 the thymus marker *Foxn1* is strongly expressed in the thymus domain of the third pouch (Gordon et al., 2001), and most or all of the cells in the primordium have acquired either a parathyroid or thymus fate.

Gcm2 is currently the earliest known parathyroid specific marker (Gordon et al., 2001). While *Gcm2* is required for the survival of parathyroid, fate commitment is more likely caused by *Tbx1*. A *Gcm2* negative parathyroid domain is found in *Gcm2* null mice that contains *Tbx1, CasR* and *CCL21* mRNA at E10.5; this domain survives until E12 when it undergoes coordinated apoptosis (Liu et al., 2007). The parathyroid is also sensitive to changes in *Tbx1* dosage. *Tbx1* expression in endoderm is required for survival of pharyngeal pouches and mice that are *Tbx1* null or have a deletion of endodermal *Tbx1* lack both thymus and parathyroid due to absence of pouch endoderm (Jerome and Papaioannou 2001, Arnold et al., 2006; Zhang et al., 2006). *Tbx1* heterozygous mice have an ectopic parathyroid and mice with *Tbx1* over expression

have either an ectopic or missing parathyroids, depending on dosage (Merscher et al., 2001; Liao et al., 2004). Incorrect *Tbx1* dosage is also associated with migration failure of the thymus and parathyroids (Liao et al., 2004).

Thymus and parathyroid organogenesis is known to depend on epithelial-mesenchymal interactions between pouch endoderm and neural crest cells. Neural crest cells form the mesenchymal capsule that surrounds the thymus and is required for proliferation of the organ rudiment (Revest et al., 2001; Itoi et al., 2007; Foster et al., 2008). Signaling between the thymic capsule and the thymic epithelium are also essential for Fgf10 expression (Ohuchi 2000), which is required for TEC proliferation after E12.5 (Revest et al., 2001). *Fgf8* is expressed in pharyngeal endoderm and ectoderm and is also important for survival of neural crest cells. Hypomorphic *Fgf8* embryos have increased cell death of neural crest cells in regions next to lowered *Fgf8* expression, in addition to a reduction in third and fourth pouch size (Abu-Issa et al., 2002). The thymic capsule may also be involved in thymus migration. Several studies have shown failed migration when Bmp4 signaling is blocked in neural crest (Ohnemus et al., 2002; Wang et al., 2006; Gordon et al. 2010). More support for thymic capsule mediated migration comes from the neural crest deletion of Ephrin β2 in which the thymus and parathyroids form and separate from the pharynx, but fail to migrate (Foster et al., 2010).

Analysis of Splotch mice has also identified a role for neural crest cells in the allocation of thymus and parathyroid fates within the developing 3rd pouch-derived organ rudiment. Splotch mice, which have a point mutation in *Pax3*, are neural crest cell deficient as *Pax3* is essential to the survival, proliferation, and differentiation of neural crest cells (Conway et al., 2000; Epstein et al., 2000; Pani et al., 2002). Although initial work with Splotch mice suggested that the thymus was hypoplastic or aplastic (Franz et al., 1989; Conway et al., 1997; Machado et

al., 2001), recent work has shown that the thymus in Splotch mice is instead large but ectopic (Griffith et al., 2009). This large ectopic thymus is accompanied by a hypoplastic parathyroid, and these changes in size can be traced back to a domain boundary shift within the developing third pouch (Griffith et al., 2009). This result showed that signals from neural crest cells to the developing endodermal primordia determine the location of the border between thymus and parathyroid domains, and thus final organ size.

Sonic hedgehog is also involved in establishing thymus and parathyroid pouch fate. In the absence of Sonic hedgehog there is no parathyroid domain and the Foxn1 domain expands throughout the pouch and into the pharynx (Moore-Scott and Manley, 2005). While recent work in zebrafish, chicken, and mouse suggests that differential Shh signaling throughout the pharyngeal region is required to place the Gcm2 domain in a location where there is little or no Shh signaling (Grevellec et al., 2011), our data suggest that in mice Shh signaling is present in the dorsal third pouch is required for parathyroid fate (Moore-Scott and Manley, 2005). Evidence of Shh signaling in the form of increased *Patched* expression is found in a small domain of pouch endoderm proximal to the pharynx as well as in the adjacent neural crest mesenchyme (Moore-Scott and Manley, 2005). Based on this study, we proposed that a Shh-Tbx1-Gcm2 regulatory pathway is responsible for establishing initial parathyroid development (Liu et al., 2007). Because Patched expression is not found in most of the pouch and because Foxn1 takes over the entire third pouch in the absence of Shh, and especially in light of the Splotch findings, it is possible that Shh signaling is acting in part through neural crest mesenchyme to regulate domain boundaries.

To address the respective contributions of Shh signaling to neural crest and pouch endoderm in 3rd pouch patterning and organ development, we used tissue specific Cre driver

strains to selectively delete or ectopically activate Shh signaling in neural crest mesenchyme or pharyngeal endoderm by manipulating the expression or activity of *Smoothened*. Loss of Shh signaling from neural crest mesenchyme did not recapitulate the full Splotch phenotype although there were some similarities. Our data suggest that while Shh signaling to neural crest mesenchyme is not sufficient to cause the domain border shift seen in Splotch mice, it does contribute to border placement. Furthermore, loss of Shh signaling from pouch endoderm did not phenocopy the absent Gcm2 domain observed in Shh null mice, indicating that Shh signaling to pouch endoderm alone is not necessary or sufficient for parathyroid organogenesis. Our results show that Shh signaling to both neural crest and endoderm is required for parathyroid fate specification and for proper organ domain placement during thymus and parathyroid organogenesis. We further show that the establishment of the border between thymus and parathyroid fate normally involves a transient stage of cell mixing between the two organ fates, that is gradually resolved to non-overlapping organ domains.

Materials and Methods

Mice:

Smo^{fx}, Rosa26SmoM2, Wnt1Cre, and $Foxa2Cre^{ERT2}$ mice were purchased from The Jackson Laboratory (Bar Harbor, ME) and crossed to generate Wnt1Cre;Smo^{fx}, $Foxa2Cre^{ERT2}$;Smo^{fx}, Wnt1Cre;Rosa26SmoM2 and $Foxa2Cre^{ERT2}$;Rosa26SmoM2 embryos and littermate controls.

Matings were monitored on a daily basis and the day of the vaginal plug was designated embryonic day 0.5. Embryos were also staged by somite number and morphological cues such as eye and limb development. Genotyping was performed on yolk sac DNA using previously

described primers (Long et al., 2001; Jeong et al., 2004). All experiments were carried out with the approval of the UGA Committee for Animal Use in Research and Education.

Tissue preparation:

All embryos collected were fixed in 4% PFA and dehydrated. Embryos collected for frozen immunostaining were briefly fixed (20 min (E10.5), 30 min (E11.5-E13.5)), thoroughly washed in PBS (10 2' washes), dehydrated in sucrose (1 hour 5% sucrose, 4 hours 15% sucrose), and embedded in OCT. Sections were cut on a cryostat at 8 μm thickness. Embryos collected for paraffin immunostaining were fixed for 1 hour, thoroughly washed in PBS, dehydrated in an ethanol gradient, permeabilized in xylenes, and embedded in paraffin. Sections for immunostaining were cut on a Leica RM2155 microtome at 8 μm thickness. Embryos collected for *in situ* were kept cold at all steps and RNase free reagents were used. Sections for *in situ* were cut at 12 μm thickness.

Section and whole-mount *In situ hybridization*:

Whole mount and paraffin section *in situ* hybridizations were performed as described (Manley and Capecchi, 1995; Moore-Scott and Manley, 2005), using mutant embryos and littermate controls. Each probe was analyzed on a minimum of 2-3 embryos per stage. Probes for *Pax1* (Manley and Capecchi, 1995), *Fgf8* (Crossley and Martin, 1995), *Ptc1* (Goodrich et al. 1996), *Tbx1* (Chapman et al., 1996), *Gcm2, Foxn1, Bmp4* (Gordon et al., 2001), and *Fgf10* (Belluschi et al., 1997), have been previously described. Probe template was made by PCR using plasmid with primers for T3, T7, and SP6. Probes for single color *in situ* were made using DIG-UTP. FITC-UTP was also used to make a *Foxn1* probe for dual color *in situ*. Single color *in situs* were counterstained with nuclear fast red. Dual color *in situs* were not counterstained. Dual *in situs* were performed as described (Moore-Scott and Manley, 2005) up to the first color

reaction. At this time a protocol by Pringle and Richardson was adapted for the second color reaction utilizing INT-BCIP for the second chromogen.

Immunostaining:

Immunostaining was performed on paraffin embedded or frozen tissue fixed in 4% PFA. Paraffin embedded tissue was washed twice in xylene to remove the paraffin and then briefly washed in 100%, 90%, 70%, and 30% EtOH before being placed in PBS. Paraffin embedded immunostaining required an antigen retrieval step in which tissue was boiled in AR buffer (10mM Na_3Citrate pH6, 0.05% Tween20) for 30 minutes. Slides were allowed to cool to room temperature in the buffer for an additional 20 minutes. Slides were then incubated overnight with primary antibody, 5% donkey serum, and .05% Triton-X in PBS. The next day slides were washed once in PBS and then incubated with secondary antibody in PBS for one hour at room temperature in the dark. Slides were then washed three times in PBS with the middle wash containing DAPI. Slides were mounted with EMS-Fluorogel and coverslipped for visualization. Frozen tissue was processed as described above with the exception of xylene, rehydration and antigen retrieval. Antibodies used were goat anti-Foxn1 (1:200 Santa Cruz G-20), rabbit anti-Gcm2 (1:200 abcam ab64723), rabbit anti-Tbx1 (1:100 abcam ab18530), rabbit anti-Cleaved Caspase-3 (1:200 cell signaling), rat anti-BrdU (1:10, Serotec, OBT0030S), Ikaros (1:100, Santa Cruz, M-20), rat anti-E-Cadherin (1:400 Invitrogen 13-1900), and rabbit anti-Fibronectin (MP Biomedicals 55038). All secondaries were DyLight (Jackson Immunoresearch) dyes: Alexa (Invitrogen) dyes were used as a last resort if DyLight dyes were unavailable.

X-gal staining:

Embryos for X-gal staining were processed as described (Gordon et al., 2001). After staining, whole mount pictures were taken using a Zeiss SteRIO dissecting microscope and then

embryos were processed for paraffin embedding and sectioned on a Leica RM2155 microtome at 10 μm thickness.

Cell counting:

Cell counting was performed manually using serial sections taken on a Zeiss Axioplan using the events feature in AxioVision Rel. 4.8 software.

Three dimensional reconstruction:

3-D reconstructions were made from serial sections using SurfDriver WinSurf 4.3 software.

Results

Tissue specific regulation of Shh signaling using the signal transducer Smoothened.

In order to manipulate Shh signaling in a tissue-specific manner in either the neural crest or pharyngeal endoderm during mouse embryonic development, we chose to target Smoothened (*Smo*), an intracellular signal transducer of Shh signaling. We utilized both a conditional allele and an inducible allele of *Smo* that have been shown to efficiently delete or activate Shh signaling after Cre-mediated recombination. The Smo^{fx} conditional allele has loxp sites surrounding the first coding exon allowing for its inactivation when crossed to a Cre expressing driver strain (Long et al., 2001). R26SmoM2 expresses an inducible dominant active allele of *Smo* after Cre-mediated recombination (Jeong et al., 2004). SmoM2 contains a point mutation in the transmembrane domain which prevents Patched (Ptch) from binding to and inhibiting Smo, resulting in constitutive activation of Shh signaling, in either the presence or absence of Shh itself.

To determine if Shh signaling to neural crest cells regulates organ domain boundaries within the third pharyngeal pouch, we used the Wnt1Cre neural crest specific driver (Danielian

et al., 1998; Jiang et al., 2000) (Fig 1A). When crossed to the Smo^{fx} allele, Wnt1Cre deleted Shh signaling in neural crest cells, as assayed by *Patched* expression (Fig1B). When crossed to the R26SmoM2 allele, Wnt1Cre induced Shh signaling in neural crest mesenchyme (Jeong et al., 2004), increasing Shh signaling in its normal domain, and ectopically activating it around the entire pouch (Fig 1C).

To determine the role of Shh signaling within pouch endoderm, we used the $Foxa2^{CreERT2}$ allele, which is expressed in endoderm, notochord, and floorplate (Park et al., 2008). Injection of tamoxifen at E5.5 resulted in Cre activation throughout the pharyngeal endoderm (Fig 1D). Shh signaling in pouch endoderm was eliminated by crossing $Foxa2^{CreERT2}$ with the Smo^{fx} allele resulting in no Shh signaling in pouch endoderm as assayed by *Ptch* expression (Fig 1E). Ectopically activation was accomplished by crossing $Foxa2^{CreERT2}$with the R26SmoM2 allele, resulting in ectopic Shh signaling throughout the pouch endoderm (Fig 1F).

Initial patterning is normal when Shh signaling is deleted or ectopically activated in neural crest mesenchyme or pouch endoderm.

We assayed *Fgf8, Tbx1, Foxg1*, and *Gcm2* expression in tissue specific null mutants to determine if they resembled the Shh null or Splotch mutant phenotype at these early stages. At E10.5, *Fgf8* is normally expressed in the otic vesicle, the second, third, and fourth pharyngeal pouches, and cleft ectoderm (Fig 2A). Initial *Fgf8* patterning at E9.5 is normal in *Shh* null mice. By E10.5 *Fgf8* is upregulated in the second pouch but still normal in the third and fourth pouches indicating that *Shh* negatively regulates *Fgf8* in the second pouch but not the third or fourth pouches (Moore-Scott and Manley, 2005). Whole mount in situ hybridization showed *Fgf8* expression to be normal in Wnt1Cre;Smo^{fx} and $Foxa2Cre^{ERT2}$;Smo^{fx} embryos at E10.5 (Fig 2B, 2C). *Fgf8* expression was also normal in Wnt1Cre;R26SmoM2 embryos (Fig. 2D). These

results showed that activation or deletion of Shh signaling in neural crest mesenchyme or deletion in pouch endoderm did not alter *Fgf8* expression suggesting that Shh signaling in either cell type was sufficient to rescue the abnormal *Fgf8* expression seen in *Shh* null mice.

Tbx1 expression depends on Shh signaling; *Foxa2* mediated regulation of *Tbx1* decreases starting at E9.5 in pharyngeal endoderm in *Shh* null mice (Yamagishi et al., 2003). *Tbx1* is absent in the pharyngeal endoderm and downregulated in the mesodermal core of pharyngeal arches in *Shh* null embryos at E10.5 (Garg et al., 2001). *Tbx1* expression was present at E10.5 in the prospective parathyroid domain in the dorsal-anterior third pouch, cardiac mesenchyme, pharyngeal arch mesoderm, and the otic vesicle (Fig 2E). Tbx1 expression appeared normal in Wnt1Cre;Smo^{fx} and Foxa2Cre^{ERT2};Smo^{fx} embryos at E10.5 (Fig 2F, 2G). Neither the endodermal deletion nor the neural crest mesenchyme deletion of Shh signaling mimicked the Shh null embryo. Furthermore, consistent with the *Shh* null, deletion of Shh signaling from either neural crest mesenchyme or pouch endoderm does not alter early patterning of the 3rd pouch endoderm by *Fgf8* or *Tbx1*.

Foxg1 is an additional early marker of the prospective thymus domain (Wei and Condie, in press), and is also expressed in the brain where it has been shown to act downstream of Shh signaling (Danesin et al., 2009). *Foxg1* is expressed in the second and third pharyngeal pouches as well as the otic vesicle at early E10.5 (Fig 2H) and is restricted to the ventral third pharyngeal pouch by late E10.5 (Wei and Condie, in press). Foxg1 expression was also comparable to wild type in both Wnt1Cre;Smo^{fx} and Foxa2Cre^{ERT2};Smo^{fx} embryos at E10.5 (Fig 2I, 2J).

Gcm2 is first expressed in the pharyngeal region at E9.5 and is confined to the anterior dorsal region of the third pouch by E10.5 (Gordon et al., 2001). Gcm2 is absent in the Shh null and the Gcm2 domain is reduced in size in Splotch mice (Moore-Scott and Manley, 2005;

Griffith et al., 2009). Gcm2 was expressed in approximately 25% of the wild-type 3rd pouch at E10.5 as assayed by 3-D reconstruction of serial section immunostaining (Fig 2K). The size and location of Gcm2 staining was similar to wild type at E10.5 after deletion of *Smo* in either neural crest or endoderm (Fig 2L, 2M). The percentage of *Gcm2* within the pouch was also comparable to wild type in Wnt1Cre;R26SmoM2 embryos at E10.5, although total pouch size was reduced and the Gcm2 domain was displaced toward the ventral part of the pouch (Fig 2N).

Intermingling between Foxn1- and Gcm2–positive cells at E11-11.5

The 3rd pharyngeal pouch endoderm has two potential fates: thymus or parathyroid. While the parathyroid marker Gcm2 is expressed in the 3rd pharyngeal pouch at E9.5, the earliest defined thymus specific marker, Foxn1, is not detected until E11 (40 somites) in the ventral most regions of the pouch (Gordon et al., 2001). Because understanding precisely how *Foxn1* and *Gcm2* are patterned within the pouch could lead to a better understanding of the mechanism of thymus and parathyroid fate establishment, we examined Foxn1 and Gcm2 expression at the protein level at embryonic stages from first expression of *Foxn1* at E11 (40 somites) to the stage that thymus and parathyroid separate (60 somites).

At 40 somites Foxn1 and Gcm2 were found at ventral and dorsal ends of the pouch respectively. The pouch also contained a central region of cells that did not express Foxn1 or Gcm2 at 40 somites (Fig. 3A). While the two domains were distinct at this stage, regions of 'intermingling' were also found where both Foxn1- and Gcm2-positive cells were present. These regions of intermingling were further classified as Foxn1 positive cells within the normal Gcm2 domain, or Gcm2 positive cells within the normal Foxn1 domain (Fig. 3C, 3D). All cells in the pouch were positive for either Foxn1 or Gcm2 by 44 somites (Fig. 3B). We found that intermingling of Foxn1positive cells within the Gcm2 domain was more common than the

presence of Gcm2 positive cells within the Foxn1 domain, and that intermingling events decreased in frequency from 48 somites onward. The two organ domains were fully distinct by 60 somites (Fig. 3E) (Table 1). At this stage thymus and parathyroid are completely distinct populations of cells with a well-defined border between the two domains.

***Foxn1* expression is altered within the 40 somite pouch when Shh signaling is manipulated in pouch endoderm.**

We hypothesized that Shh signaling to neural crest mesenchyme is responsible for boundary placement between the thymus and the parathyroid, while Shh signaling to pouch endoderm is sufficient for parathyroid fate. In this model the dorsal region of pouch endoderm, which had *Patched* expression in wild type, is required for *Gcm2* expression and inhibits *Foxn1* expression. To test this hypothesis we deleted and ectopically activated Shh signal transducer *Smoothened* in pouch endoderm and examined pouch fate between 40 and 50 somites.

As shown above, the earliest stage when both Foxn1 and Gcm2 are both present within the 3rd pouch is at 40 somites (Fig 4A). Dividing the 40 somite pouch into five regions from ventral-most to dorsal-most, all *Foxn1* positive cells are found in the three ventral most regions of the pouch (regions one to three) with a majority of these cells belonging to regions one and two (Fig 4D). *Gcm2* is found in the three more dorsal regions of the pouch (regions three to five) (Fig 4G). Region 3 is therefore the zone where the two initially intermingle.

Because of the *Shh* null phenotype, we were surprised to find that *Gcm2* is expressed in the absence of endodermal Shh signaling. Similar to controls, Foxn1 was found primarily in regions one and two (Fig 4C, 4F), region three was primarily Gcm2 positive with some intermingling of Foxn1 positive cells, while region four contained only Gcm2 positive cells. Only region five was abnormal in Foxa2Cre^{ERT2};Smo^{fx} embryos. A small patch of Foxn1 positive

cells was found in region five in five out of six pouches examined at 40-41 somites (Fig 3I). Foxn1 positive cells in region five were completely separate from the *Foxn1* cells of regions one and two. This phenotype has some resemblance to the Splotch phenotype, because both phenotypes have multiple regions of Foxn1 expression, including ectopic domains in the dorsal region and into the pharynx (Griffith et al., 2009). Because a *Gcm2* domain was found in the absence of endodermal Shh signaling, we conclude that endodermal Shh signaling is not necessary for initiation of the *Gcm2* domain.

Expression of *Foxn1* remains altered at 48 somites when Shh signaling is manipulated in pouch endoderm.

Although not necessary for *Gcm2* domain initiation, it was possible that Shh signaling to pouch endoderm regulates expansion or maintenance of the *Gcm2* domain at later stages. To test this possibility we examined the primordium at 48 somites. In wild type embryos at E11.5, the *Foxn1* domain covered approximately 72% of the pouch while the *Gcm2* domain covered the remaining 28% (Table 2). Similar to E10.5, the *Gcm2* domain was found in the anterior dorsal region of the pouch. At this stage, *Foxn1* had expanded from E10.5 to include all of the non-parathyroid fated pouch (Fig 5A, 5C, 5E, 5G).

Total cell number within 3rd pouch was comparable between Foxa2Cre^{ERT2};Smo^{fx} embryo and wild type littermate at 48 somites (Fig 5J). While cell numbers of both the *Foxn1* and *Gcm2* positive domains were normal, organization was abnormal. Similar to the 40 somite phenotype, a region of *Foxn1* cells was found in a more anterior dorsal region of the pouch that would be occupied by *Gcm2* positive cells in a wild type pouch. The dorsal *Foxn1* positive region was connected to the main Foxn1 domain toward the posterior part of the pouch (Fig 4D). Levels of intermingling between *Foxn1* and *Gcm2* positive cells in zone 3 were comparable to wild type.

Deletion of Shh signaling in pouch endoderm therefore resulted in a mostly normal primordium with an additional abnormal anterior dorsal domain of *Foxn1* expressing cells.

To further understand the role of Shh signaling in pouch endoderm, we ectopically overexpressed Shh signaling throughout the primordium. Based on our initial hypothesis we expected to see an expanded parathyroid domain and no thymus domain. As expected, overall pouch size was normal in Foxa2Cre^{ERT2};R26SmoM2 embryos at 48 somites (Fig 5L), and the *Foxn1* domain had fewer cells than wild type. However, the *Gcm2* domain was comparable to wild type in size and location rather than being expanded. Instead, a domain of Foxn1 and Gcm2 negative cells was located between the Gcm2 and foxn1 positive domains in Foxa2Cre^{ERT2};R26SmoM2 embryos. The number of marker negative cells plus the number of *Foxn1*+ cells was comparable to the total number of *Foxn1*+ cells in a wild type pouch at this stage (Fig 5H, 5L). This negative zone between the Foxn1 and Gcm2 domains also resulted in significantly less intermingling (Fig 5H). Because the *Gcm2* cell count was normal and the total number of *Foxn1* cells plus unstained cells is equal to total *Foxn1* cells in a wild type mouse, we concluded that this region would have been *Foxn1* positive in the absence of ectopic Shh signaling. Thus, the induction of ectopic Shh signaling throughout the pouch did not completed block Foxn1 expression, but instead resulted in a failure of *Foxn1* expression to spread up to the border of Gcm2 expressing cells, without expanding Gcm2 expression.

The *Foxn1*/*Gcm2* negative pouch in Foxa2Cre^{ERT2};R26SmoM2 embryos is unique, and raised questions about what else was different in the unstained region. Ectopic *Tbx1* expression was also found in the region of marker negative pouch (Fig 6F), suggesting that ectopic Shh signaling in the endoderm induced *Tbx1* expression, at least in this central domain of the pouch. These data further suggest that this ectopic Tbx1 may repress *Foxn1* in this region, although the

most ventral domain does not turn on Tbx1, and Foxn1 initial expression remains normal. These data suggest that the response to Shh signaling is not uniform throughout the pouch, and raise the possibility that other signals may compete with Shh signaling to affect the establishment of organ fate.

Gcm2 positive cells are located further toward the ventral part of the pouch at E10.5 when Shh signaling is deleted or ectopically active in neural crest mesenchyme.

The Shh null mouse is aparathyroid and has an expanded Foxn1 domain that includes the entire pouch as well as parts of the pharynx by E11.5, while Splotch mice have a shift in domain sizes that results in a hyperplastic thymus and hypoplastic parathyroids, and a delay in separation causing ectopic organs (Moore-Scott and Manley, 2005; Griffith et al., 2009). Because of these results we hypothesized that downstream targets of Shh signaling within the neural crest mesenchyme in turn act on the pouch endoderm to regulate the thymus and parathyroid domains. To determine where and how loss of Shh signaling in neural crest regulates the Foxn1 and Gcm2 domains within the pouch we examined the number and organization of Foxn1 and Gcm2 cells at 40 somites in Wnt1Cre;Smo^{fx} embryos.

Similar to wild type, Foxn1 and Gcm2 positive cells began at the ventral and dorsal ends of the pouch respectively (regions one and five) in Wnt1Cre;Smo^{fx} embryos at E11 (Fig 4B, 3H). While Foxn1 was still found primarily in regions one and two with a few cells in region three, Gcm2 positive cells were found further into the ventral pouch in region two, which is a Foxn1 specific region in wild type pouch (Fig 4E). Region three contained both Foxn1 positive cells and Gcm2 positive cells and served as a mixing domain in the 3rd pouch endoderm of both wild-type and Wnt1Cre;Smo^{fx} embryos. In contrast, Gcm2 positive cells within the Foxn1 domain were uncommon in wild type, while Gcm2 positive cells within region two of the Foxn1 domain

were found at a significantly higher rate when Shh signaling was deleted in neural crest mesenchyme (Fig 4J). Intermingling of Gcm2 cells within the Foxn1 domain was also seen at 48 somites in Wnt1Cre;Smo^{fx} embryos, although intermingling was reduced at 48 somites in comparison to 40 somites, similar to wild type. Furthermore Wnt1Cre;Smo$^{fx/+}$ embryos had an intermediate intermingling phenotype at 48 somites, suggesting dosage dependency (data not shown). This result suggests that Shh signaling to neural crest mesenchyme plays some role in boundary formation within the primordium.

Shh signaling from neural crest mesenchyme regulates Gcm2 expression within the 3rd pharyngeal pouch at 48 somites.

At E11.5 Splotch mice have altered domain sizes for *Foxn1* and *Gcm2* expression in comparison to wild type (Table 2). If Shh signaling to the neural crest mesenchyme was responsible for the domain shift seen in Splotch mice, we would expect to find a similar domain shift in Wnt1Cre;Smo^{fx} embryos.

Total cell numbers of both the Foxn1 and Gcm2 domains within the 3rd pouch was comparable between Wnt1Cre;Smo^{fx} embryos and wild type littermates at E11.5 (48 somites) (Fig 5I). However, numerous patterning defects were found in the Wnt1Cre;Smo^{fx} mutants, including Foxn1 and Gcm2 positive cells in the pharynx, as well as multiple lumens and increased intermingling of the Foxn1 and Gcm2 domains (Fig 5B and Supplemental Figure 1). Taken together, these results indicate that deletion of Shh signaling in neural crest mesenchyme resulted in a defect in later patterning but no changes in initial patterning, or in proliferation or cell death. These data show that, contrary to our initial model, Shh signaling to neural crest mesenchyme is not responsible for the boundary shift seen in *Splotch* mice.

To fully understand the role of Shh signaling to neural crest mesenchyme, we also induced ectopic Shh signaling in neural crest mesenchyme, by activating the R26SmoM2 transgene with Wnt1Cre. Overall pouch size was reduced in Wnt1Cre;R26SmoM2 embryos at 50 somites (Fig 5K). There was also a reduction in relative parathyroid size from 26.7% of total pouch size to 15.7% of total pouch size (Table 2). Proliferation in Wnt1Cre;R26SmoM2 embryos was variable with either a long and thin primordium that contained proliferating cells, or a small round primordium with no proliferation (Supplemental Figure 1). Similar to the E10.5 phenotype, the Gcm2 domain extended further posterior in the pouch than in wild type. While intermingling of Gcm2 positive cells in the Foxn1 domain was normal there was significantly less intermingling of Foxn1 positive cells in the Gcm2 domain compared to wild type intermingling (Fig 5F). These data showed that ectopic Shh signaling in neural crest cells resulted in a lack of proliferation causing a hypoplastic parathyroid and thymus, and a shift towards thymus fate. The organization of Foxn1 and Gcm2 expressing cells within the Wnt1Cre;R26SmoM2 pouch was also novel.

Changes in pouch organization in Wnt1Cre;Smo^{fx} embryos are accompanied by more fibronectin in the Foxn1 domain.

The fact that Wnt1Cre;Smo^{fx} embryos had changes in organization without changes in initial patterning, proliferation, or cell death suggested a possible role for cell adhesion molecule regulation by Shh signaling from neural crest mesenchyme. To test this possibility we looked at E-cadherin and fibronectin. E-cadherin is tightly regulated and highly expressed in epithelial cells, and is differentially expressed in the thymus and parathyroid domains at E12.5 during morphogenesis (Shook and Keller., 2003; Gordon et al., 2010). At 51 somites (late E11.5) and 56 somites (E12), E-cadherin was uniformly high throughout the wild type pouch as detected by

immunohistochemistry (Fig. 7A, 7B). It is unlikely that E-cadherin is involved in the increased intermingling of Gcm2 cells within the Foxn1 domain however as Wnt1Cre;Smo^{fx} E-cadherin staining was similar to wild type at 51 and 56 somites (Fig. 7C, 7D).

Fibronectin is a protein of the extracellular matrix and is upregulated to allow for cell mobility (Miyamoto et al., 1998). Fibronectin is restricted to the presumptive parathyroid domain, the exterior of all pouch, and the lumen in a wild type pouch at 51 somites (Fig. 7E, 7F). By 56 somites, it is found at high levels throughout both the parathyroid and the thymus (Fig. 7G, 7H). Fibronectin is found at low levels in the thymus domain of the Wnt1Cre;Smo^{fx} pouch at 51 somites. This result suggested that fibronectin staining in Wnt1Cre;Smo^{fx} pouch may be temporally ahead of wild type fibronectin in thymus and parathyroid, and this change could contribute to the messy boundaries found in Wnt1Cre;Smo^{fx} pouch at E11.5.

Known signaling targets of Shh are normal when Shh signaling is manipulated in neural crest mesenchyme or pouch endoderm.

In order for Shh signaling from neural crest mesenchyme to act on the third pharyngeal pouch, a second signaling molecule downstream of *Shh* would need to act directly on the pouch. Previous studies have shown that *Fgf10* and *Bmp2/4* act downstream of *Shh* in palatal mesenchyme (Lan and Jiang., 2009). Both *Fgf10* and *Bmp4* are found in mesenchyme surrounding the pouch and could potentially regulate pouch fate.

Fgf7 and *Fgf10* are expressed in mesenchyme surrounding the thymus and have been shown to interact with *FgfR2-IIIb* to promote thymus growth and TEC differentiation (Revest et al., 2001). *Fgf10* was present in mesenchyme surrounding the ventral and lateral sides of the pouch as well as low expression within the pouch by section *in situ* hybridization at E11.5. *Fgf10* was not found near the pharynx or above the dorsal part of the 3rd pouch (Fig 9A, 9C).

Similar to wild type, *Fgf10* expression surrounded the ventral and lateral sides of the pouch and was found in the pouch as well in Wnt1Cre;Smo^{fx} embryos at E11.5. Overall, the *Fgf10* pattern was very similar between wild type and Wnt1Cre;Smo^{fx} . *Fgf10* expression was also comparable to wild type in Foxa2Cre^{ERT2};Smo^{fx} embryos at E11.5, with expression in ventral and lateral mesenchyme as well as in the pouch endoderm (Fig 9D). Because neither the Wnt1Cre;Smo^{fx} phenotype nor the Foxa2Cre^{ERT2};Smo^{fx} phenotype mimics the *Splotch* pouch boundary shift we cannot rule out the possibility that *Fgf10* is the mechanism by which neural crest regulates domain size within the pouch; however, normal *Fgf10* expression in both neural crest mesenchyme and pouch endoderm deletion of Shh signaling suggests that *Fgf10* does not act downstream of *Shh* in mesenchyme surrounding the 3rd pouch.

Bmp4 and *Shh* are often antagonists and work in palatogenesis has shown that *Bmp4* regulates *Shh* and is able to repress it (Watanabe et al., 1998; Zhang et al., 2000; Zhao et al., 2000). In early thymus development, Bmp4 signaling to mesenchyme is required for thymic capsule formation and separation of thymus and parathyroid (Gordon et al., 2010). In later thymus development *Bmp4* from both TEC and neural crest mesenchyme are required for thymus survival, and a smaller primordium with a large lumen is found in *Bmp4*'s absence (Bleul and Boehm, 2005; Gordon et al., 2010).

At 49 and 50 somites some variability in *Bmp4* expression was found in Wnt1Cre;Smo^{fx} embryos. *Bmp4* expression in a wild type pouch was found in mesenchyme on the ventral side of the pouch as well as within the pouch by *in situ* hybridization (Fig 9E, 9F). Of the twelve mutant pouches examined, seven pouches had *Bmp4* expression in the ventral mesenchyme that was flush with the pouch while five pouches were more similar to wild type, in that some of the pouch was not contacting Bmp4 expressing cells (Fig 9G, 9H). Because the earliest pouch

phenotypes in the neural crest deletion of Shh signaling began at 40 somites, we looked at Bmp4 signaling at 41 somites to determine if the slight variability in *Bmp4* expression location at E11.5 was responsible for the intermingling phenotype. All four pouches from Wnt1Cre;Smo^{fx} embryos examined at 41 somites were similar to wild type in that there were *Bmp4* negative cells between the *Foxn1* domain and the region of *Bmp4* expression in adjacent mesenchyme (Fig. 9P, 8Q). Contrary to the independence of Bmp4 signaling from the deletion of Shh signaling in neural crest mesenchyme, Bmp4 signaling was altered when Shh signaling was ectopically overexpressed in neural crest mesenchyme. *Bmp4* expression was significantly reduced from the mesenchyme surrounding the primordium in Wnt1Cre;R26SmoM2 embryos, confirming the antagonistic role observed between *Shh* and *Bmp4* in the *Shh* null embryo (Fig 9S-V). *Bmp4* expression in pouch endoderm and on the ventral side of the pouch comparable to wild type expression in these embryos (Fig. 9K-L).

Differences between Fgf10 and Bmp4 signals in wild type and Shh signaling deletion mutants are subtle if present. The lack of significant difference in known signaling targets suggests that Shh signaling works outside of known pathways to cause the changes seen in Wnt1Cre;Smo^{fx} and Foxa2Cre^{ERT2};Smo^{fx}. It is also likely that a Shh independent signal from neural crest mesenchyme is involved in regulating pouch fate because Wnt1Cre;Smo^{fx} embryos lack the striking pouch boundary differences found in *Splotch* mice.

Pharynx shape is affected by Shh signaling to the neural crest

Pharynx shape is altered in Shh null mice and takes a smaller and more rounded shape (Moore-Scott and Manley, 2005). To further compare similarities between the Shh null phenotype and manipulation of Shh signaling in pouch endoderm we examined pharynx shape in Foxa2Cre^{ERT2};Smo^{fx} and Foxa2Cre^{ERT2};R26SmoM2 embryos. In wild-type embryos at E11.5,

the 3rd pharyngeal pouch was found next to the pharynx and remained attached in the anterior region of the pouch. The pharynx near the 3rd pouch had an arch-like shape and the 3rd pouch projected ventrally as assayed by 3-D reconstruction of serial section subjected to in situ hybridization for both *Foxn1* and *Gcm2* (Fig. 8A, 8D, 8G, 8J). In Foxa2Cre^{ERT2};Smo^{fx} and Foxa2Cre^{ERT2};R26SmoM2 embryos, pharynx shape remained normal and the pouch was found in a comparable location to wild type (Fig 8E, 8F, 8K, 8L). These results suggest that Shh signaling within pouch endoderm alone does not influence pharynx shape.

In contrast to the endoderm, pharynx shape was altered in Wnt1Cre;Smo^{fx} embryos. When Shh signaling in neural crest mesenchyme was deleted the dorsal side of the pharynx remained similar to wild type while the distance between dorsal and ventral sides of the pharynx was increased and the point where the pharynx and the 3rd pouch joined was raised to a more dorsal location within the embryo (Fig 8B, 8C). This change in location may explain the altered Bmp4 expression seen in some of the mutant pouches. Pharynx shape was also altered in Wnt1cre;R26SmoM2 embryos. Although the pharynx was still faintly arch shaped, it reached further laterally across the embryo and placed the 3rd pouch in a location closer to the surface of the embryo (Fig 8H, 8I). Both Wnt1Cre;Smo^{fx} embryos and Wnt1cre;R26SmoM2 embryos had changes in pharynx shape in response to altered Shh signaling suggesting that Shh signaling from neural crest mesenchyme helps to shape the pharynx. However whether the pharynx shape is changed by altered pouch location or change in pharynx shape causes altered pouch location is unknown.

Discussion

In this paper we investigated the contributions of Shh signaling within the pouch endoderm and neural crest mesenchyme to organization of the third pouch, and the possible link

between the *Splotch* mutant and *Shh* null phenotypes. Contrary to our original hypothesis, we did not find that Shh signaling to neural crest mesenchyme was responsible for the shift in organ fate boundaries seen in *Splotch* mice, nor did we find that Shh signaling to pouch endoderm was sufficient for Gcm2 expression of parathyroid fate establishment. We found that Shh signaling to both neural crest mesenchyme and third pouch endoderm are required for normal organization of the thymus and parathyroid and that no tissue specific deletion is able to mimic the *Shh* null phenotype. Shh signaling to neural crest mesenchyme helps to pattern the size and location of the parathyroid domain within the endoderm. This result implies the existence of a second signal, other than Bmp4 or Fgf10, acting downstream of Shh. Furthermore, overexpression of Shh signaling to neural crest mesenchyme is able to repress Bmp4 signaling in mesenchyme surrounding the ventral part of the pouch supporting an antagonistic role between Shh signaling and Bmp4 signaling. Shh signaling within pouch endoderm does not affect parathyroid domain size, but appears to block thymus organ fate, in part via influencing the expression of the known *Shh* target gene *Tbx1*. Ectopic Shh signaling within the endoderm induces *Tbx1,* which in turn appears to inhibit *Foxn1* expression. However, although SmoM2 activation induces Shh signaling throughout the pouch, the most ventral domain is protected from its effects, possibly by the persistence of Bmp4 expression within this ventral domain.

Based on these findings we propose a model in which Shh signaling controls pouch patterning directly via *Tbx1* expression to inhibit *Foxn1* and permit *Gcm2* expression, and indirectly regulates the location of the border between the Foxn1 and Gcm2 domains through inhibition of Bmp4 signaling and/or an as of yet identified second signal from neural crest mesenchyme (Fig. 10).

Shh signaling from endoderm alone is not sufficient for parathyroid fate.

In the Shh null embryo the thymus domain encompasses the entire third pouch in the absence of a parathyroid domain. We predicted that Shh signaling within the pouch endoderm was necessary to induce or maintain *Tbx1* and *Gcm2* expression to establish the parathyroid domain. Surprisingly, Shh signaling within the pouch endoderm was not required for *Gcm2* expression, although the location was shifted with relation to the pharynx when Shh signaling was deleted in pouch endoderm. One possible explanation for this result is that a second, mesenchyme-derived signal is sufficient to induce *Gcm2* expression. This signal would itself need to be downstream of Shh signaling within the neural crest, as knocking out Shh globally eliminates Gcm2 expression in mice (Moore-Scott and Manley, 2005).

Ectopic Tbx1 expression within the pouch inhibits Foxn1 expression.

Just as the *Gcm2* domain is not lost in the endoderm-specific knockout of *Smo*, the *Gcm2* domain is also not expanded to fill the entire pouch in Foxa2Cre^{ERT2};R26SmoM2 embryos. Instead, we found a central region of cells within the pouch between the Foxn1 and Gcm2 domains that expressed neither organ marker at E11.5, well after organ fates have spread to encompass the entire primordial in wild-type embryos. Because the total combined size of marker negative pouch and the *Foxn1* positive domain in Foxa2Cre^{ERT2};R26SmoM2 embryos is equal to the size of a wild type *Foxn1* domain, it seems likely that this region would have otherwise expressed *Foxn1*. Based on the lack of either *Foxn1* or *Gcm2* expression in the central domain of the pouch and the ectopic *Tbx1* expression, we propose that *Tbx1* acts downstream of Shh signaling within the third pouch to repress *Foxn1* expression in wild type development. However, *Tbx1* expression is not sufficient for *Gcm2* expression. It is possible that *Tbx1* is upstream of *Gcm2,* but that *Gcm2* requires activation from an additional regionally restricted

signal from the neural crest. Gcm2 expression could also be suppressed in the more ventral regions of the pouch. Although not covered in the scope of this study, it would be informative to look at later organ morphogenesis in Foxa2Cre^{ERT2};R26SmoM2 embryos to determine if this marker-negative domain survives and if so, what its ultimate fate may be.

Shh signaling from neural crest mesenchyme is not sufficient for domain border regulation within the third pharyngeal pouch.

Splotch mice have a domain shift within the third pouch, increasing the thymus domain at the expense of the parathyroid domain (Griffith et al., 2009). Because of similarities between the Splotch phenotype and the Shh null phenotype we predicted that neural crest cells regulate pouch fate via a second signal that is a downstream target of Shh signaling. This model predicts that deleting Shh signaling in neural crest cells would cause a domain shift similar to that seen in *Splotch* mice. We tested this hypothesis in Wnt1Cre;Smo^{fx} embryos, and while there were some similarities between Wnt1Cre;Smo^{fx} and *Splotch* mice (i.e. disrupted organ domain borders and multiple lumens), no domain shift was found in Wnt1Cre;Smo^{fx} embryos.

Because the Wnt1Cre;Smo^{fx} phenotype does not mimic the domain shift phenotype of *Splotch* mice, this suggests that a Shh independent signal from neural crest mesenchyme regulates domains within the third pouch. Our data rule out the two most likely candidates, *Bmp4* and *Fgf10*. Although the *Splotch* phenotype implicates the neural crest, we cannot rule out the possibility that the signal responsible for the domain shift comes from mesoderm that is ectopically located near the pouch endoderm in the absence of neural crest cells. In this model, the amount of mesenchymal tissue lost in *Splotch* mice is greater than in Wnt1Cre;Smo^{fx} mice, placing the pouch closer to an additional currently unknown mesodermal signal that influences organ domains within the pouch.

It is interesting that deletion of Shh signaling within third pouch associated neural crest mesenchyme did not alter *Bmp4* or *Fgf10* expression, as recent work in palatal development shows the opposite result when Shh signaling is deleted in palatial mesenchyme (Lan and Jiang, 2009). This result further supports earlier work suggesting that high levels of Shh signaling to the first and second pharyngeal pouches acts differently than low levels of Shh signaling to the third and fourth pouches (Moore-Scott and Manley, 2005; Grevellec et al., 2011).

Although organ domain borders are different between *Splotch* mice and Wnt1Cre;Smo^{fx} mice there are some similarities between the two phenotypes. Both phenotypes have multiple lumens and irregular borders, suggesting that Shh signaling within neural crest cells is partially responsible for the *Splotch* phenotype. Both of these phenotypes could be related to fibronectin, as fibronectin is important for cell mobility and could be involved in lumen closure (Miyamoto, 1998). The cell mixing may also contribute to separation and migration defects at later stages. Although thymus and parathyroid are normally separate from one another and not attached to the pharynx at E13.5, both primordia are found next to each other at an ectopic location next to pharynx in Wnt1Cre;Smo^{fx} embryos. Wnt1Cre;$Smo^{fx/+}$ mice also have organ separation and migration defects, with a second small ectopic thymus and a long thin parathyroid attachment to the primary thymus (data not shown). These heterozygous phenotypes suggest that precise levels of Shh signaling from neural crest mesenchyme are required for normal thymus and parathyroid patterning and morphogenesis but that Shh signaling alone from neural crest mesenchyme is not responsible for the boundary shift seen in *Splotch* mice.

Our initial model of domain boundary establishment in which Shh signaling to neural crest mesenchyme activates a signal that regulates boundary placement predicted that overexpression of Shh signaling in neural crest mesenchyme would cause a reversal of the

Splotch phenotype, with a larger parathyroid and a small (or no) thymus. Instead we saw an overall smaller primordium with a domain shift towards thymus fate, similar to *Splotch* mutants. The primordium size discrepancy in Wnt1Cre;R26SmoM2 embryos is most likely due to a lack of proliferation. The size difference between the thymus and parathyroid domains in wild-type mice is created in part by differentiation proliferation – the thymus domain undergoes rapid expansion, while the parathyroid domain has much lower rates of proliferation (Gordon et al., 2004; Manley and Selleri et al., 2004). The reduced proliferation within the pouch endoderm in Wnt1Cre;R26SmoM2 embryos suggests that this differential proliferation may in part be influenced by signals from the neural crest – positive signals in the ventral mesenchyme, but also suppressive signals from the dorsal mesenchyme acting downstream of Shh signaling.

Shh signaling in neural crest mesenchyme influences pharynx shape.

Pharynx shape in Shh null mice is also altered relative to wild type. Whereas wild type pharynx is a flat curved structure with sharp branching points for each of the pharyngeal pouches, the Shh null pharynx is more rounded with the pouches forming nubs attached to a tube-like pharynx. Pharynx shape in *Splotch* mice is more similar to wild type than to the Shh null. Neither Foxa2Cre^{ERT2};Smo^{fx} nor Foxa2Cre^{ERT2};R26SmoM2 have a change in pharynx shape suggesting that endodermal Shh signaling has minimal effect on pharynx shape and pouch placement. The pharynx shape of Wnt1Cre;Smo^{fx} mice is intermediate between the Shh null pharynx and the *Splotch* pharynx. The neural crest-specific deletion may be milder that the null in part due to other anatomical defects in the null mutant that exacerbate pharynx shape. In any event, our data implicate neural crest derived signals acting downstream of Shh in mediating pharynx shape.

In conclusion, our data show that third pouch endoderm is sensitive to both direct Shh signaling within the pouch, and indirect Shh signaling within the neural crest mesenchyme. We have shown that Shh signaling alone does not regulate organ borders within the pouch as initially predicted, although it may contribute to border formation on a smaller scale. We have also shown that endodermal Shh signaling alone is sufficient for parathyroid fate, that ectopic *Tbx1* within the pouch may inhibit *Foxn1* expression and is not sufficient for *Gcm2* expression, and that ectopic Shh signaling in neural crest mesenchyme is able to inhibit Bmp4 signaling. Future work should look outside of Shh signaling for the neural crest mesenchyme signal responsible for boundary regulation within the pouch, and further investigate the relationships of *Foxn1*, *Gcm2*, and *Tbx1* within the third pouch.

Figures and Figure Legends

Figure 2.1

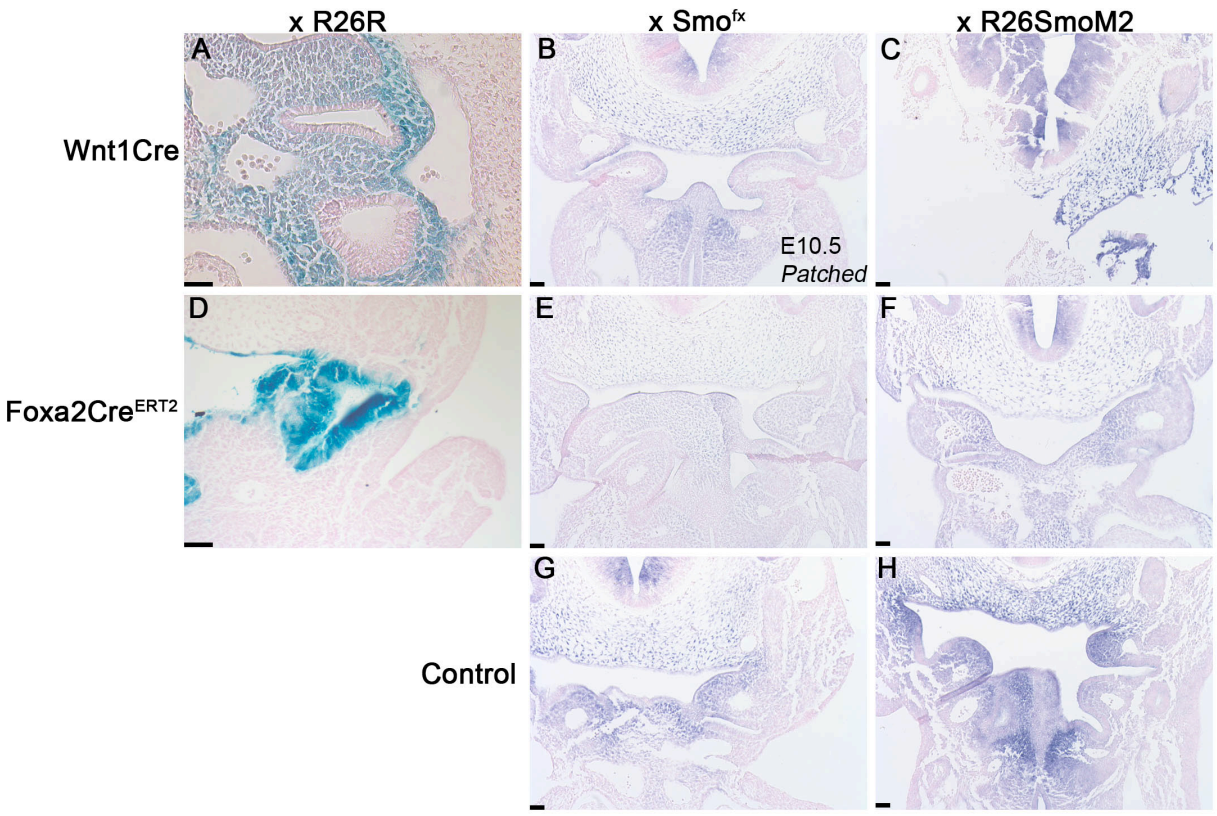

Fig. 2.1: A tissue specific strategy for manipulation of Shh signaling.

(A-F) Transverse sections of β-gal and coronal sections of in situ hybridization at E10.5. Wnt1Cre marks neural crest cells surrounding the third pharyngeal pouch (A). When crossed to Smo^{fx}, Wnt1Cre is used to delete Shh signaling in neural crest (B). When crossed to R26SmoM2, Wnt1Cre is used to ectopically activate Shh signaling in neural crest (C). $Foxa2Cre^{ERT2}$ marks pouch endoderm and a small number of neural crest cells when activated by tamoxifen at E5.5 (D). When crossed to Smo^{fx}, $Foxa2Cre^{ERT2}$ is used to delete Shh signaling in pouch endoderm (E). When crossed to R26SmoM2, $Foxa2Cre^{ERT2}$ is used to ectopically activate Shh signaling in pouch endoderm (F). *Patched* expression is found in the anterior-most part of the third pouch at E10.5 (G & H). Scale bars indicate 50 μm.

Figure 2.2

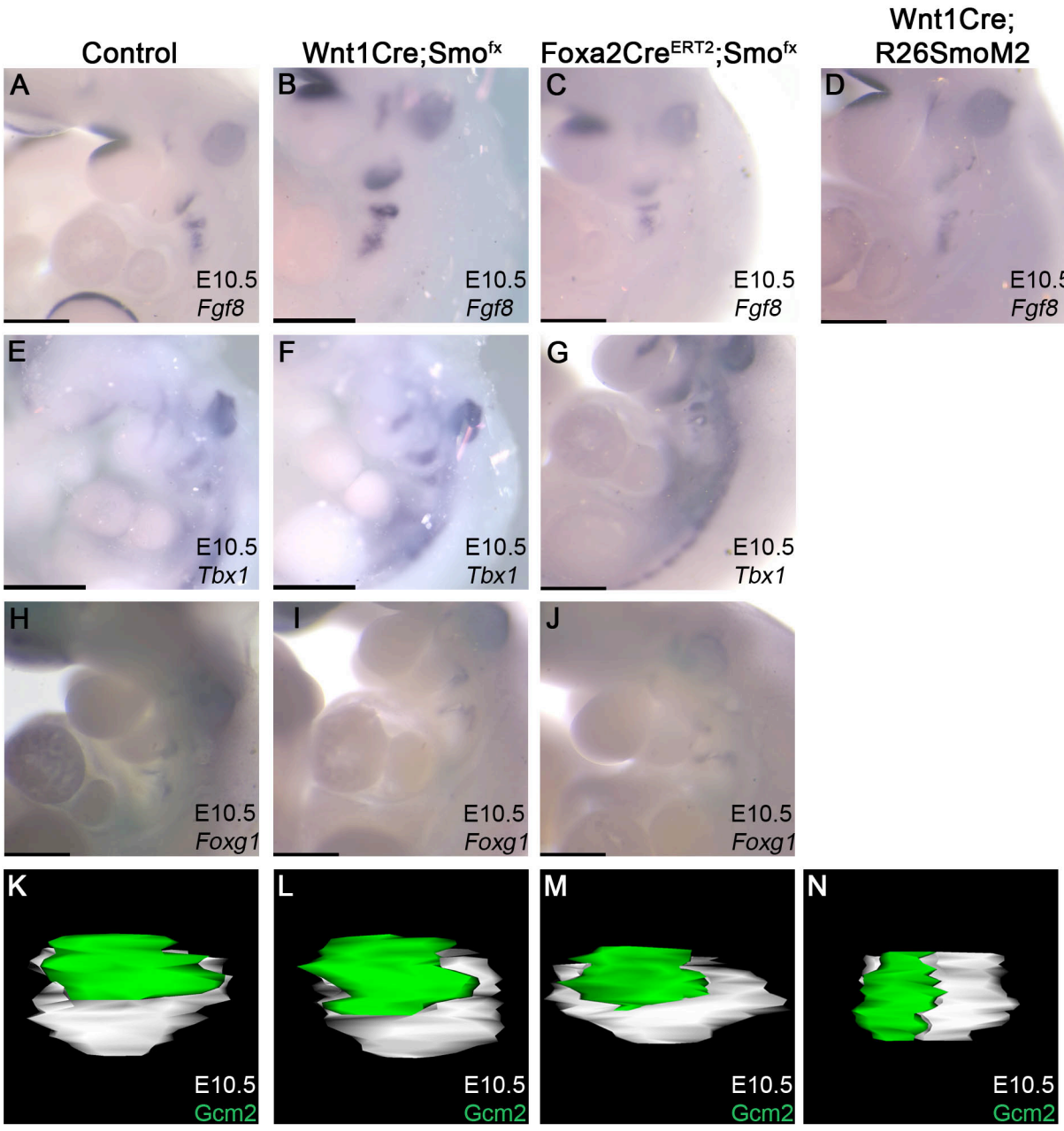
Control
Wnt1Cre;Smo^fx
Foxa2Cre^ERT2;Smo^fx
Wnt1Cre;
R26SmoM2
A
B
C
D
E10.5
Fgf8
E
F
G
E10.5
Tbx1
H
I
J
E10.5
Foxg1
K
L
M
N
E10.5
Gcm2

Fig. 2.2: Initial patterning is normal when Shh signaling is deleted or constitutively expressed in neural crest mesenchyme or deleted in pouch endoderm.

(A-J) Lateral views of wholemount in situs at E10.5 at high magnification to show the pharyngeal pouches. (A-D) Fgf8 expression at E10.5. Fgf8 is found in the second third and fourth pharyngeal pouches in wild type mice at E10.5 (A). Fgf8 remains unchanged in the second, third, and fourth pouches in $Smo^{flx/flx}$;Wnt1Cre (B), $Smo^{flx/flx}$;Foxa2Cre (C), and SmoM2;Wnt1Cre (D) embryos at E10.5. (E-G) Tbx1 expression at E10.5. Tbx1 is found in the dorsal third pouch, cardiac mesenchyme, mesenchyme surrounding the pharyngeal pouches, and otic vesicle at E10.5 in wild type mice (E). Tbx1 remains unchanged in $Smo^{flx/flx}$;Wnt1Cre (F) and $Smo^{flx/flx}$;Foxa2Cre (G) embryos at E10.5. (H-J) Foxg1 expression at E10.5. Foxg1 is found in the second and third pharyngeal pouches as well as the otic vesicle at early E10.5 in wild type mice (H). Foxg1 remains unchanged in $Smo^{flx/flx}$;Wnt1Cre (I) and $Smo^{flx/flx}$;Foxa2Cre (J) embryos at E10.5. (K-N) Anterior views of 3-D reconstructions of Gcm2 expression within the third pharyngeal pouch at E10.5. Gcm2 is found in the dorsal most region of the third pharyngeal pouch at E10.5 in wild type mice (K). The Gcm2 domain locates to the dorsal most region of the third pharyngeal pouch in both $Smo^{flx/flx}$;Wnt1Cre (L) and $Smo^{flx/flx}$;Foxa2Cre (M). The Gcm2 domain is slightly altered in SmoM2;Wnt1Cre embryos at E10.5 in that it does not cover the entire dorsal pouch. Scale bars indicate 1 mm.

Figure 2.3

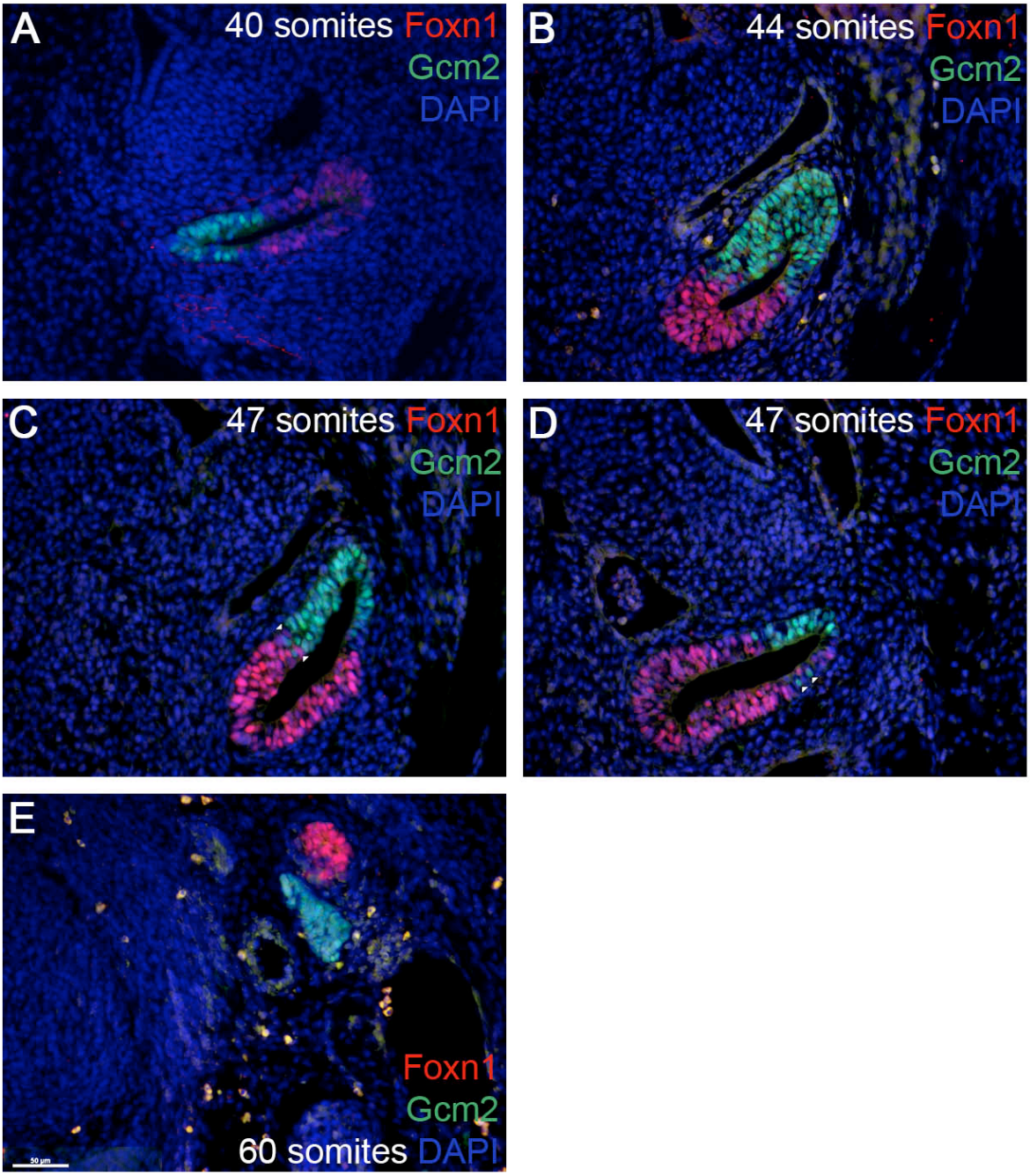
A
40 somites Foxn1
Gcm2
DAPI
B
44 somites Foxn1
Gcm2
DAPI
C
47 somites Foxn1
Gcm2
DAPI
D
47 somites Foxn1
Gcm2
DAPI
E
Foxn1
Gcm2
60 somites DAPI
50 µm

Fig. 2.3 The *Foxn1* and *Gcm2* domains share regions of intermingling before the 60 somite stage.

(A – E) Transverse and saggital sections from wild type embryos stained for Foxn1 and Gcm2. Foxn1 and Gcm2 positive cells are found within the 40 somite pouch (A). All pouch stains for Foxn1 or Gcm2 by 44 somites (B). Cells intermingle at early stages and Foxn1 cells can be found in the Gcm2 domain (C) and Gcm2 cells can be found in the Foxn1 domain (D). Intermingling is indicated by white arrowheads. Foxn1 and Gcm2 positive cells do not intermingle by 60 somites (E). Scale bar indicates 50 μm.

Figure 2.4

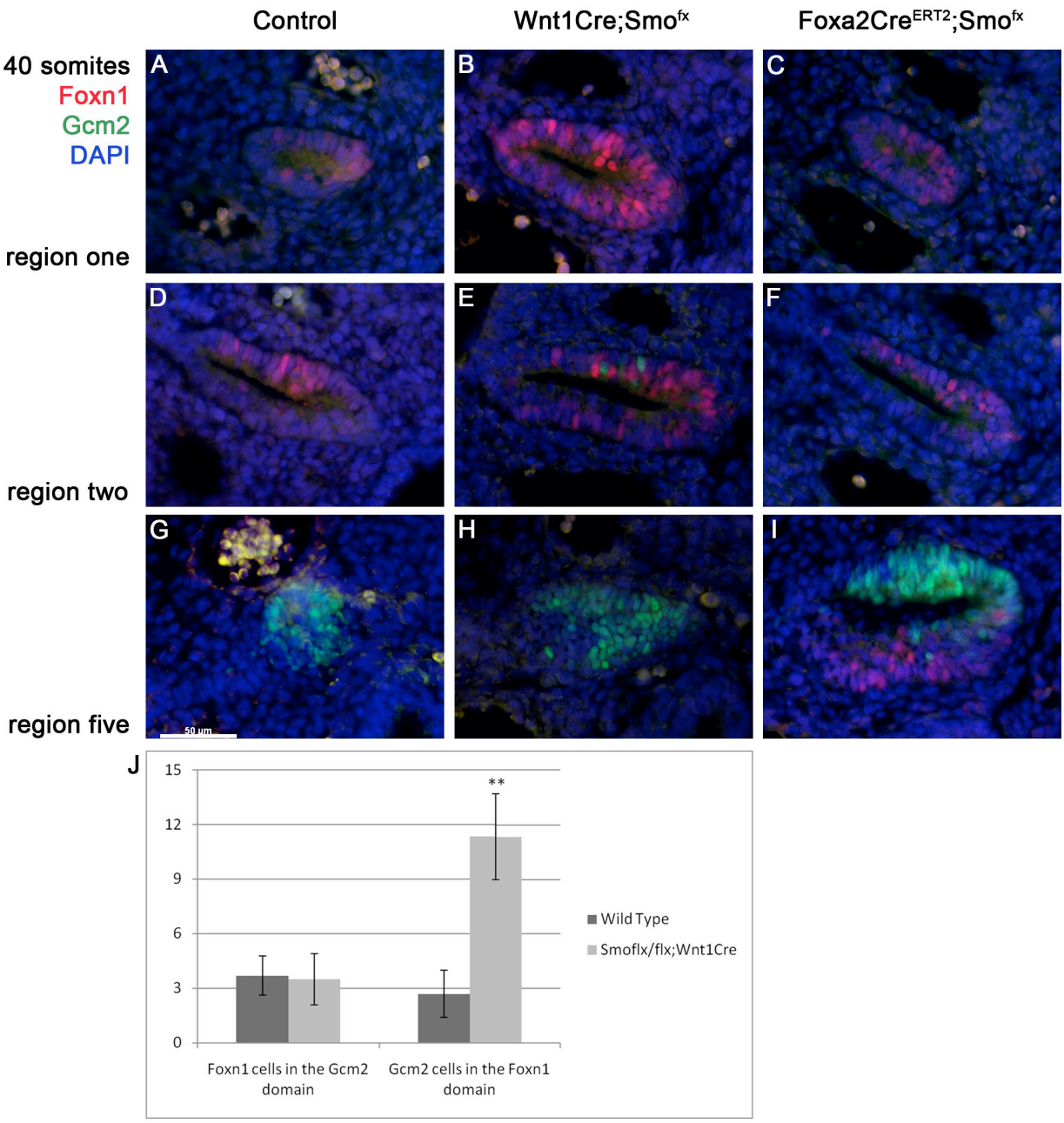
Control
Wnt1Cre;Smo^fx
Foxa2Cre^ERT2;Smo^fx
40 somites
Foxn1
Gcm2
DAPI
region one
region two
region five
A
B
C
D
E
F
G
H
I
50 µm
J
15
12
9
6
3
0
**
Wild Type
Smoflx/flx;Wnt1Cre
Foxn1 cells in the Gcm2 domain
Gcm2 cells in the Foxn1 domain

Fig. 2.4 Gcm2 travels further in the absence of Shh signaling in neural crest mesenchyme at E10.5.

(A-I) Immunostaining of Foxn1 (red) and Gcm2 (green) within coronal sections of third pharyngeal pouch at 40 somites. Foxn1 is first found in the ventral most region of the pouch at 40 somites in wild type embryos (A). Foxn1 is also found in the ventral most regions of Wnt1Cre;Smo^{fx} (B) and $Foxa2Cre^{ERT2}$;Smo^{fx} mutant pouches at 40 somites. Foxn1 positive cells continue to be found through the ventral most half of the pouch at 40 somites in wild type (D) and $Foxa2Cre^{ERT2}$;Smo^{fx} (F) embryos. Although Foxn1 positive cells are also found in the ventral half of the Wnt1Cre;Smo^{fx} embryo a few Gcm2 positive cells are found as well. Gcm2 is found in the dorsal half of the pouch at 40 somites in wild type embryos (G). Gcm2 extends to the dorsal most region of the pouch in both Wnt1Cre;Smo^{fx} and $Foxa2Cre^{ERT2}$;Smo^{fx} embryos (H & I). Significantly more Gcm2 positive cells are found within the Foxn1 domain of the Wnt1Cre;Smo^{fx} pouch (N=6) than in wild type (N=10) at 40 somites (J). The number of Foxn1 cells in the Gcm2 domain is similar between wild type and mutant pouch. Scale bar indicates 50 μm.

Figure 2.5

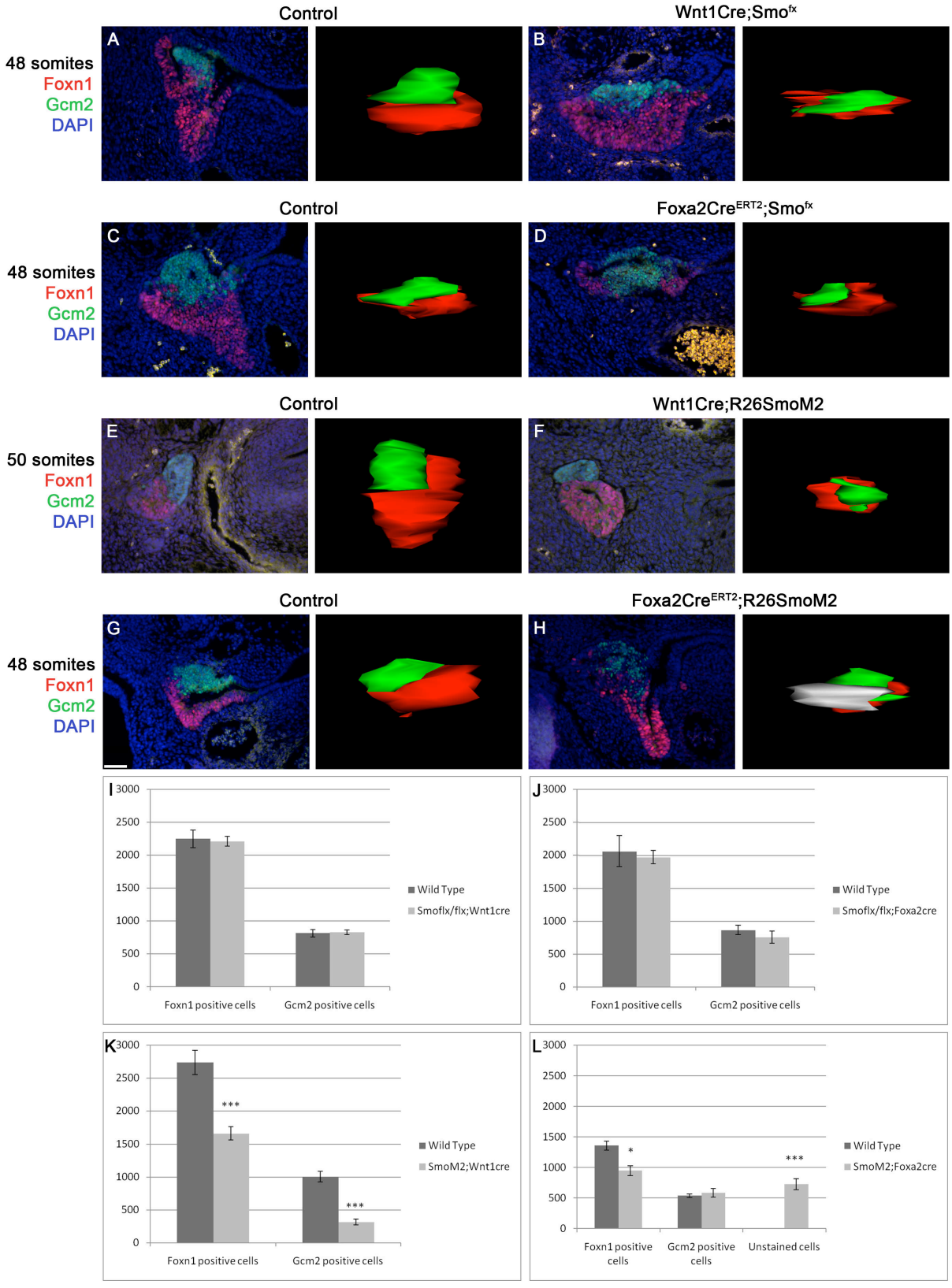
Control
Wnt1Cre;Smo^fx
48 somites
Foxn1
Gcm2
DAPI
A
B
Control
Foxa2Cre^ERT2;Smo^fx
C
D
Control
Wnt1Cre;R26SmoM2
50 somites
E
F
Control
Foxa2Cre^ERT2;R26SmoM2
G
H
I
J
K
L
Wild Type
Smoflx/flx;Wnt1cre
Smoflx/flx;Foxa2cre
SmoM2;Wnt1cre
SmoM2;Foxa2cre
Foxn1 positive cells
Gcm2 positive cells
Unstained cells
***
*

Fig. 2.5. Shh signaling from both neural crest mesenchyme and pouch endoderm regulate the Foxn1 and Gcm2 domains of the third pharyngeal pouch.

(A-H) Immunostaining of Foxn1 (red) and Gcm2 (green) domains within transverse sections of third pharyngeal pouch at E11.5 accompanied by whole pouch 3-D reconstructions. The Gcm2 domain is found in the anterio-dorsal most region of the third pouch at E11.5 while the Foxn1 domain covers the remaining pouch in a wild embryo at E11.5 (A, C, E, G). The third pouch is at a higher dorsal location and extends further laterally in Wnt1Cre;Smo^{fx} embryos at E11.5 (B). The Gcm2 domain extends to a more ventral and central location within the pouch in Foxa2Cre^{ERT2};Smo^{fx} embryos at E11.5 (D). Overall pouch size is smaller and the Gcm2 domain covers the entire dorso-ventral axis of the pouch in Wnt1Cre;R26SmoM2 embryos at E11.5 (F). Part of the pouch fails to express Foxn1 or Gcm2 at E11.5 in Foxa2Cre^{ERT2};R26SmoM2 embryos (H). (I-L) A comparison of cells positive for Foxn1 and Gcm2 at E11.5 in each of the mutant pouches. There is no difference between number of Foxn1 or Gcm2 positive cells in Wnt1Cre;Smo^{fx} (N=6)and littermate controls (N=4) (I) or Foxa2Cre^{ERT2};Smo^{fx} (N=6) and littermate controls (N=4) (J) at E11.5. There are fewer Foxn1 and Gcm2 positive cells in Wnt1Cre;R26SmoM2 embryos (N=6) than littermate controls (N=4) at E11.5 (K). Gcm2 positive cells are comparable between Foxa2Cre^{ERT2};R26SmoM2 embryos (N=8) and littermate controls (N=6). While there are fewer Foxn1 cells in Foxa2Cre^{ERT2};R26SmoM2 embryos, there is a region of unstained cells that compensates for the missing Foxn1 cells (L). All 3-D reconstructions except H are oriented so that the X-axis ranges from anterior (up) to posterior (down) and the Z-axis ranges from dorsal (shown) to ventral (not shown). H is shown with dorsal to ventral in the Y-axis to show the unstained region of the pouch. Scale bar indicates 50 μm.

Figure 2.6

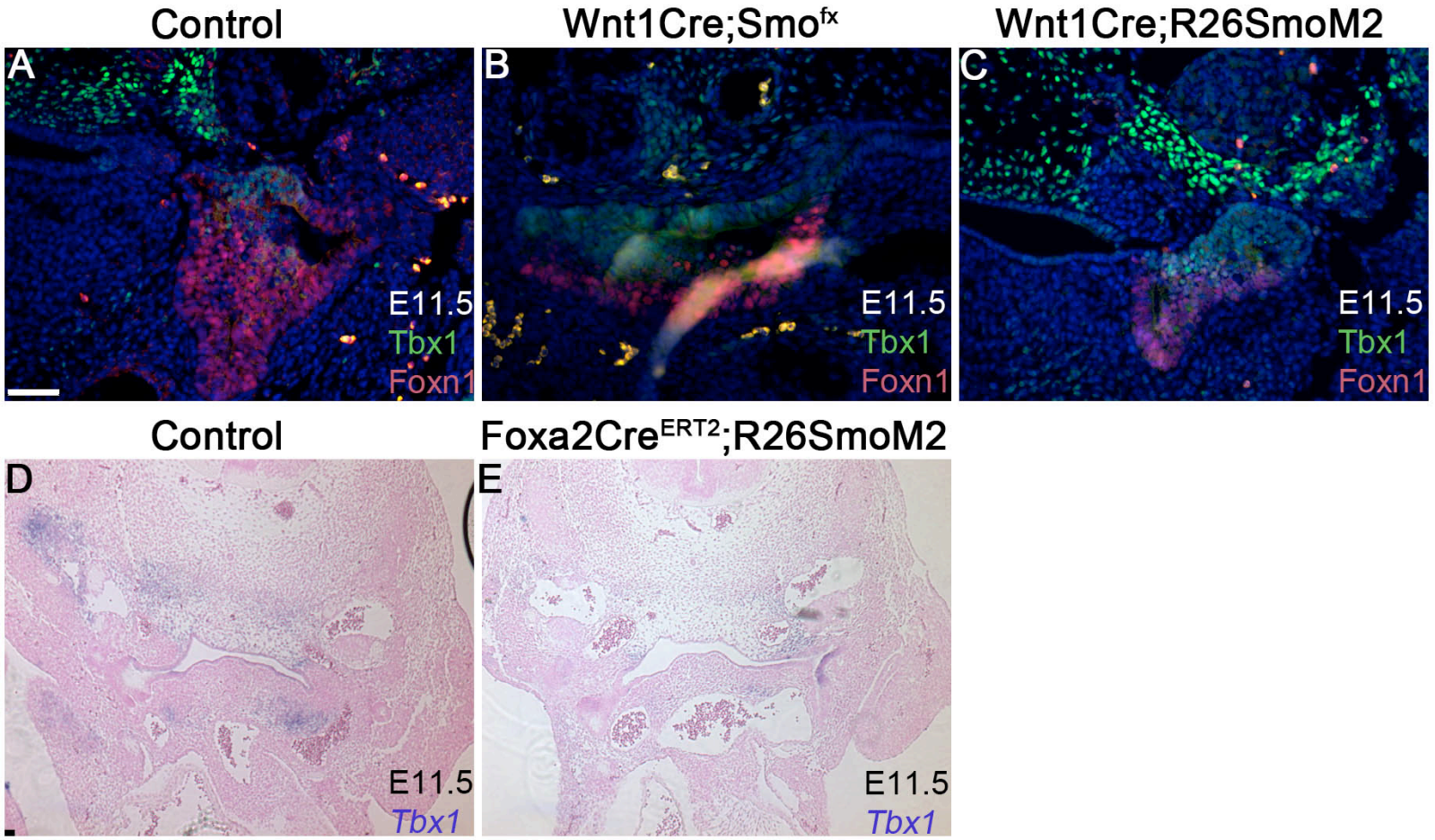
Control
Wnt1Cre;Smo^fx
Wnt1Cre;R26SmoM2
A
B
C
E11.5
Tbx1
Foxn1
Control
Foxa2Cre^ERT2;R26SmoM2
D
E
E11.5
Tbx1

Fig 2.6 *Tbx1* expression is altered in response to altered Shh signaling.

(A – C) Immunostaining for Foxn1 and Tbx1 at E11.5. Tbx1 is found in the parathyroid domain and mesenchyme in wild type mice (A). Changes in Tbx1 staining are subtle in Wnt1Cre;Smo^{fx} mice (B). Tbx1 staining in the mesenchyme above the pouch extends further toward the surface of the embryo (C). (D – E) *Tbx1 in situ* at E11.5. *Tbx1* expression is comparable to immunostaining in wild type mice (D). An ectopic domain of intense *Tbx1* expression is found in a region similar to the unstained pouch reported in Figure 5H (E).

Scale bars indicate 50 μm.

Figure 2.7

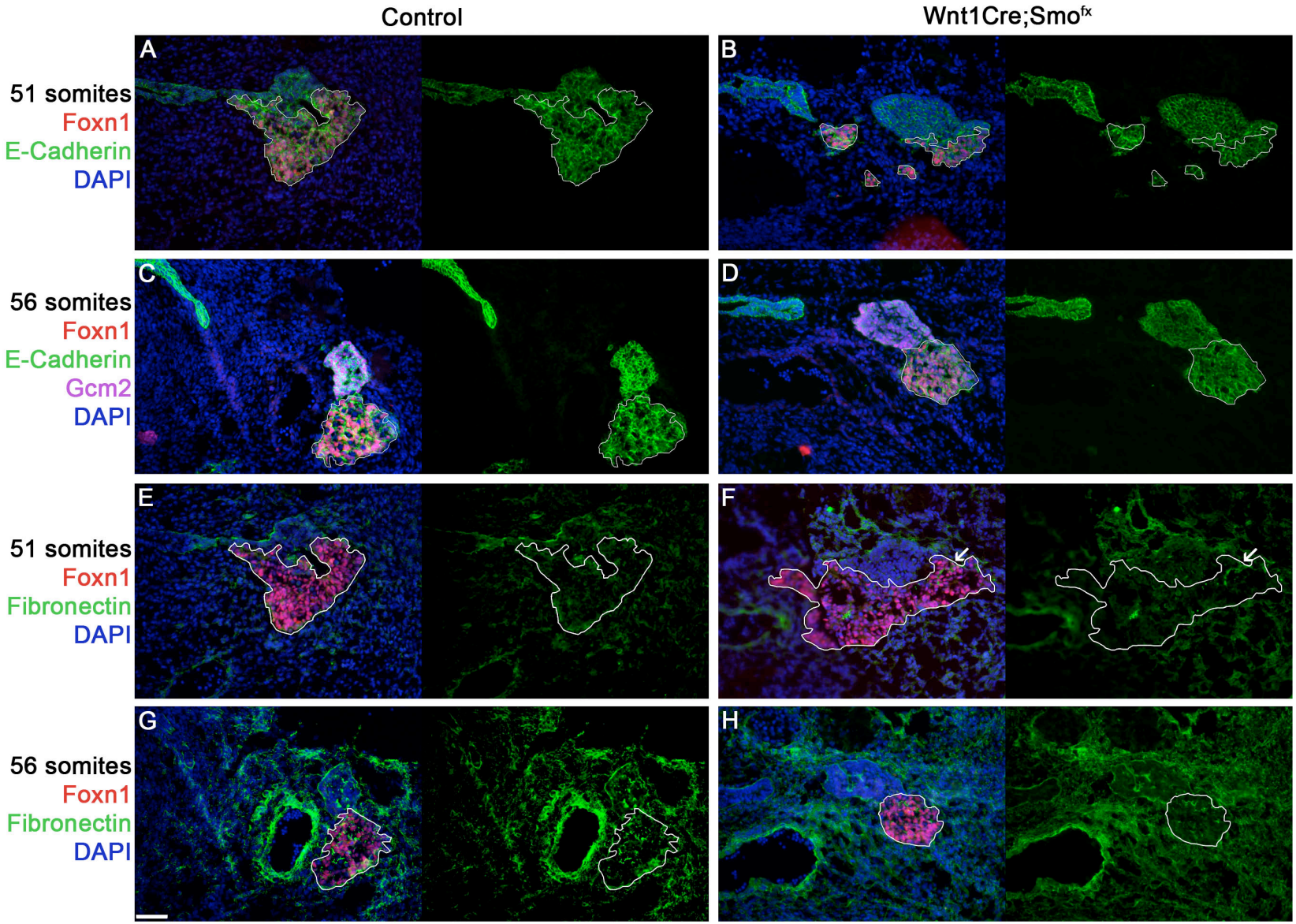
Control
Wnt1Cre;Smo^fx
A
B
51 somites
Foxn1
E-Cadherin
DAPI
C
D
56 somites
Foxn1
E-Cadherin
Gcm2
DAPI
E
F
51 somites
Foxn1
Fibronectin
DAPI
G
H
56 somites
Foxn1
Fibronectin
DAPI

Fig 2.7 Changes in organization in Wnt1Cre;Smo^{fx} embryos are accompanied by changes in fibronectin organization.

(A – D) Immunostaining for Foxn1, Gcm2, and E-cadherin at 51 and 56 somites. E-cadherin staining was uniform throughout thymus and parathyroid at 51 and 56 somites (A & C) and Wnt1Cre;Smo^{fx} fibronectin staining was comparable to wild type (B & D).

(E – H) Immunostaining for Foxn1 and Fibronectin at 51 and 56 somites. Fibronectin staining was found primarily in parathyroid at 51 somites in wild type (E). Parathyroid-like fibronectin staining was found in the Foxn1 domain (arrow) of Wnt1Cre;Smo^{fx} embryos at 51 somites. Fibronectin staining is found in parathyroid and thymus by 56 somites in wild type (G). Wnt1Cre;Smo^{fx} Fibronectin staining is comparable to wild type at 56 somites (H).

Scale bar indicates 50 μm

Figure 2.8

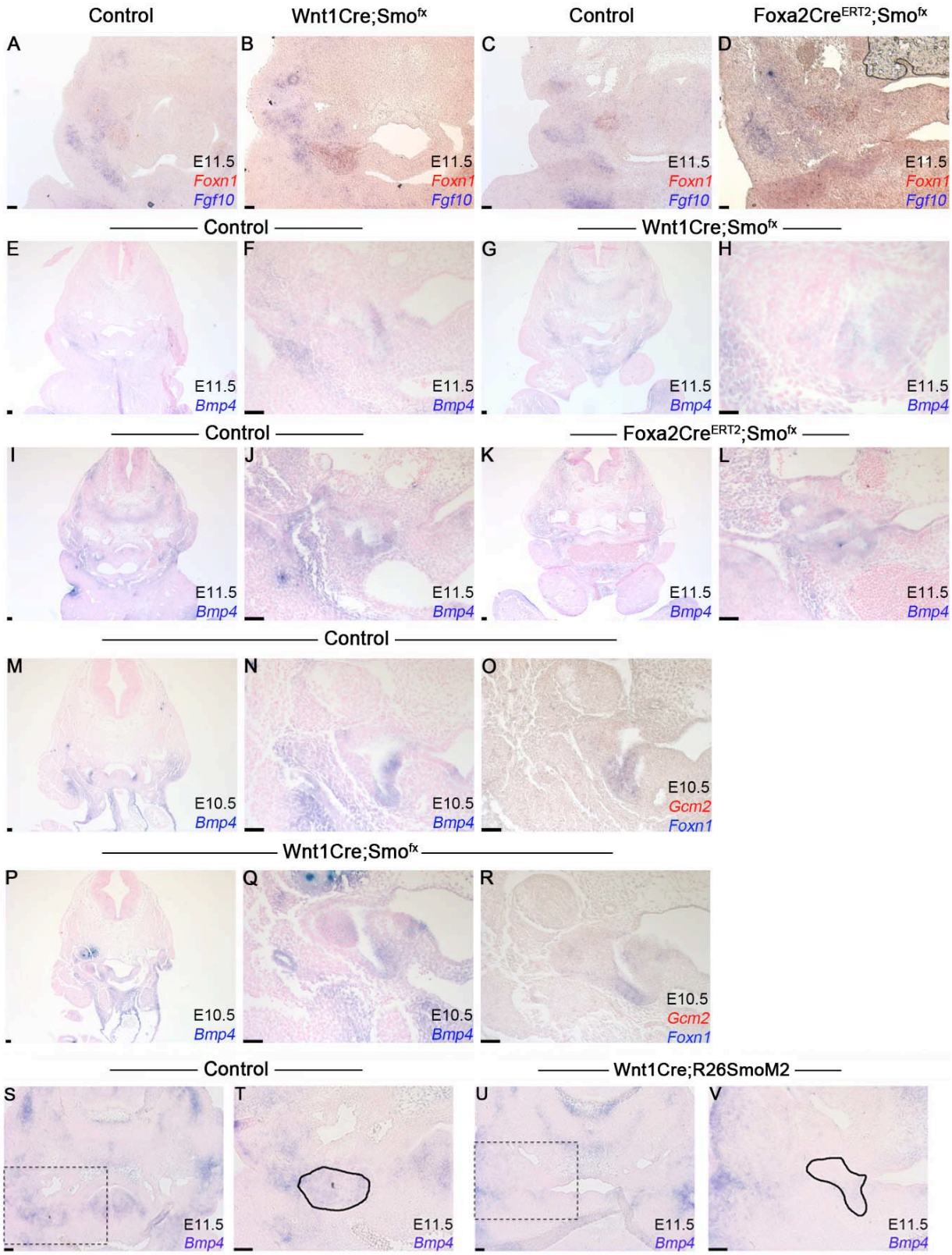
Control
Wnt1Cre;Smofx
Control
Foxa2CreERT2;Smofx
A
B
C
D
E11.5
Foxn1
Fgf10
Control
Wnt1Cre;Smofx
E
F
G
H
E11.5
Bmp4
Control
Foxa2CreERT2;Smofx
I
J
K
L
E11.5
Bmp4
Control
M
N
O
E10.5
Bmp4
E10.5
Gcm2
Foxn1
Wnt1Cre;Smofx
P
Q
R
E10.5
Bmp4
E10.5
Gcm2
Foxn1
Control
Wnt1Cre;R26SmoM2
S
T
U
V
E11.5
Bmp4

Fig. 2.8. Known mesenchymal signals surrounding the third pharyngeal pouch are normal when Shh signaling is deleted in neural crest mesenchyme or pouch endoderm.

(A-D) Transverse sections of dual Foxn1 (red) and Fgf10 (purple) in situs at E11.5. Fgf10 is found in mesenchyme surrounding the Foxn1 domain (A, C) as well as within the pouch (not shown) in wild type embryos at E11.5. Fgf10 expression in mesenchyme surrounding the Wnt1Cre;Smo^{fx} pouch (B) is similar to wild type at E11.5. Fgf10 expression in mesenchyme surrounding the Foxa2Cre^{ERT2};Smo^{fx} pouch (D) is also similar to wild type at E11.5. (E-L) Transverse sections of Bmp4 in situs at E11.5. Bmp4 is found in mesenchyme ventral to the pouch as well as in the presumptive Foxn1 domain of the pouch at E11.5 in wild type embryos (E, F, I, J). Very similar Bmp4 expression is found in Wnt1Cre;Smo^{fx} embryos (G, H) and Foxa2Cre^{ERT2};Smo^{fx} embryos (K, L). (M-R) Transverse sections of every other section Bmp4 (purple) and dual Foxn1(purple) and Gcm2 (red) in situs at 41 somites. Similar to E11.5, Bmp4 is found in ventral mesenchyme adjacent to the pouch as well as in the Foxn1 domain of the pouch in 41 somite wild type embryos (M – O). Bmp4 is found in ventral mesenchyme adjacent to the pouch as well as throughout the pouch of Wnt1Cre;Smo^{fx} embryos at 41 somites (P – R). Scale bars indicate 50 μm.

Figure 2.9

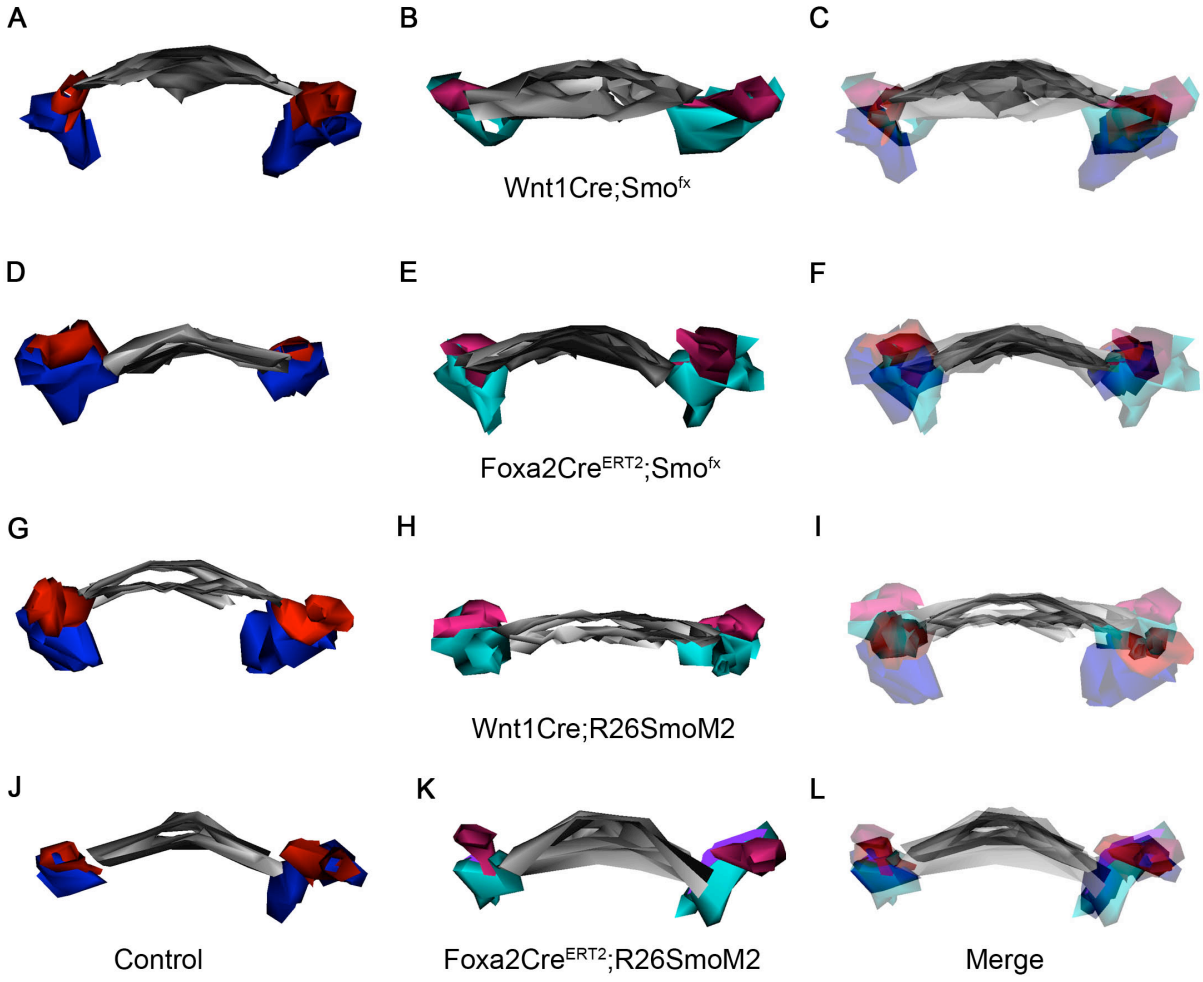
A
B
C
Wnt1Cre;Smo^fx
D
E
F
Foxa2Cre^ERT2;Smo^fx
G
H
I
Wnt1Cre;R26SmoM2
J
K
L
Control
Foxa2Cre^ERT2;R26SmoM2
Merge

Fig 2.9: Pharynx shape is altered at E11.5 when Shh signaling is deleted or constitutively activated in neural crest mesenchyme but is unchanged by altering Shh signaling in pouch endoderm.

(A, D, G, J) Anterior views of 3-D reconstructions of wild type littermates at E11.5. The Gcm2 domain (blue) is found at a more anterio-dorsal position within the pouch while the Foxn1 domain (red) is found at a more posterior-ventral position. The anterior pouch is still attached to the pharynx (gray). (B, E, H, K) Anterior views of 3-D reconstructions of Wnt1Cre;Smo^{fx} (B), Foxa2Cre^{ERT2};Smo^{fx} (E), Wnt1Cre;R26SmoM2 (H), and Foxa2Cre^{ERT2};R26SmoM2 (K) embryos at E11.5. Mutant pouches are shown in turquoise (Foxn1) and magenta (Gcm2). Unstained pouch is shown in purple. (C, F, I, L) Merged views of 3-D reconstructions of wild type littermates and mutant pouches for Wnt1Cre;Smo^{fx} (C), Foxa2Cre^{ERT2};Smo^{fx} (F), Wnt1Cre;R26SmoM2 (I), and Foxa2Cre^{ERT2};R26SmoM2 (L). Pharynx shape and pouch location change in response to deleting (C) or constitutively expressing (I) Smo in neural crest mesenchyme. Pharynx shape and pouch location are normal when Smo is deleted or constitutively expressed in pouch endoderm (F & L). All reconstructions made from transverse dual *in situs* for Foxn1 and Gcm2 (data not shown).

Figure 2.10

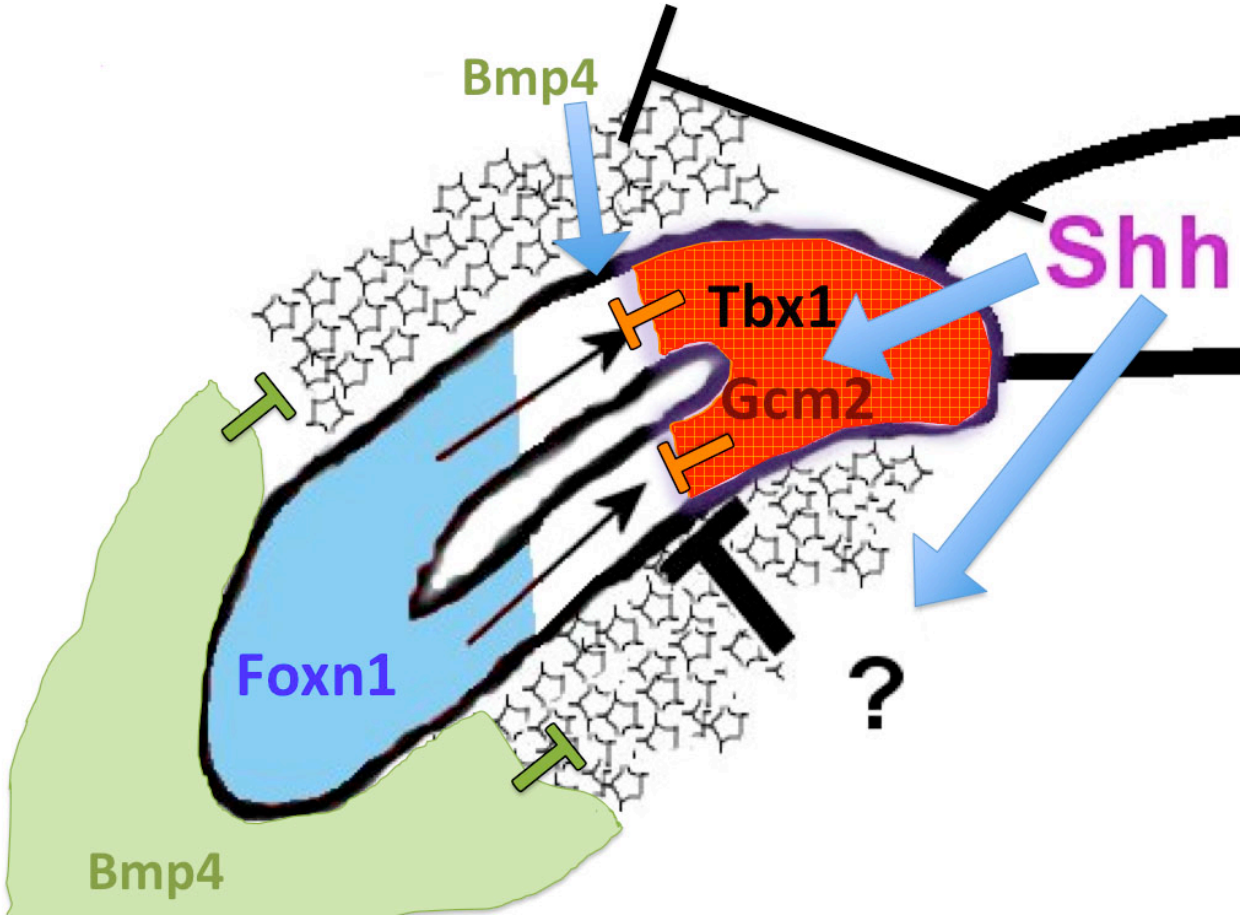

Fig 2.10 A model for the role of Shh signaling in third pouch boundary formation.

Shh signaling controls pouch patterning directly via *Tbx1* expression to inhibit *Foxn1* and permit *Gcm2* expression, and indirectly regulates the location of the border between the Foxn1 and Gcm2 domains through an as of yet identified second signal from neural crest mesenchyme. Shh signaling to neural crest mesenchyme is also able to inhibit Bmp4 expression and Bmp4 expression at and around the ventral-most region of the primordium may protect this Foxn1 positive region from the effects of Shh signaling.

Figure S.1

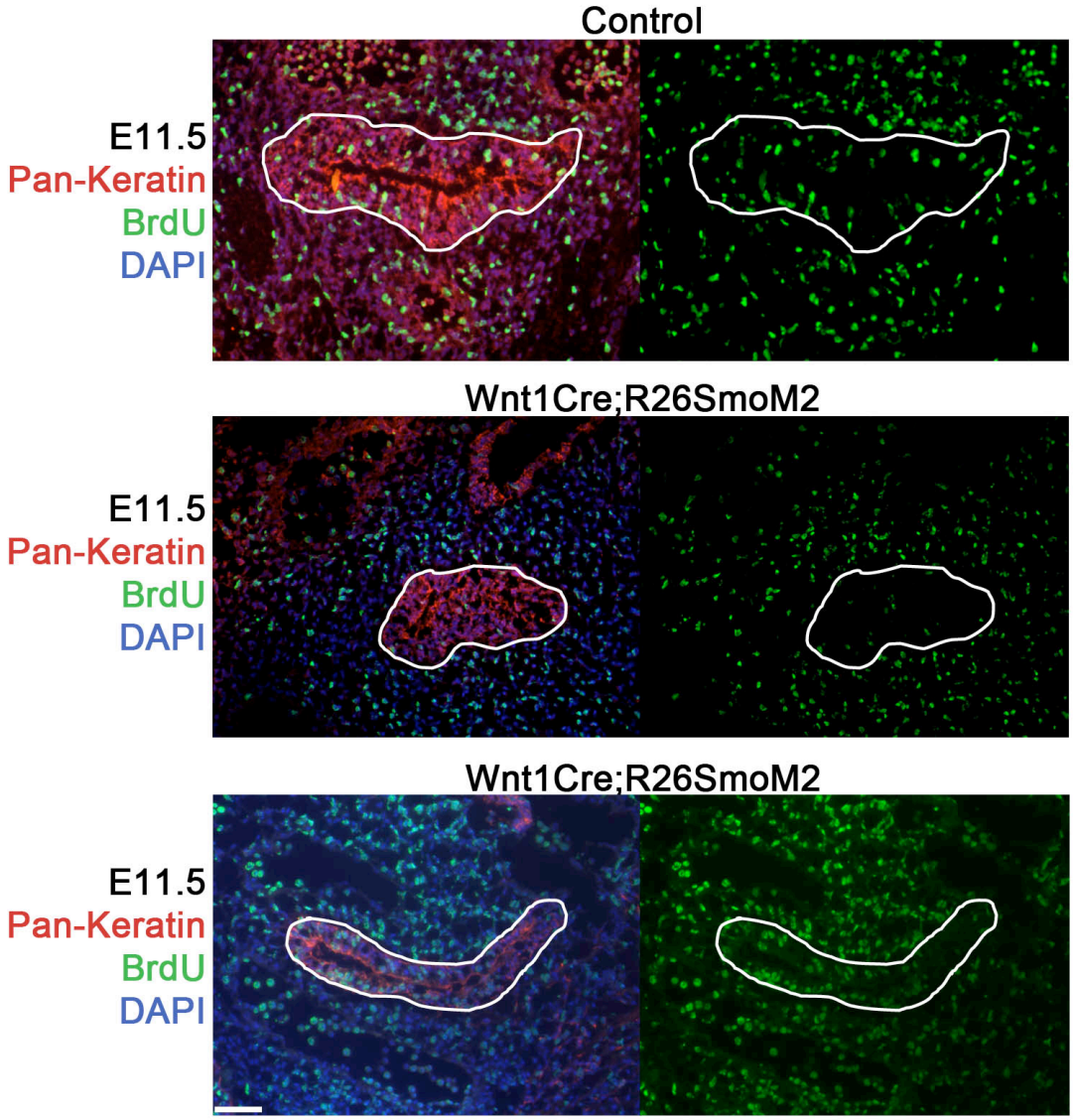
Control
E11.5
Pan-Keratin
BrdU
DAPI
Wnt1Cre;R26SmoM2
E11.5
Pan-Keratin
BrdU
DAPI
Wnt1Cre;R26SmoM2
E11.5
Pan-Keratin
BrdU
DAPI

Supplemental Figure 1: Proliferation is variable when Shh signaling is ectopically activated in neural crest mesenchyme

Proliferation occurs with common frequency in a wild type pouch at E11.5.

In one Wnt1Cre;Rosa26SmoM2 phenotype, the primordium was still essentially a single layer of epithelial cells, and the lumen was large. Many of the cells were BrdU-positive.

In another Wnt1Cre;Rosa26SmoM2 phenotype, the primordium on both sides was long and thin and it seemed many of the cells were BrdU-positive.

Scale bar indicates 50 μm.

Tables

Table 2.1: Intermingling between Foxn1 and Gcm2 positive cells decreases after 48 somites.

Somite Number	Foxn1 cells in Gcm2 domain	Gcm2 cells in Foxn1 domain
39	0	0
40	1.75 +/- .9	3.25 +/- 1
41	.17 +/- .2	1.17 +/- 1
42	10.75 +/- 1.5	6.75 +/- 1.3
45	15 +/- 4.0	9 +/- 4.2
46	12.5 +/- 1.5	5
47	18 +/- 2	8.33 +/- 1.2
48	19.29 +/- 2.7	6.86 +/- .8
49	8 +/- 1.6	3.75 +/- .5
50	7 +/- 1	4
56	0	0
60	0	0

Table 2.2. Percentage of the pouch covered by Foxn1 and Gcm2 domains in Shh signaling mutants with comparison to the Splotch mouse at E11.5.

	Domain split of various mutants				Wild type littermate controls			
	Foxn1 domain		Gcm2 domain		Foxn1 domain		Gcm2 domain	
Wnt1Cre;Smo^{fx}	72.8	$^{+}$/-2.2%	27.2	$^{+}$/-1.1%	73.4	$^{+}$/-3.8%	26.6	$^{+}$/-1.6%
Foxa2Cre^{ERT2};Smo^{fx}	72.3	$^{+}$/-3.8%	27.7	$^{+}$/-3.4%	70.0	$^{+}$/-8.0%	30.0	$^{+}$/-2.4%
Wnt1Cre;R26SmoM2	**84.0**	$^{+}$/-5.1%	**16.0**	$^{+}$/-2.2%	73.3	$^{+}$/-4.6%	26.7	$^{+}$/-3.4%
Foxa2Cre^{ERT2};R26SmoM2	**41.9**	$^{+}$/-3.6%	26.0	$^{+}$/-3.1%	71.7	$^{+}$/-3.8%	28.3	$^{+}$/-1.4%
Splotch	**78**%		**22**%		71%		29%	

References

Abu-Issa, R., G. Smyth, et al. (2002). "Fgf8 is required for pharyngeal arch and cardiovascular development in the mouse." Development 129(19): 4613-4625.

Arnold, J. S., U. Werling, et al. (2006). "Inactivation of Tbx1 in the pharyngeal endoderm results in 22q11DS malformations." Development 133(5): 977-987.

Bellusci, S., J. Grindley, et al. (1997). "Fibroblast growth factor 10 (FGF10) and branching morphogenesis in the embryonic mouse lung." Development 124(23): 4867-4878.

Blackburn, C. C. and N. R. Manley (2004). "Developing a new paradigm for thymus organogenesis." Nature reviews. Immunology 4(4): 278-289.

Bleul, C. C. and T. Boehm (2005). "BMP Signaling Is Required for Normal Thymus Development." The Journal of Immunology 175(8): 5213-5221.

Bockman, D. and M. Kirby (1984). "Dependence of thymus development on derivatives of the neural crest." Science 223(4635): 498-500.

Chapman, D. L., N. Garvey, et al. (1996). "Expression of the T-box family genes, Tbx1–Tbx5, during early mouse development." Developmental Dynamics 206(4): 379-390.

Conway, S. J., D. J. Henderson, et al. (1997). "Development of a lethal congenital heart defect in the splotch (Pax3) mutant mouse." Cardiovascular Research 36(2): 163-173.

Conway, S. J., J. Bundy, et al. (2000). "Decreased neural crest stem cell expansion is responsible for the conotruncal heart defects within the Splotch (Sp2H)/Pax3 mouse mutant." Cardiovascular Research 47(2): 314-328.

Crossley, P. H. and G. R. Martin (1995). "The mouse Fgf8 gene encodes a family of polypeptides and is expressed in regions that direct outgrowth and patterning in the developing embryo." Development 121(2): 439-451.

Danesin, C., J. N. Peres, et al. (2009). "Integration of telencephalic Wnt and hedgehog signaling center activities by Foxg1." Developmental cell 16(4): 576-587.

Danielian, P. S., D. Muccino, et al. (1998). "Modification of gene activity in mouse embryos in utero by a tamoxifen-inducible form of Cre recombinase." Current Biology 8(24): 1323-S1322.

Epstein, J. A., J. Li, et al. (2000). "Migration of cardiac neural crest cells in Splotch embryos." Development 127(9): 1869-1878.

Foster, K., J. Sheridan, et al. (2008). "Contribution of Neural Crest-Derived Cells in the Embryonic and Adult Thymus." The Journal of Immunology 180(5): 3183-3189.

Foster, K. E., J. Gordon, et al. (2010). "EphB‚Äìephrin-B2 interactions are required for thymus migration during organogenesis." Proceedings of the National Academy of Sciences 107(30): 13414-13419.

Franz, T. (1989). "Persistent truncus arteriosus in the Splotch mutant mouse." Anat Embryol (Berl). 180(5): 457-464.

Garg, V., C. Yamagishi, et al. (2001). "Tbx1, a DiGeorge syndrome candidate gene, is regulated by sonic hedgehog during pharyngeal arch development." Developmental biology 235(1): 62-73.

Goodrich, L. V., R. L. Johnson, et al. (1996). "Conservation of the hedgehog/patched signaling pathway from flies to mice: induction of a mouse patched gene by Hedgehog." Genes & Development 10(3): 301-312.

Gordon, J., A. R. Bennett, et al. (2001). "Gcm2 and Foxn1 mark early parathyroid- and thymus-specific domains in the developing third pharyngeal pouch." Mechanisms of Development 103(1-2): 141-143.

Gordon, J., V. A. Wilson, et al. (2004). "Functional evidence for a single endodermal origin for the thymic epithelium." Nature immunology 5(5): 546-553.

Gordon, J., S. R. Patel, et al. (2010). "Evidence for an early role for BMP4 signaling in thymus and parathyroid morphogenesis." Developmental biology 339(1): 141-154.

Gordon, J. and N. R. Manley (2011). "Mechanisms of thymus organogenesis and morphogenesis." Development 138(18): 3865-3878.

Grevellec, A., A. Graham, et al. (2011). "Shh signalling restricts the expression of Gcm2 and controls the position of the developing parathyroids." Developmental biology 353(2): 194-205.

Griffith, A. V., K. Cardenas, et al. (2009). "Increased thymus- and decreased parathyroid-fated organ domains in Splotch mutant embryos." Developmental biology 327(1): 216-227.

Itoi, M., N. Tsukamoto, et al. (2007). "Mesenchymal cells are required for functional development of thymic epithelial cells." International Immunology 19(8): 953-964.

Jeong, J., J. Mao, et al. (2004). "Hedgehog signaling in the neural crest cells regulates the patterning and growth of facial primordia." Genes & Development 18(8): 937-951.

Jerome, L. A. and V. E. Papaioannou (2001). "DiGeorge syndrome phenotype in mice mutant for the T-box gene, Tbx1." Nat Genet 27(3): 286-291.

Jiang, X., D. H. Rowitch, et al. (2000). "Fate of the mammalian cardiac neural crest." Development 127(8): 1607-1616.

Lan, Y. and R. Jiang (2009). "Sonic hedgehog signaling regulates reciprocal epithelial-mesenchymal interactions controlling palatal outgrowth." Development 136(8): 1387-1396.

Liao, J., L. Kochilas, et al. (2004). "Full spectrum of malformations in velo-cardio-facial syndrome/DiGeorge syndrome mouse models by altering Tbx1 dosage." Human molecular genetics 13(15): 1577-1585.

Liu, Z., S. Yu, et al. (2007). "Gcm2 is required for the differentiation and survival of parathyroid precursor cells in the parathyroid/thymus primordia." Developmental biology 305(1): 333-346.

Long, F., X. M. Zhang, et al. (2001). "Genetic manipulation of hedgehog signaling in the endochondral skeleton reveals a direct role in the regulation of chondrocyte proliferation." Development 128(24): 5099-5108.

Machado, A. F., L. J. Martin, et al. (2001). "Pax3 and the splotch mutations: structure, function, and relationship to teratogenesis, including gene-chemical interactions." Curr Pharm Des. 7(9): 751-785.

Manley, N. R. and M. R. Capecchi (1995). "The role of Hoxa-3 in mouse thymus and thyroid development." Development 121(7): 1989-2003.

Manley, N. R., L. Selleri, et al. (2004). "Abnormalities of caudal pharyngeal pouch development in Pbx1 knockout mice mimic loss of Hox3 paralogs." Developmental biology 276(2): 301-312.

Manley, N. R. and B. G. Condie (2010). "Transcriptional Regulation of Thymus Organogenesis and Thymic Epithelial Cell Differentiation." 92: 103-120.

Merscher, S., B. Funke, et al. (2001). "TBX1 Is Responsible for Cardiovascular Defects in Velo-Cardio-Facial/DiGeorge Syndrome." Cell 104(4): 619-629.

Miyamoto, S., B.-Z. Kathz, et al. (1998). "Fibronectin and Integrins in Cell Adhesion, Signaling, and Morphogenesis." Annals of the New York Academy of Sciences 857(1): 119-129.

Moore-Scott, B. A. and N. R. Manley (2005). "Differential expression of Sonic hedgehog along the anterior-posterior axis regulates patterning of pharyngeal pouch endoderm and pharyngeal endoderm-derived organs." Developmental biology 278(2): 323-335.

Ohnemus, S., B. Ã. Kanzler, et al. (2002). "Aortic arch and pharyngeal phenotype in the absence of BMP-dependent neural crest in the mouse." Mechanisms of Development 119(2): 127-135.

Ohuchi, H., Y. Hori, et al. (2000). "FGF10 Acts as a Major Ligand for FGF Receptor 2 IIIb in Mouse Multi-Organ Development." Biochemical and Biophysical Research Communications 277(3): 643-649.

Pani, L., M. Horal, et al. (2002). "Rescue of neural tube defects in Pax-3-deficient embryos by p53 loss of function: implications for Pax-3- dependent development and tumorigenesis." Genes & Development 16(6): 676-680.

Park, E. J., X. Sun, et al. (2008). "System for tamoxifen-inducible expression of cre-recombinase from the Foxa2 locus in mice." Developmental dynamics : an official publication of the American Association of Anatomists 237(2): 447-453.

Patel, S. R., J. Gordon, et al. (2006). "Bmp4 and Noggin expression during early thymus and parathyroid organogenesis." Gene expression patterns : GEP 6(8): 794-799.

Pringle, N. P. and W. D. Richardson "In situ hybridization protocols." www.ucl.ac.uk/~ucbzwdr/In%20Situ%20Protocol.pdf.

Revest, J.-M., R. K. Suniara, et al. (2001). "Development of the Thymus Requires Signaling Through the Fibroblast Growth Factor Receptor R2-IIIb." The Journal of Immunology 167(4): 1954-1961.

Shook, D. and R. Keller (2003). "Mechanisms, mechanics and function of epithelial‚Äìmesenchymal transitions in early development." Mechanisms of Development 120(11): 1351-1383.

Wang, J., A. Nagy, et al. (2006). "Defective ALK5 signaling in the neural crest leads to increased postmigratory neural crest cell apoptosis and severe outflow tract defects." BMC developmental biology 6(1): 51.

Watanabe, Y., D. Duprez, et al. (1998). "Two domains in vertebral development: antagonistic regulation by SHH and BMP4 proteins." Development 125(14): 2631-2639.

Wei, Q. and B. G. Condie (in press). "Data mining and in situ hybridization screen identify potential transcription regulators of thymus development." PLoS ONE.

Yamagishi, H., J. Maeda, et al. (2003). "Tbx1 is regulated by tissue-specific forkhead proteins through a common Sonic hedgehog-responsive enhancer." Genes & Development 17(2): 269-281.

Zhang, Y., Z. Zhang, et al. (2000). "A new function of BMP4: dual role for BMP4 in regulation of Sonic hedgehog expression in the mouse tooth germ." Development 127(7): 1431-1443.

Zhang, Z., T. Huynh, et al. (2006). "Mesodermal expression of Tbx1 is necessary and sufficient for pharyngeal arch and cardiac outflow tract development." Development 133(18): 3587-3595.

Zhao, X., Z. Zhang, et al. (2000). "Transgenically ectopic expression of Bmp4 to the Msx1 mutant dental mesenchyme restores downstream gene expression but represses Shh and Bmp2 in the enamel knot of wild type tooth germ." Mechanisms of Development 99(1-2): 29-38.

CHAPTER 3

AP-2α CONTROLS CELL DEATH OF ECTODERMAL CLEFT DURING THYMUS ORGANOGENESIS.

To be submitted to *Developmental Biology*. Virginia Bain, Julie Gordon, Brian Hartley, Trevor Williams, and Nancy Manley

Abstract

The four pharyngeal pouches form between E8.5 and E9.5 in mice and are endodermal tissue pockets that extend from the pharynx to the surface ectoderm at the earliest stages. The parathyroid domain is patterned within the third pharyngeal pouch by E10.5 and the remaining pouches expresses the thymus marker *Foxn1* by E11.25. At the same time, the thymus rudiment contacts both the surface ectoderm and the pharynx. To develop normally, the thymus and the parathyroids must separate from the pharynx, the surface ectoderm, and one another. To date, mutants have been identified that affect each of these processes, except for separation from the ectoderm. Evidence from *AP-2α* null mice indicates a role for *AP-2α* in separation of the thymus from surface ectoderm.

The transcription factor *AP-2α* is expressed in ectoderm and neural crest cells and is involved in the closure of the ventral body wall and the neural tube. In *AP-2α* mutants the thymus fails to dissociate from the ectoderm and is located ectopically. We used a genetic approach to determine if *AP-2α* expression in ectoderm or neural crest is required for separation of the thymus from ectoderm. We find that when *AP-2α* is deleted globally, the thymus marker *Foxn1* is expressed in all cells of the thymus rudiment, including cells at the surface of the embryo, while parathyroid formation and separation of the thymus from the pharynx are relatively normal. We find dosage sensitivity in the global *AP-2α* deletion with a less severe thymus phenotype in heterozygous littermates. We did not find a more severe phenotype when *AP-2α* is deleted only in ectoderm or in neural crest (Brewer et al 2004). These data suggest a model in which *AP-2α* from ectoderm and neural crest mesenchyme are both sufficient at precise levels to separate thymus from ectodermal cleft.

Introduction

AP-2α is a member of the AP-2 family of transcription factors, which are involved in establishment of neural crest cell identity and survival of surrounding tissues (Nottoli et al 1998). Evidence suggests the roles of AP-2 transcription factors in establishing neural crest cell identity and ectoderm survival are separate, and that neural crest cell identity is a cell autonomous role while ectoderm survival is non-cell autonomous (Knight et al 2005).

AP-2α is expressed mostly in ectoderm and neural crest cells. It is found in the progress zone of the limb bud, in the kidney, in the eye, and at the surface ectoderm (Mitchell et al 1991). Recently, *AP-2α* has also been shown to have multiple roles in neural crest development: an early role mediating Wnt signaling in establishment and maintenance of the neural border and a later role in neural crest maintenance (Crozé et al 2011). *AP-2α* is also expressed in cardiac neural crest cells, which are involved in the development of the thymus, parathyroid, and thyroid (Brewer et al 2002).

Because *AP-2α* is expressed in several places and has multiple functions, recent experiments have used gene-mediated Cre knockouts of *AP-2α* to determine tissue specific roles of *AP-2α*. *AP-2α* null embryos are an ideal system to study body wall closure defects because they have a fully penetrant ventral body wall defect but are viable throughout gestation (Brewer et al 2004). However, *AP-2α* is unique among mutants with body wall closure defects in that other body wall closure deficient mice do not report ectopic thymi and thymus is shown comparable to wild type in size and location in TGFβ2$^{-/-}$;TGFβ3$^{-/-}$ embryos (Suzuki et al 1996, Manley et al 2001, Dunker et al 2002). The lack of a thymus phenotype in most body wall closure deficient mice indicates that ectopic thymus is not a secondary effect of body wall closure defects and instead suggests a unique role for *AP2α* in thymus morphogenesis.

The thymus and parathyroid derive from third pharyngeal pouch endoderm. This endoderm begins as a single cell layer that extends laterally within the embryo from pharynx to surface ectoderm by E9.5. This 3rd pharyngeal pouch endoderm continues to proliferate and undergoes patterning to establish parathyroid and thymus domains that express organ-specific genes by E10.5 and E11.25, respectively (Gordon et al., 2001). For successful organogenesis, the thymus and parathyroid must separate from the pharynx, ectoderm, and each other before migrating to their correct anatomical position (Gordon and Manley 2011). The *AP-2α* mutant has a unique phenotype among third pouch mutants in that the thymus remains attached at the surface of the embryo, but does separate from the pharynx (Brewer et al 2002).

The *AP-2α* mutant's thymus phenotype raises a question about which sources of *AP-2α* within the embryo contribute to thymus and opens the possibility of altered fate of the tissue at the surface of the embryo. To investigate the role of *AP-2α* we examined thymus development in an ectoderm specific deletion of *AP-2α*, a neural crest specific deletion of *AP-2α*, and the *AP-2α* null. We identified the precise time of separation of thymus from ectodermal cleft as the 47 - 49 somite stage. We found that *AP-2α* from neural crest is required for cell death of the ectodermal cleft, that this requirement is dosage sensitive, and that in the absence of this cell death the thymus fails to separate properly. We also found that the ectodermal cleft fails to die in the *AP-2α* null mutant, and expresses markers for both thymus and parathyroid. We interpret these data to mean that the ectodermal cleft is fusing with the proper thymus and parathyroid domains from the 3rd pouch-derived endodermal primordium, and acquiring a new fate. We found no involvement of *AP-2α* in thymus or parathyroid development from ectoderm alone.

Materials and Methods

Mice:

$Gcm2^{EGFP}$ mice, tdTomato mice, and Foxn1Cre mice were purchased from The Jackson Laboratory (Bar Harbor, ME) and crossed to generate $Gcm2^{EGFP}$;$Foxn1Cre^{tdTomato}$ embryos.

Matings were monitored on a daily basis and the day of the vaginal plug was designated embryonic day 0.5. Embryos were also staged by somite number and morphological cues such as eye and limb development. Genotyping was performed on yolk sac DNA using previously described primers ().

AP-2a:$LacZ^{KI/KI}$ and EctoCre;AP-2a:$LacZ^{KI/fx}$ mice were provided and genotyped by our collaborators from the Williams lab (Brewer et al., 2002; Brewer et al., 2004). All experiments were carried out with the approval of the UGA Committee for Animal Use in Research and Education.

Tissue preparation:

All embryos collected were fixed in 4% PFA and dehydrated. Embryos collected for frozen immunostaining were briefly fixed (20 min (E10.5), 30 min (E11.5-E13.5)), thoroughly washed in PBS (10 2' washes), dehydrated in sucrose (1 hour 5% sucrose, 4 hours 15% sucrose), and embedded in OCT. Sections were cut on a cryostat at 8 μm thickness. Embryos collected for paraffin immunostaining were fixed for 1 hour, thoroughly washed in PBS, dehydrated in an ethanol gradient, permeabilized in xylenes, and embedded in paraffin. Sections for immunostaining were cut on a Leica RM2155 microtome at 8 μm thickness. Embryos collected for *in situ* were kept cold at all steps and RNase free reagents were used. Sections for *in situ* were cut at 12 μm thickness.

Section and whole-mount *In situ hybridization*:

Whole mount and paraffin section *in situ* hybridizations were performed as described (Manley and Capecchi, 1995; Moore-Scott and Manley, 2005), using mutant embryos and littermate controls. Each probe was analyzed on a minimum of 2-3 embryos per stage. Probes for *Pax1* (Manley and Capecchi, 1995), *Fgf8* (Crossley and Martin, 1995), *Tbx1* (Chapman et al., 1996), and *Foxn1*(Gordon et al., 2001), have been previously described. Probe template was made by PCR using plasmid with primers for T3, T7, and SP6. Probes for single color *in situ* were made using DIG-UTP. Single color *in situs* were counterstained with nuclear fast red.

Immunostaining:

Immunostaining was performed on paraffin embedded or frozen tissue fixed in 4% PFA. Paraffin embedded tissue was washed twice in xylene to remove the paraffin and then briefly washed in 100%, 90%, 70%, and 30% EtOH before being placed in PBS. Paraffin embedded immunostaining required an antigen retrieval step in which tissue was boiled in AR buffer (10mM Na_3Citrate pH6, 0.05% Tween20) for 30 minutes. Slides were allowed to cool to room temperature in the buffer for an additional 20 minutes. Slides were then incubated overnight with primary antibody, 5% donkey serum, and .05% Triton-X in PBS. The next day slides were washed once in PBS and then incubated with secondary antibody in PBS for one hour at room temperature in the dark. Slides were then washed three times in PBS with the middle wash containing DAPI. Slides were mounted with EMS-Fluorogel and coverslipped for visualization. Frozen tissue was processed as described above with the exception of xylene, rehydration and antigen retrieval. Antibodies used were goat anti-Foxn1 (1:200 Santa Cruz G-20), rabbit anti-Gcm2 (1:200 abcam ab64723), rabbit anti-Cleaved Caspase-3 (1:200 cell signaling), and Ikaros

(1:100, Santa Cruz, M-20). All secondaries were DyLight (Jackson Immunoresearch) dyes: Alexa (Invitrogen) dyes were used as a last resort if DyLight dyes were unavailable.

X-gal staining:

Embryos for X-gal staining were processed as described (Gordon et al., 2001). After staining, whole mount pictures were taken using a Zeiss SteRIO dissecting microscope and then embryos were processed for paraffin embedding and sectioned on a Leica RM2155 microtome at 10 μm thickness.

Three dimensional reconstruction:

3-D reconstructions were made from serial sections using SurfDriver WinSurf 4.3 software.

Results

***AP-2α* is expressed in surface ectoderm and neural crest cells surrounding the third pharyngeal pouch.**

To identify all potential sources of *AP-2α* in and around the third pharyngeal pouch we examined a heterozygous AP-2α:LacZ knock-in (AP-2α:LacZ$^{KI/+}$) embryo (Brewer et al 2002). We found strong staining in the pharyngeal ectoderm next to the pharyngeal pouches at E9.5. We also found some b-galactosidase staining in neural crest cells in the mesenchyme surrounding the pouch (Fig. 1A). At E11.5, we still saw strong ectodermal expression and some neural crest expression of *AP-2α*.(Fig. 1B). We did not see *AP-2α* in the thymus primordium during the crucial window for separation from surface ectoderm; however, we did see it in the ectodermal cleft attaching pharyngeal pouch to surface ectoderm (Fig. 1C).

Initial pouch patterning is normal in the absence of *AP-2α*

While the *AP-2α* null thymus phenotype was briefly mentioned in an earlier study, several questions remain about the origin of thymus found at the surface of the embryo as well as a question of functionality. To address these questions we first looked at markers for third pouch endoderm.

Fgf8 is essential for survival of neural crest cells surrounding third pharyngeal pouch (Abu-Issa 2002). *Fgf8* is normally expressed at E10.5 in the otic vesicle, the second, third, and fourth pharyngeal pouches, and cleft ectoderm, but is not present in the thymus or parathyroid at E11.5 (Fig 2A). Because the thymus was found in an ectopic location in *AP-2α* mutants, we looked at *Fgf8* expression at E11.5. While *Fgf8* was absent in the thymus or parathyroid of AP-2α:LacZ$^{KI/KI}$ mutants at E11.5, we saw ectopic *Fgf8* expression in the ectodermal clefts (Fig 2B).

H&E staining at E10.5 (Fig 2C) also indicated that AP-2α:LacZ$^{KI/KI}$ embryos had normal morphology (Fig 2D). Normal morphology suggested that pouch development was normal at E10.5 and that the defect in AP-2α:LacZ$^{KI/KI}$ embryos occurred at a later stage, which we further confirmed by ectopic patterning gene expression at E11.5.

Lack of *AP-2a* results in an ectopic thymus and parathyroid.

By E11.5 in wild type embryos, the third pharyngeal pouch is divided into *Foxn1* positive thymus and *Gcm2* positive parathyroid domains. Foxn1 positive cells are located in the posterior and ventral thymus domain within pharyngeal endoderm, separated from the surface of the embryo by a thick layer of mesenchyme at E11.5 (Fig 3A). In an AP-2α:LacZ$^{KI/KI}$ embryo, we saw Foxn1 positive cells within the third pouch as usual, but also saw ectopic Foxn1 positive cells within ectodermal cleft and at the surface of the embryo (Fig. 3B). Pouch shape was also altered in the AP-2α:LacZ$^{KI/KI}$ embryo. While the wild type pouch at E11.5 is typically wedge-

shaped, with a small lumen and minimal attachment to pharynx, the mutant pouch fails to close and form a lumen, and attaches to ectodermal cleft in a serpentine-like structure (Fig. 3D). In an AP-2α:LacZ$^{KI/+}$ embryo, Foxn1 positive cells were present within the third pouch and (fewer) in the ectodermal cleft; in addition the pouch was in an ectopic location closer to the surface of the embryo than in wild-type (Fig 3E). Gcm2 positive cells were also present in the anterior dorsal parathyroid domain within pharyngeal endoderm at E11.5 in wild type mice (Fig 3A). In an AP-2α:LacZ$^{KI/KI}$ mouse, we found Gcm2 positive cells within the third pouch as well as within ectodermal cleft (Fig. 3D). It is possible that the ectodermal cleft expresses both *Foxn1* and *Gcm2* with little domain specific regulation as Fig 3B and Fig 3D are consecutive sections. In contrast, we found Gcm2 positive cells in a location comparable to wild type in an AP-2α:LacZ$^{KI/+}$ embryo at E11.5 (Fig 3F).

At E12.5 the wild type thymus was no longer attached to surface ectoderm or pharynx but the thymus had yet to begin migration (Fig. 3G). We found the parathyroid interior to the arch artery, yet the thymus remained outside of the arch artery. In an AP-2α:LacZ$^{KI/KI}$ embryo at E12.5 the thymus had detached from the pharynx, but had not detached from the surface ectoderm and was located at the surface of the embryo (Fig. 3H). Additional thymus connected to the primary thymus and the surface of the embryo was also found in a location where third pharyngeal pouch originated from, suggesting that thymus came from two sources in AP-2α:LacZ$^{KI/KI}$ embryos: third pouch endoderm and ectodermal cleft. In addition to its abnormal location, the AP-2α:LacZ$^{KI/KI}$ thymus had several cysts as of E12.5. In AP-2α:LacZ$^{KI/+}$ embryos the thymus was still attached to the ectodermal cleft (Fig. 3I); however, when following thymus and cleft throughout transverse serial sections, we found a break between the cleft attached to thymus and unattached ectodermal cleft (Fig. 5E).

By E14.5, the wild type thymus has migrated posteriorly and ventrally and it is located just anterior to the heart (Fig. 3J). As shown by 3-D reconstruction, normal development of the thymus and parathyroid entails migration of the thymus (red) to a posterior location above the heart. This migration pulls the parathyroid (turquoise) to a location between the pouch origin and the heart next to thyroid (purple) (Fig 3P). In an AP-2α:LacZ$^{KI/KI}$ embryo, the thymus was still attached to the surface of the embryo, and extended ventrally and posteriorly such that the most posterior location was slightly ectopic to the wild-type location (Fig. 3K). The capsule surrounding the portion of thymus found at the surface of the embryo failed to cover the exposed side of the thymus but was otherwise comparable to wild type (Fig. 3L, 3M). Parathyroid was comparable to wild type at this stage as shown by 3-D reconstruction of H&E sections. In an AP-2α:LacZ$^{KI/+}$ embryo thymus morphology was more similar to wild type, but was still attached to the surface ectoderm. Ectopic thymus lobes were found next to parathyroids, but extended to contact the surface of the embryo in the most anterior region of the thymus. Thymus lobes were longer than wild type along the anterior/posterior axis and the more posterior limit of the AP-2α:LacZ$^{KI/+}$ thymus was similar to wild type (Fig. 3N). Organization of the thymic capsule of the AP-2α:LacZ$^{KI/+}$ embryo was abnormal, in that it impinged on the epithelial thymus rudiment in some places (Fig. 3O).

Separation of thymus from surface ectoderm occurs at the ectodermal cleft.

Earlier work from the Manley lab indicated that separation of thymus from ectoderm occurred at the ectodermal cleft sometime between E11.75 and E12 (Gordon et al 2004). To precisely identify the timing of cell death in the ectodermal cleft, embryos with transgenic markers for Foxn1 and Gcm2 from 45 – 50 somite stages were stained with an antibody for cleaved-caspase 3. We found that cell death in the ectodermal cleft occurred between 47 and 49

somites (Fig 4A). After this cell death, the ectodermal cleft was no longer visible and thymus was not attached to ectoderm as shown by a break in E-Cadherin staining at 51 somites (Fig 4B).

We next examined the ectodermal cleft in AP-2α:LacZ$^{KI/KI}$ embryos to determine if separation was impaired. While cell death occurred in the ectodermal cleft at 47 somites in AP-2α:LacZ$^{KI/KI}$ embryos, the pattern of cell death was not restricted to ectodermal cleft and instead was found in cleft and pouch whereas wild type pouch had little cell death at this time, and the thymus failed to separate from the ectodermal cleft (Fig 4C). Cell death was also abnormal in AP-2α:LacZ$^{KI/+}$ embryos, suggesting that cell death of the ectodermal cleft required tight regulation of AP-2α (Fig 4D).

Ectodermal AP-2α is not required for patterned cell death within the ectodermal cleft.

To address potential contributions of AP-2α from surface ectoderm and neural crest mesenchyme, we utilized a conditional allele of AP-2α (Alflox) crossed to tissue specific Cre strains for ectoderm or Wnt1, as well as one copy of the knock-in allele (Danielian 1998, Brewer 2004). Neural crest contributions of AP-2α were addressed in a previous study. No thymus phenotype was reported in the Wnt1-Cre mediated deletion of AP-2α, suggesting that AP-2α from neural crest downstream of Wnt signaling was not required for thymus development (Brewer 2004).

To address contributions of AP-2α from surface ectoderm, the AP-2α:LacZ^{ki} allele was crossed to an ectoderm specific cre strain, and EctoCre;AP-2α:LacZ$^{ki/+}$ offspring were mated to homozygous Alflox mice to produce EctoCre;AP-2α:LacZ$^{ki/flx}$ mutants. Specificity of the Ectoderm-cre was confirmed using Rosa26LacZ, which showed activity throughout the ectoderm and little expression in endoderm or mesenchyme at E11.5, and was completely ectoderm specific by E12.5 (Fig 5A, 5B). Surprisingly, EctoCre;AP-2α:LacZ$^{ki/+}$ mutants were not more

severe than AP-2α:LacZ$^{KI/+}$ embryos at any stage assayed. (Fig 5C, 5D, 5E, 5F). These data indicate that complete deletion of AP-2α from ectoderm did not exacerbate global haploinsufficiency for AP-2α.

Thymus function is reduced or delayed in the absence of *AP-2α*.

The thymus provides specific microenvironments required for T-cell differentiation. For thymus to function normally, it must attract lymphoid progenitor cells and provide specific microenvironments within thymic epithelial cells to select for and against T-cells (Blackburn and Manley 2004). To assay thymus function, we looked at lymphoid progenitor cell attraction and organization of medulla and cortex. In wild type embryos and AP-2α:LacZ$^{KI/+}$ embryos, lymphoid progenitor cells were attracted to the third pharyngeal pouch by CCL25 signaling, starting at E11.5 (Fig 6A, 6B). However, in AP-2α:LacZ$^{KI/KI}$ embryos, lymphoid progenitor cells were greatly reduced at E11.5 (Fig 6C). These results suggest that although Foxn1 is expressed in the thymus domain, there may be additional defects in thymic epithelial cell differentiation that affect thymus function.

Discussion

In this paper we examined the role of *AP-2α* in thymus development. We confirmed earlier work suggesting that in wild type mice the thymus separates from the ectodermal cleft by precisely patterned cell death from 47 – 49 somites. We found that *AP-2α* is required for proper placement of cell death within the ectodermal cleft from 47 – 49 somites and that this requirement is haploinsufficient. We also found that in the absence of *AP-2α*, the ectodermal cleft acquires expression of third pouch patterning genes that allow it to adopt thymus and parathyroid fate. Finally, we found that the thymus formed in the absence of *AP-2α* lacks proper function. Taken together, these findings suggest that *AP-2α* is necessary for separation of third

pouch endoderm from ectodermal cleft and that *AP-2α* may serve several roles in thymus development.

Patterning is normal at E10.5 in the absence of *AP-2α*; however, ectopic patterning within the ectodermal clefts persists at E11.5.

The *AP-2α* null pouch closely resembled wild type at E10.5, both in morphology and patterning. Both *Fgf8* and *Tbx1* are expressed in wild type third pharyngeal pouch and are required to establish organ fates, and *Fgf8* is also found in ectodermal clefts at E10.5. By E11.5 *Fgf8* is no longer expressed in or near the third pharyngeal pouch in a wild type embryo; however, ectopic *Fgf8* was found in the ectodermal clefts of AP-2α:LacZ$^{ki/ki}$ embryos at E11.5. These clefts also ectopically expressed *Foxn1* and *Gcm2* in the *AP-2α* null. We hypothesize that mis-expression of Fgf8 in the ectodermal clefts allowed it to adopt a third pouch fate. *AP-2α* is involved in establishing anterior-posterior identity within an embryo and *Fgf8* is normally found in the first ectodermal cleft at E11.5. Possibly, in the absence of *AP-2α*, all ectodermal clefts express *Fgf8* at E11.5 allowing other pouch patterning genes near the third ectodermal cleft to induce third pouch identity. These may include signaling molecules normally repressed in the neural crest near the surface ectoderm that are de-repressed in the absence of *AP-2α*.

Separation of thymus from ectoderm is caused by *AP-2α* induced cell death of the ectodermal cleft from 47 – 49 somites.

The third pharyngeal pouch is attached to the surface of the embryo at the third ectodermal cleft until 47 – 49 somites, at which time the cleft undergoes apoptosis to detach the pouch endoderm from the surface ectoderm. In *AP-2α* heterozygous and null mice, cell death in and around the third ectodermal cleft is still present; however, the precise pattern of cell death necessary to detach endoderm from ectoderm fails to occur. In *AP-2α* heterozygous mice,

detachment is delayed by a day and occurs after migration begins. It is possible that the connection between cleft and pouch is tenuous due to present but unpatterned apoptosis within the cleft and pouch and that tension from migration is sufficient to break the connection. The thymus is still attached to ectodermal cleft when it starts migrating and it is possible that this attachment alters the shape of the thymus and may be related to abnormal organization of the thymic capsule in some places. However, it is also possible that AP-2α in neural crest cells has some function in capsule organization. We do not know if this role for *AP-2α* is independent of altered patterning genes in ectodermal cleft. While *AP-2α* is only expressed in ectoderm and neural crest cells, improper regulation of cell death in *AP-2α* heterozygous and null mice causes ectopic cell death within the third pouch, as well as a dispersal of the expected cell death within the ectodermal cleft. Because altered patterning of *Fgf8* only occurs in ectodermal cleft and not within the pouch, patterning and cell death regulation may be two separate functions for *AP-2α* .

Thymus development is dosage sensitive to *AP-2α* but indifferent to its location.

While the *AP-2α* null phenotype is quite severe, with fusion of third pouch and ectodermal cleft and its persistent attachment to the surface of the embryo, all mice heterozygous for *AP-2α* shared a much milder phenotype. Because *AP-2α* is expressed in both neural crest mesenchyme and ectoderm, we expected to see different phenotypes for tissue specific deletions of *AP-2α*. We were surprised to find that both the neural crest deletion and the ectoderm deletion of *AP-2α* were very similar to the *AP-2α* heterozygous phenotype with respect to thymus development. These data suggest a signal (or signals) downstream of *AP-2α* in both tissues is required to place cell death within the ectodermal cleft. This signal may also restrict cell death from third pharyngeal pouch.

AP-2α is required for separation of thymus from ectodermal cleft. In the absence of *AP-2α*, ectodermal cleft both fails to die and adopts third pouch fate. We were unable here to identify unique contributions of *AP-2α* from ectoderm or neural crest to placement of cell death and ectodermal cleft patterning. Identifying the signals downstream of *AP-2α* in both neural crest and ectoderm that are responsible for placement of cell death within cleft ectoderm and establishment of ectopic cell fates would be an interesting follow-up study.

Figures and Figure Legends

Figure 3.1

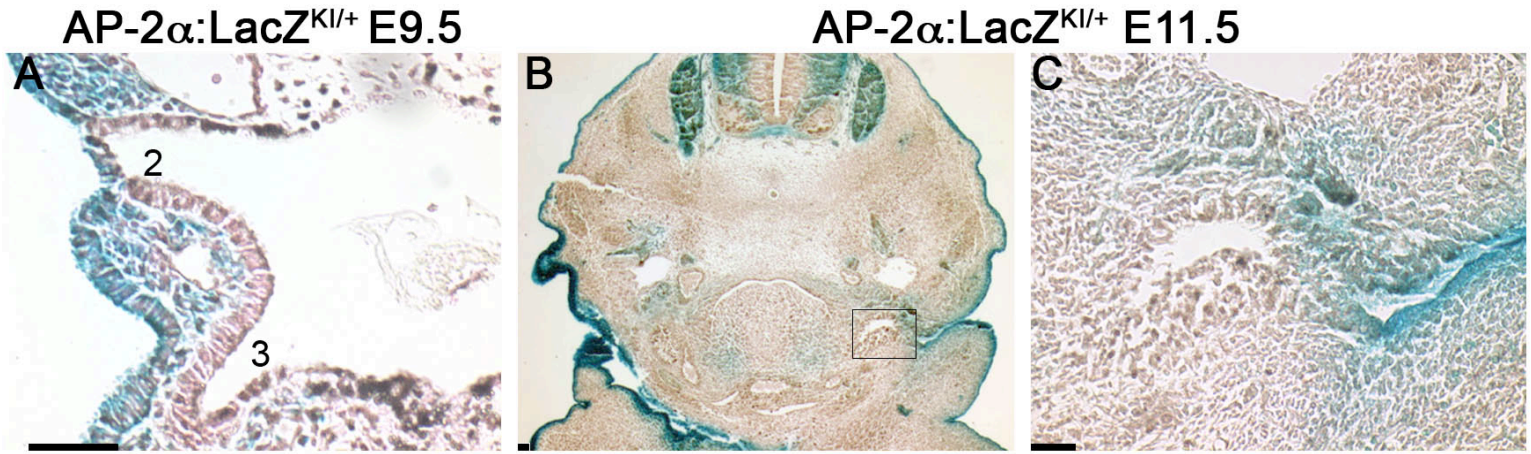

Figure 3.1: *AP-2α* is expressed in neural crest mesenchyme and surface ectoderm surrounding the 3rd pharyngeal pouch.

β-gal expression of AP-2α in the 3rd pharyngeal pouch at E9.5 (A) and E11.75 (B). C. Enlarged view of the third pouch from 1B. Scale bar indicates 50 μm.

Figure 3.2

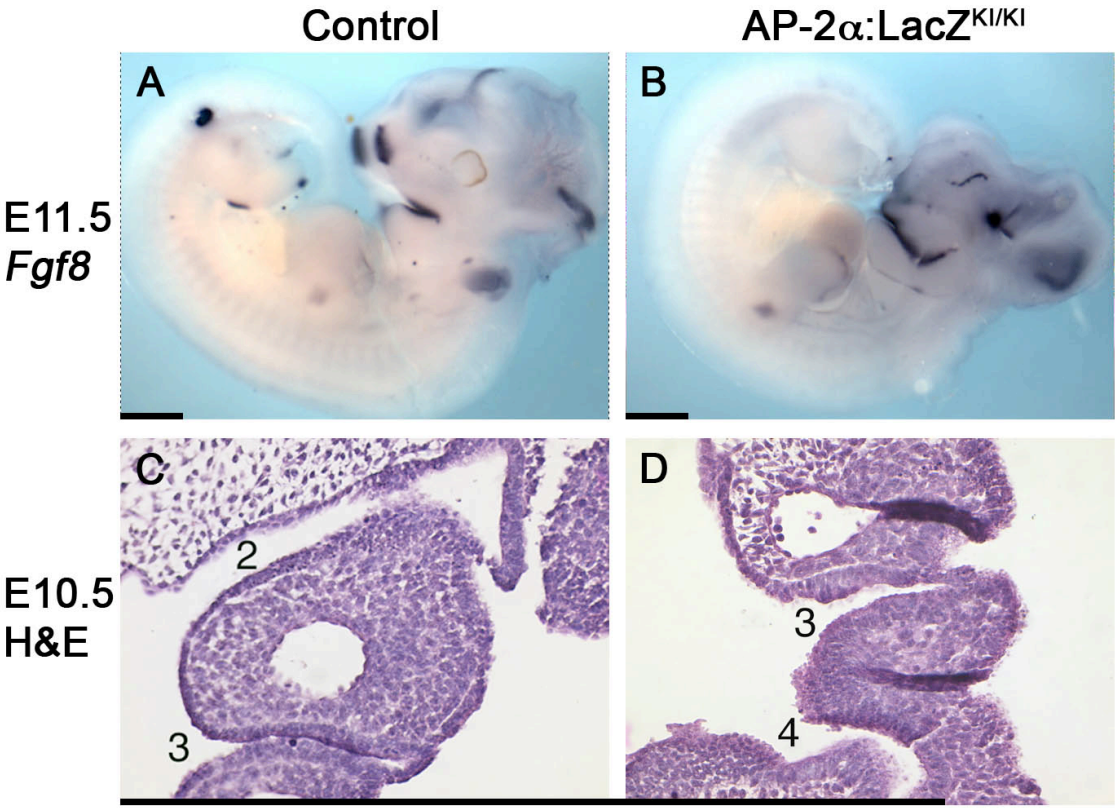

Figure 3.2: Pouch morphology is normal at E10.5 in the absence of *AP-2α*; however, ectopic endoderm identity genes are found in cleft ectoderm at E11.5.

(A – B) Wholemount *in situ* for *Fgf8* at E11.5. *Fgf8* is not found in third pouch endoderm or ectodermal cleft at E11.5 in wild type (A). Ectopic *Fgf8* is found in the ectodermal cleft of AP-2$\alpha^{KI/KI}$ embryos at E11.5 (B). (C – D) H&E staining at E10.5. Initial pouch morphology is similar between wild type (C) and AP-2$\alpha^{KI/KI}$ embryos (D) at E10.5. Scale bar indicates 1 mm.

Figure 3.3

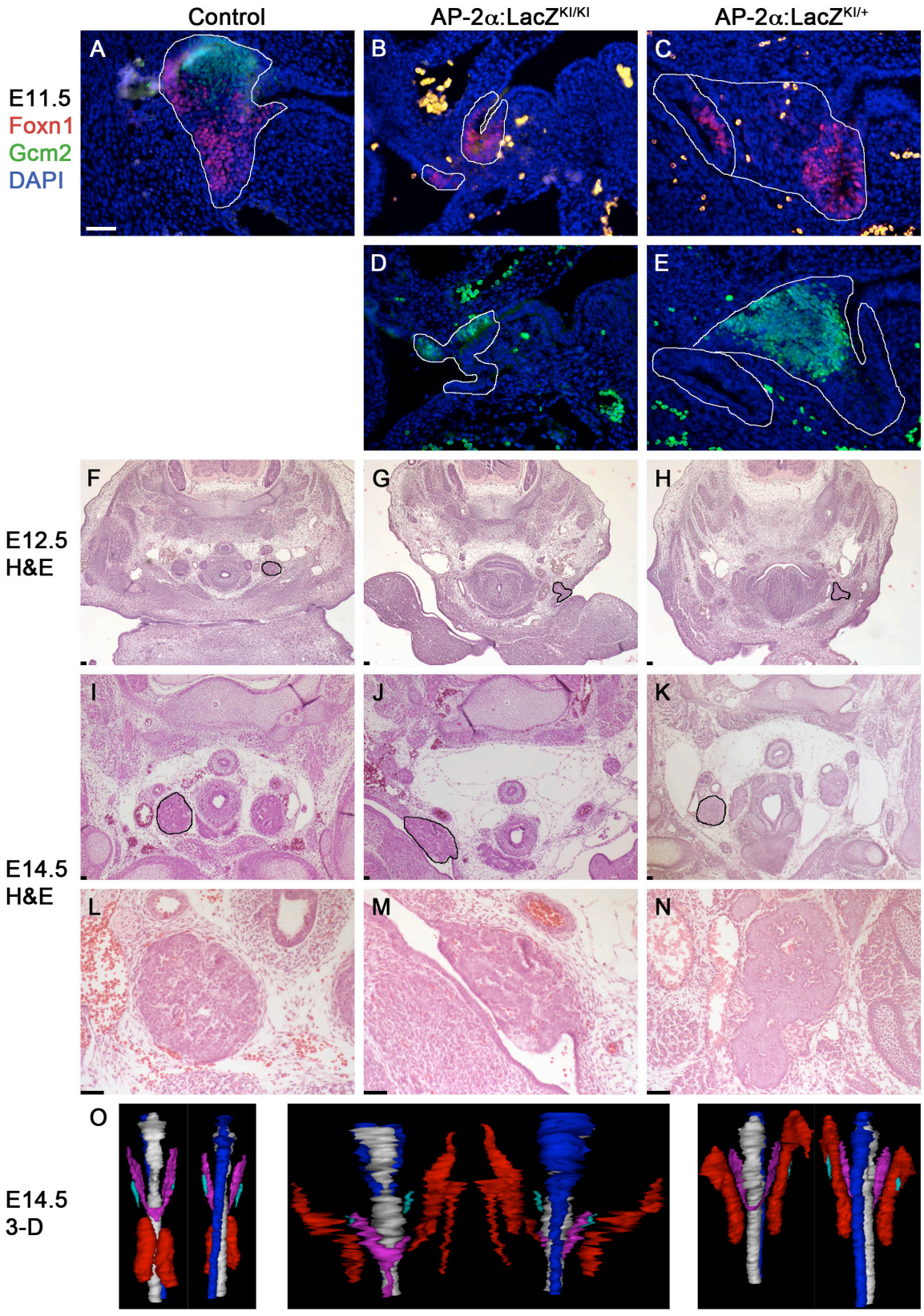
Control
AP-2α:LacZ^KI/KI
AP-2α:LacZ^KI/+
E11.5
Foxn1
Gcm2
DAPI
A
B
C
D
E
E12.5
H&E
F
G
H
E14.5
H&E
I
J
K
L
M
N
E14.5
3-D
O

Figure 3.3: Lack of *AP-2α* results in ectopic parathyroid and thymus

(A – E) Foxn1 and Gcm2 immunostaining at E11.5 in wild type, AP-2α:LacZ$^{KI/KI}$, and AP-2 α:LacZ$^{KI/+}$ embryos. Foxn1 and Gcm2 are found as relatively distinct domains only within third pouch endoderm at E11.5 (A). Foxn1 and Gcm2 are found as distinct domains within third pouch endoderm in AP-2α:LacZ$^{KI/KI}$ embryos; however, an indistinct region of Foxn1 and Gcm2 expression is found in the ectodermal cleft as well at E11.5 (B & D). Foxn1 is found in the ectodermal cleft in AP-2 α:LacZ$^{KI/+}$ embryos at E11.5 in addition to normal Foxn1 and Gcm2 staining found within pouch endoderm (C & E). (F – N) H&E staining at E12.5 and E14.5 in wild type, AP-2 α:LacZ$^{KI/KI}$, and AP-2 α:LacZ$^{KI/+}$ embryos. AP-2α:LacZ$^{KI/KI}$ (G & J) and AP-2 α:LacZ$^{KI/+}$ (H & K) are found in an ectopic location in comparison to wild type (F & I) at E12.5 and E14.5. The thymic capsule surrounds the thymus in wild type (L) but fails to surround thymus exposed at the surface in the AP-2α:LacZ$^{KI/KI}$ embryo (M). Strange disorganization of cells surrounding the thymus was found in AP-2 α:LacZ$^{KI/+}$ embryos (N).

(O) 3-D reconstruction of wild type, AP-2 α:LacZ$^{KI/KI}$, and AP-2 α:LacZ$^{KI/+}$ pharyngeal derived organs at E14.5. Thymus is red, parathyroid is turquoise, thyroid is purple, pharynx is white, and esophagus is blue. Scale bar indicates 50 μm.

Figure 3.4

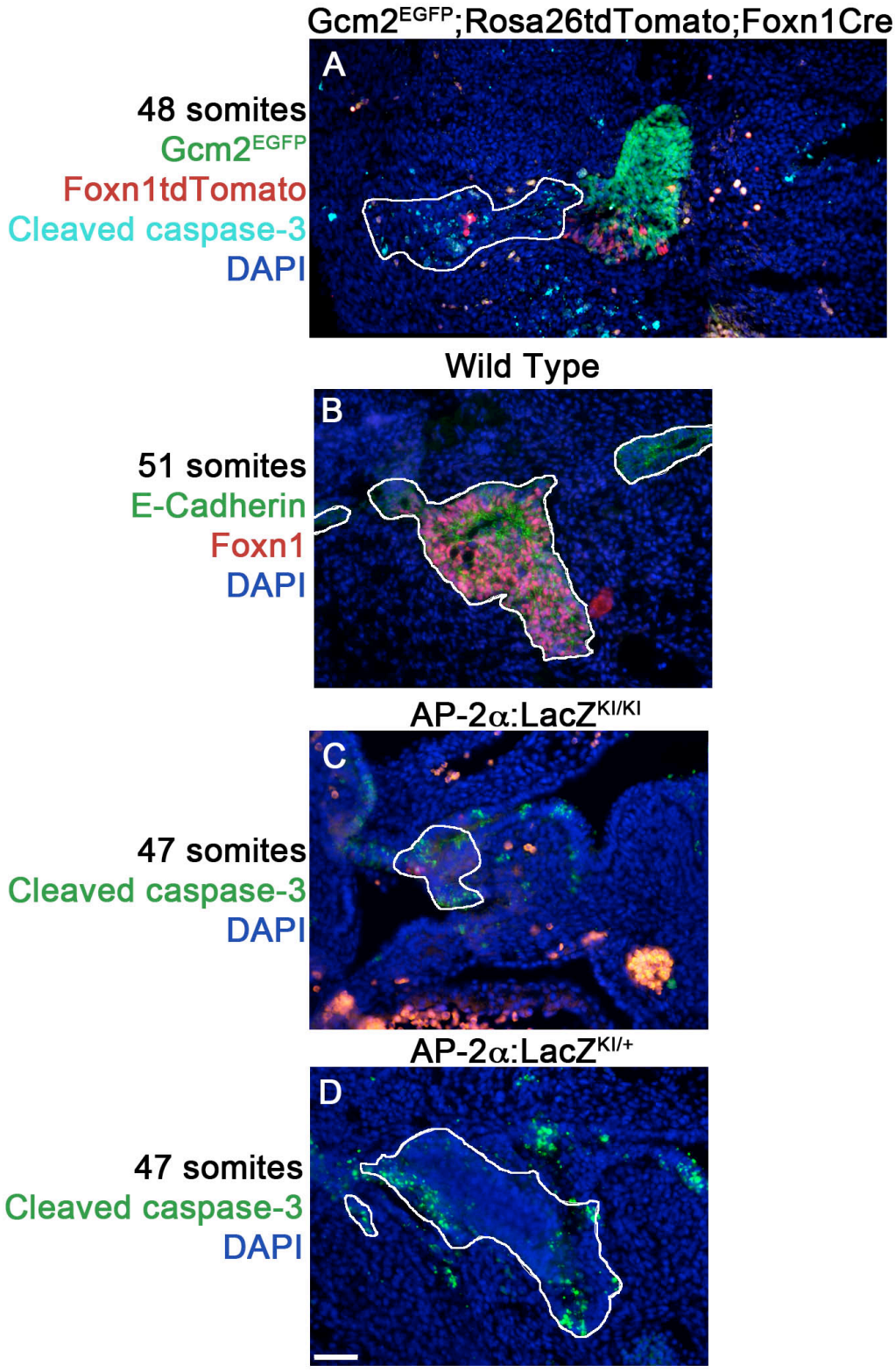
Gcm2EGFP;Rosa26tdTomato;Foxn1Cre
A
48 somites
Gcm2EGFP
Foxn1tdTomato
Cleaved caspase-3
DAPI
Wild Type
B
51 somites
E-Cadherin
Foxn1
DAPI
AP-2α:LacZKI/KI
C
47 somites
Cleaved caspase-3
DAPI
AP-2α:LacZKI/+
D
47 somites
Cleaved caspase-3
DAPI

Figure 3.4: Cell death at the ectodermal cleft is necessary for separation of thymus from ectodermal cleft

(A – D) Immunostaining to show cell death at the ectodermal cleft. In a wild type embryo, thymus detaches from ectodermal cleft by tightly regulated cell death from 47 – 49 somites (A). There is little to no cell death in the pouch endoderm at this stage. The cleft is separate from the thymus by 50 somites (51 somites shown here) (B). Cell death is present in cleft ectoderm and pouch endoderm in both AP-2 α:LacZ$^{KI/KI}$ embryos (C) and AP-2 α:LacZ$^{KI/+}$ embryos (D). Scale bar indicates 50 μm.

Figure 3.5

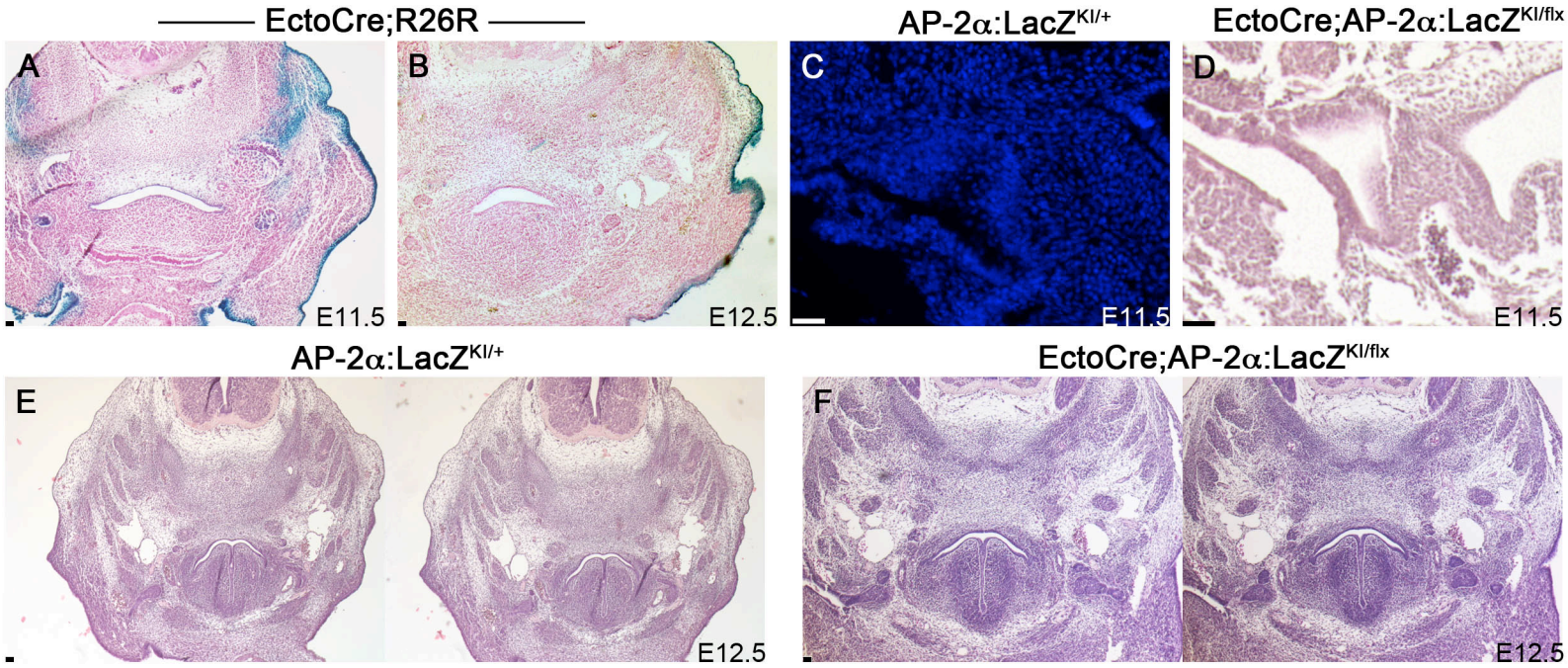
EctoCre;R26R
AP-2α:LacZ^KI/+
EctoCre;AP-2α:LacZ^KI/flx
A
B
C
D
E11.5
E12.5
E11.5
E11.5
AP-2α:LacZ^KI/+
EctoCre;AP-2α:LacZ^KI/flx
E
F
E12.5
E12.5

Figure 3.5: EctoCre;AP-2α:LacZ$^{KI/flx}$ embryos are morphologically identical to AP-2α:LacZ$^{KI/+}$ embryos at E11.5 and E12.5.

(A – B) Expression of EctoCre. β-gal stain shows that EctoCre is active at E11.5 (A) and fully ectoderm specific by E12.5 (B). (C – F) H&E and DAPI stain to compare morphology of EctoCre;AP-2α:LacZ$^{KI/flx}$ embryos and AP-2α:LacZ$^{KI/+}$ embryos. The thymus is found at the surface of the embryo in both genotypes at E11.5 (C &D). Elongated thymus stretching toward ectodermal cleft is found in both genotypes at E12.5 and a break between thymus and cleft is found in each embryo (E & F). Scale bar indicates 50 μm.

Figure 3.6

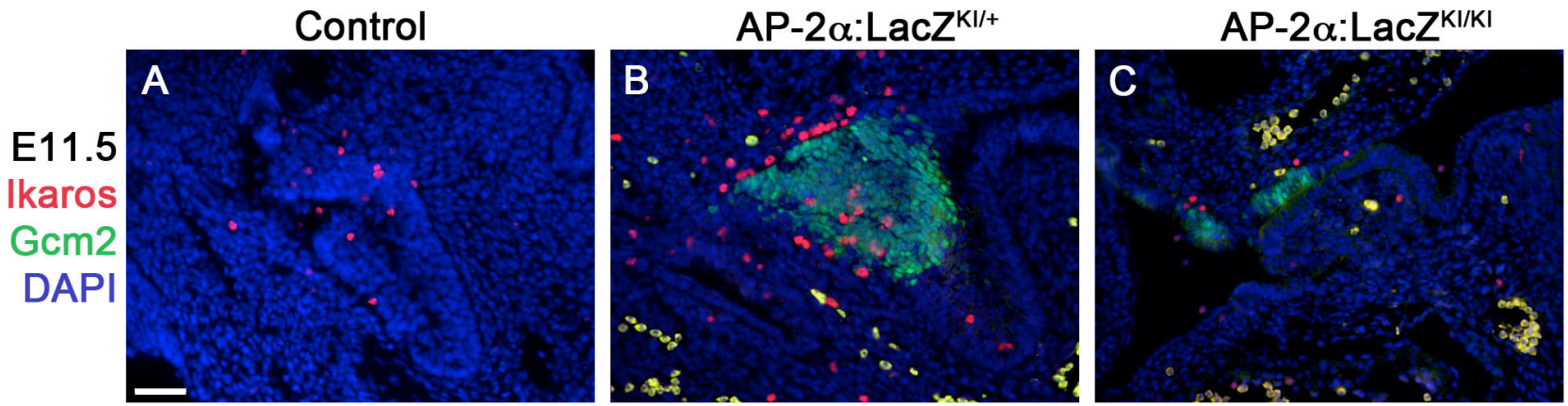
Control
AP-2α:LacZ^KI/+
AP-2α:LacZ^KI/KI
A
B
C
E11.5
Ikaros
Gcm2
DAPI

Figure 3.6: Thymus function is deficient or delayed in the absence of *AP-2α*

(A – C) Ikaros positive lymphoid progenitor cells colonize the thymus starting at E11.5. Ikaros positive cells are attracted to the thymus via the parathyroid and CCL25 at E11.5 in wild type mice (A). Ikaros positive cells are also attracted to the thymus via CCL25 in AP-2α:LacZ$^{KI/+}$ mice (B). Fewer Ikaros positive cells are attracted to the thymus in AP-2α:LacZ$^{KI/KI}$ mice (C). Scale bar indicates 50 μm.

References

Abu-Issa, R., G. Smyth, et al. (2002). "Fgf8 is required for pharyngeal arch and cardiovascular development in the mouse." Development 129(19): 4613-4625.

Blackburn, C. C. and N. R. Manley (2004). "Developing a new paradigm for thymus organogenesis." Nature reviews. Immunology 4(4): 278-289.

Brewer, S., W. Feng, et al. (2004). "Wnt1-Cre-mediated deletion of AP-2alpha causes multiple neural crest-related defects." Developmental biology 267(1): 135-152.

Brewer, S., X. Jiang, et al. (2002). "Requirement for AP-2Œ± in cardiac outflow tract morphogenesis." Mechanisms of Development 110(1-2): 139-149.

Brewer, S. and T. Williams (2004). "Loss of AP-2alpha impacts multiple aspects of ventral body wall development and closure." Developmental biology 267(2): 399-417.

Chapman, D. L., N. Garvey, et al. (1996). "Expression of the T-box family genes, Tbx1–Tbx5, during early mouse development." Developmental Dynamics 206(4): 379-390.

Crossley, P. H. and G. R. Martin (1995). "The mouse Fgf8 gene encodes a family of polypeptides and is expressed in regions that direct outgrowth and patterning in the developing embryo." Development 121(2): 439-451.

Danielian, P. S., D. Muccino, et al. (1998). "Modification of gene activity in mouse embryos in utero by a tamoxifen-inducible form of Cre recombinase." Current Biology 8(24): 1323-S1322.

de Croze, N., F. Maczkowiak, et al. (2011). "Reiterative AP2a activity controls sequential steps in the neural crest gene regulatory network." Proceedings of the National Academy of Sciences of the United States of America 108(1): 155-160.

Dunker, N. and K. Krieglstein (2002). "Tgfbeta2 -/- Tgfbeta3 -/- double knockout mice display severe midline fusion defects and early embryonic lethality." Anatomy and embryology 206(1-2): 73-83.

Gordon, J., A. R. Bennett, et al. (2001). "Gcm2 and Foxn1 mark early parathyroid- and thymus-specific domains in the developing third pharyngeal pouch." Mechanisms of Development 103(1-2): 141-143.

Gordon, J. and N. R. Manley (2011). "Mechanisms of thymus organogenesis and morphogenesis." Development 138(18): 3865-3878.

Gordon, J., V. A. Wilson, et al. (2004). "Functional evidence for a single endodermal origin for the thymic epithelium." Nature immunology 5(5): 546-553.

Knight, R. D., Y. Javidan, et al. (2005). "AP2-dependent signals from the ectoderm regulate craniofacial development in the zebrafish embryo." Development 132(13): 3127-3138.

Manley, N. R. and M. R. Capecchi (1995). "The role of Hoxa-3 in mouse thymus and thyroid development." Development 121(7): 1989-2003.

Manley, N. R., J. R. Barrow, et al. (2001). "Hoxb2 and hoxb4 act together to specify ventral body wall formation." Developmental biology 237(1): 130-144.

Mitchell, P. J., P. M. Timmons, et al. (1991). "Transcription factor AP-2 is expressed in neural crest cell lineages during mouse embryogenesis." Genes & Development 5(1): 105-119.

Moore-Scott, B. A. and N. R. Manley (2005). "Differential expression of Sonic hedgehog along the anterior-posterior axis regulates patterning of pharyngeal pouch endoderm and pharyngeal endoderm-derived organs." Developmental biology 278(2): 323-335.

Nottoli, T., S. Hagopian-Donaldson, et al. (1998). "AP-2-null cells disrupt morphogenesis of the eye, face, and limbs in chimeric mice." Proceedings of the National Academy of Sciences 95(23): 13714-13719.

Suzuki, N., P. A. Labosky, et al. (1996). "Failure of ventral body wall closure in mouse embryos lacking a procollagen C-proteinase encoded by Bmp1, a mammalian gene related to Drosophila tolloid." Development 122(11): 3587-3595.

CHAPTER 4

CONCLUSIONS AND DISCUSSION

As a final exam, I was once asked design an applet that would oscillate between red, yellow, and green (similar to a traffic signal) using visual basic. Designing an applet that turns one color on and off, or even an applet that switches between two colors does not require much code. Oscillating between three colors, as it turned out, was rather difficult to code although easy to conceptualize. Patterning of the third pharyngeal pouch into thymus and parathyroid reminds me of the traffic signal applet in that it is simple to conceptualize but in reality is a complex pathway requiring the input of many signaling molecules, transcription factors, and tissues.

Before third pharyngeal pouch endoderm forms the thymus and parathyroid, it is already patterned as endoderm. This initial patterning involves the *Hoxa3-Pax1/Pax9-Eya1-Six1/4* transcription factor network, Fgf8, and Tbx1 (Manley and Capecchi, 1995; Wallin et al., 1996; Su et al., 2001; Xu et al., 2001; Frank et al., 2002; Vitelli et al., 2002; Zou et al., 2006). Early endoderm patterning is independent of later signaling that will act on third pouch endoderm: i.e. Shh signaling (Moore-Scott and Manley, 2005). After initial patterning, several transcription factors and signals are present within the third pharyngeal pouch and may be involved in establishing thymus and parathyroid identity. We initially thought that transcription factors *Foxn1* and *Gcm2* were responsible for thymus and parathyroid fate. However, it has been shown by genetic analysis that thymus forms in the absence of *Foxn1* and parathyroid forms in the absence of *Gcm2*. Instead, *Foxn1* is responsible for TEC differentiation and *Gcm2* is responsible

for parathyroid differentiation and survival (Blackburn et al., 1996; Liu et al., 2007).

Further clues about pouch fate came from *Shh* and *Splotch* mutants. In the case of *Splotch* mice, domain boundaries were shifted within the third pouch resulting in more thymus and less parathyroid than wild type. *Splotch* mice have a defect in neural crest cells and this result suggested that a signal from neural crest mesenchyme was acting on pouch endoderm to establish or regulate pouch fate (Griffith et al., 2009). This result was similar to the *Shh* null phenotype in which the parathyroid is absent and the thymus covers all available third pouch endoderm (Moore-Scott and Manley, 2005). The first part of this dissertation sought to determine if Shh signaling in neural crest mesenchyme was responsible for the *Splotch* phenotype and to identify other roles for Shh signaling in thymus and parathyroid establishment.

Shh plays a crucial role in regulation of patterning genes within the third pharyngeal pouch.

We utilized tissue specific Cre mediated recombination to delete or induce Shh signaling (by targeting *Shh* signal transducer *Smoothened*) to identify tissue specific contributions of Shh signaling to third pharyngeal pouch fate. We found that Shh signaling acts both directly and indirectly on the third pharyngeal pouch. Surprisingly, Shh signaling to endoderm alone does not establish parathyroid fate as a normal sized parathyroid was found when Shh signaling was deleted in pouch endoderm. Furthermore, no tissue specific manipulation of Shh signaling recapitulated the *Shh* null phenotype where *Gcm2* was absent, suggesting that Shh signaling from both neural crest mesenchyme and pouch endoderm are individually sufficient for parathyroid fate. Earlier studies of the *Gcm2* null mouse found that *Tbx1* patterning was normal in the absence of *Gcm2* and suggested a *Shh-Tbx1-Gcm2* regulatory pathway for parathyroid development (Liu et al., 2007). We confirmed earlier work showing that *Shh* is upstream of both

Tbx1 and *Gcm2*; however, we found that *Tbx1* is not necessarily directly upstream of *Gcm2*. When *Shh* signaling was activated throughout the third pouch endoderm we found a region of strong *Tbx1* expression which was not accompanied by *Gcm2* expression. Interestingly this region also did not express *Foxn1* and was instead unfated third pouch endoderm. It is unclear whether this region did not express *Gcm2* because of a requirement for an additional signal or transcription factor not present in the region or if a signal or transcription factor within the unfated region (which would normally express *Foxn1*) inhibits *Gcm2* expression. Finally, the inability to phenocopy the *Splotch* mutant suggests that a signal independent of *Shh* acts on the third pouch from neural crest mesenchyme to help regulate thymus and parathyroid fate. I think this is a potential role for *Fgf10* from the neural crest mesenchyme both because of it's expression pattern in wild type embryos and because *Fgf10* expression is normal in tissue specific deletions of Shh signaling. Furthermore I think that *Fgf10* could be the signal rescuing parathyroid fate in the endoderm specific deletion of Shh signaling and that *Fgf10* expression will be altered or absent in the *Shh* null.

These findings are significant because they provide evidence that Shh signaling and *Tbx1* expression alone within the third pouch are not sufficient for parathyroid fate. Furthermore these findings suggest that Shh signaling is not the only signal involved in pouch organization and fate, nor is it the primary signal. This work is also the first evidence that *Tbx1* inhibits *Foxn1* expression. It has recently been shown that Bmp4 signaling regulates microRNAs that posttranscriptionally silence *Tbx1* and *Isl1* (Wang et al., 2010). It is possible, as was suggested after the initial study of pharyngeal development in *Shh* null mice, that Bmp signaling and Shh signaling form opposing gradients within the third pouch to establish dorsal – ventral polarity (Moore-Scott and Manley, 2005).

Separation of thymus from ectodermal cleft requires *AP-2α*.

After successful patterning, the thymus and parathyroid must separate from pharynx, ectodermal cleft, and each other before migration in order to complete normal morphogenesis. Several mutants, discussed earlier in this dissertation, have defects in separation from pharynx or failure of separation of thymus and parathyroid; however, *AP-2α* is the only gene currently known to have a role in separation of thymus from ectodermal cleft (Brewer et al., 2002). In this study, we confirmed earlier work which showed that thymus separates from ectodermal cleft by cell death at E11.75 and we determined that this cell death occurs from the 47 – 49 somites stage (Gordon et al., 2004). We found that cell death occurred in the cleft of *AP-2α* mutants; however, cell death occurred at a higher rate within pouch endoderm in the absence of *AP-2α*. Further analysis is required before we can determine how levels of cell death in mutant cleft compares to wild type cleft although initial work suggests that levels are similar but the pattern is different. We also found haploinsufficiency of *AP-2α* in thymus development. Surprisingly we did not find unique phenotypes in tissue specific knockouts of *AP-2α*. This may indicate that downstream targets of *AP-2α* from both neural crest mesenchyme and surface ectoderm work together to allow separation of third pouch from ectodermal cleft. The most surprising finding of this study was that *Fgf8* failed to be downregulated in ectodermal cleft and ectopic *Pax1* expression was found in the ectodermal cleft at E11.5. Ectodermal cleft expressed both *Foxn1* and *Gcm2* in the absence of *AP-2α*; however, the cleft lacked the organization found in third pouch endoderm. Finally preliminary work indicates that thymic function is decreased or delayed because significantly fewer ikaros positive cells were found in and around the *AP-2α* mutant thymus at E11.5.

It is interesting that wild type levels of *AP-2α* are required for normal thymus morphogenesis. It is especially interesting that the haploinsufficient phenotype for *AP-2α* is identical to the ectodermal deletion of *AP-2α* as well as later stages of the neural crest deletion of *AP-2α* - the phenotype for early stages is currently unknown (Brewer et al., 2004). This allows for the possibility that *AP-2α* from both sources is acting on different sides of the same pathway (or controls the same signal from all sources) and that any change in the level of signaling downstream of *AP-2α* causes the same failure of separation from ectodermal cleft. Because we only see refating of ectodermal cleft in the global deletion of *AP-2α*, this raises the possibility that correct placement of cell death requires *AP-2α* from both ectoderm and neural crest mesenchyme (and that any loss of *AP-2α* will result in failed or delayed separation). Global deletion of *AP-2α* results in a gain of function due to high sensitivity to some downstream signaling target of *AP-2α,* which is absent in the global deletion but present in sufficient levels in any other deletion of *AP-2α.*

In this dissertation we have continued to study the molecular mechanisms establishing third pharyngeal pouch fate and early morphogenesis of thymus and parathyroid. We have further refined our understanding of the pathway for thymus and parathyroid fate. We have found that Shh signaling to endoderm alone is not responsible for parathyroid fate, that a Shh independent signal from neural crest mesenchyme is involved in establishing fate boundary within the pouch, and that *Tbx1* can inhibit *Foxn1* within the pouch. We have also found that wild type levels of *AP-2α* are required for normal thymus morphogenesis and that in the complete absence of *AP-2α* ectodermal cleft is able to adopt third pouch fate.

It is interesting that Shh signaling helps to regulate pouch closer to the pharynx and has little to no impact on the ventral pouch, especially considering the region of *Foxn1*/*Gcm2*

positive cleft in *AP-2α* null embryos. It is possible that ventral pouch is not able to respond to Shh signaling and that if Shh signaling was able to reach the ectodermal cleft of *AP-2α* mutants, the cleft would be organized into discrete Foxn1 and Gcm2 domains, in a similar manner to the organization of a wild type pouch (Fig. 1). The presence of *Gcm2* positive cells in the ectodermal cleft of *AP-2α* mutants also supports the hypothesis that Shh signaling is not required to induce Gcm2 expression, and that a second signal from neural crest mesenchyme is also able to act on endodermal tissue to promote *Gcm2* expression.

Figures and Figure Legends

Figure 4.1

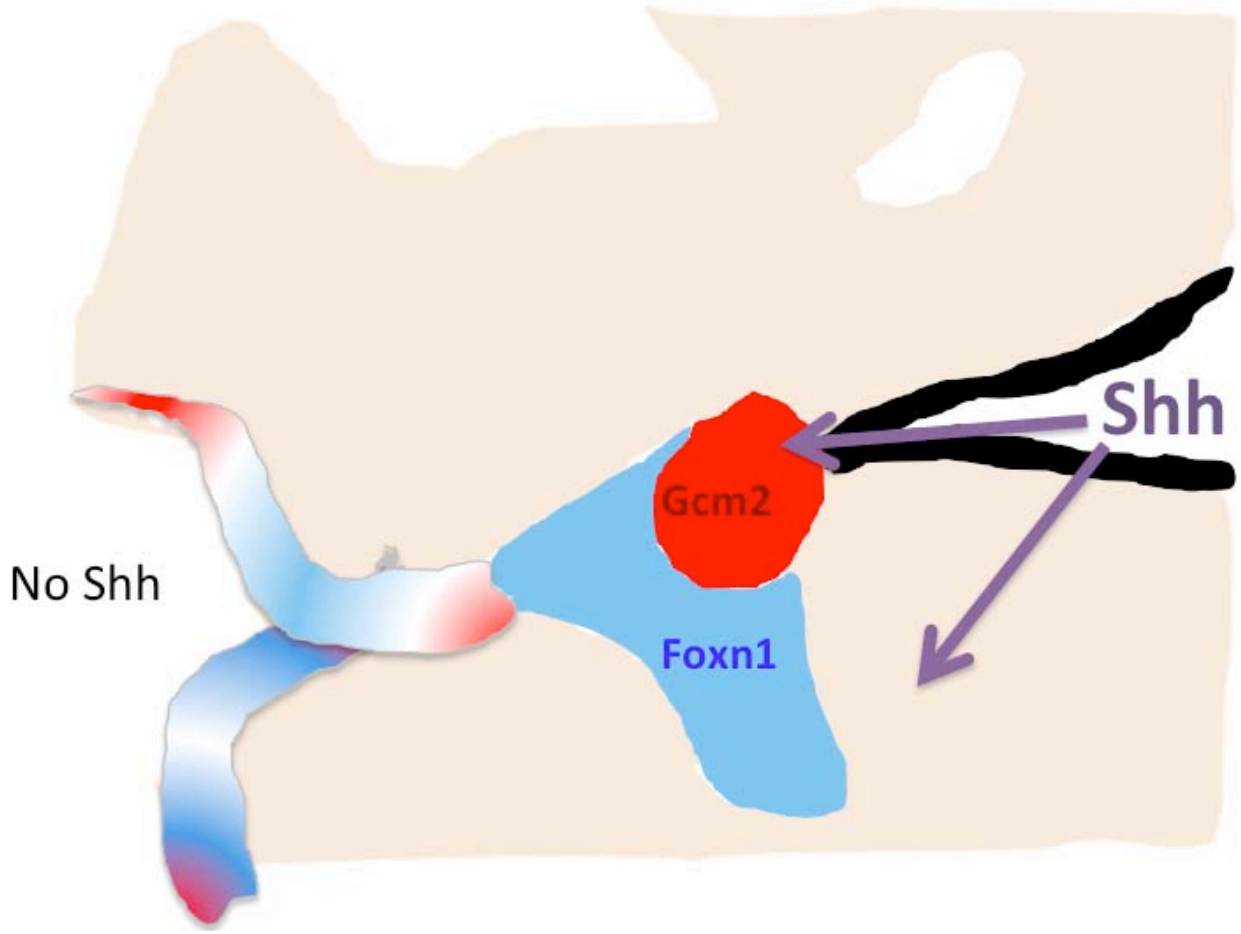

Figure 4.1: Lack of organization at the ectodermal cleft in *AP-2α* mutants

In the absence of *AP-2α* the ectodermal cleft expresses early pouch patterning genes in addition to *Foxn1* and *Gcm2*. While both pouch markers are present there is no organization within the ectodermal cleft and *Foxn1* and *Gcm2* cells intermingle. It is possible that this lack of organization is in part caused by the lack of Shh signaling at the ectodermal cleft.

References

Blackburn, C. C., C. L. Augustine, et al. (1996). "The nu gene acts cell-autonomously and is required for differentiation of thymic epithelial progenitors." PNAS 93(12): 5742-5746.

Brewer, S., W. Feng, et al. (2004). "Wnt1-Cre-mediated deletion of AP-2alpha causes multiple neural crest-related defects." Developmental biology 267(1): 135-152.

Brewer, S., X. Jiang, et al. (2002). "Requirement for AP-2α in cardiac outflow tract morphogenesis." Mechanisms of Development 110(1-2): 139-149.

Frank, D. U. et al. (2002). "An Fgf8 mouse mutant phenocopies human 22q11 deletion syndrome." Development 129(19): 4591-4603.

Gordon, J., V. A. Wilson, et al. (2004). "Functional evidence for a single endodermal origin for the thymic epithelium." Nature immunology 5(5): 546-553.

Griffith, A. V., K. Cardenas, et al. (2009). "Increased thymus- and decreased parathyroid-fated organ domains in Splotch mutant embryos." Developmental biology 327(1): 216-227.

Liu, Z., S. Yu, et al. (2007). "Gcm2 is required for the differentiation and survival of parathyroid precursor cells in the parathyroid/thymus primordia." Developmental biology 305(1): 333-346.

Manley, N. R. and M. R. Capecchi (1995). "The role of Hoxa-3 in mouse thymus and thyroid development." Development 121(7): 1989-2003.

Moore-Scott, B. A. and N. R. Manley (2005). "Differential expression of Sonic hedgehog along the anterior-posterior axis regulates patterning of pharyngeal pouch endoderm and pharyngeal endoderm-derived organs." Developmental biology 278(2): 323-335.

Su, D., S. Ellis, et al. (2001). "Hoxa3 and pax1 regulate epithelial cell death and proliferation during thymus and parathyroid organogenesis." Developmental biology 236(2): 316-329.

Vitelli, F. et al. (2002). "Tbx1 mutation causes multiple cardiovascular defects and disrupts neural crest and cranial nerve migratory pathways." Human molecular genetics 11(8): 915-922.

Wallin, J., H. Eibel, et al. (1996). "Pax1 is expressed during development of the thymus epithelium and is required for normal T-cell maturation." Development 122(1): 23-30.

Wang, J. et al. (2010). "Bmp signaling regulates myocardial differentiation from cardiac progenitors through a MicroRNA-mediated mechanism." Developmental cell 19(6): 903-912.

Xu, P.-X., W. Zheng, et al. (2002). "Eya1 is required for the morphogenesis of mammalian thymus, parathyroid and thyroid." Development 129(13): 3033-3044.

Zou, D., D. Silvius, et al. (2006). "Patterning of the third pharyngeal pouch into thymus/parathyroid by Six and Eya1." Developmental biology 293(2): 499-512.